

1/116



1-SIDED TUNNEL SYSTEM

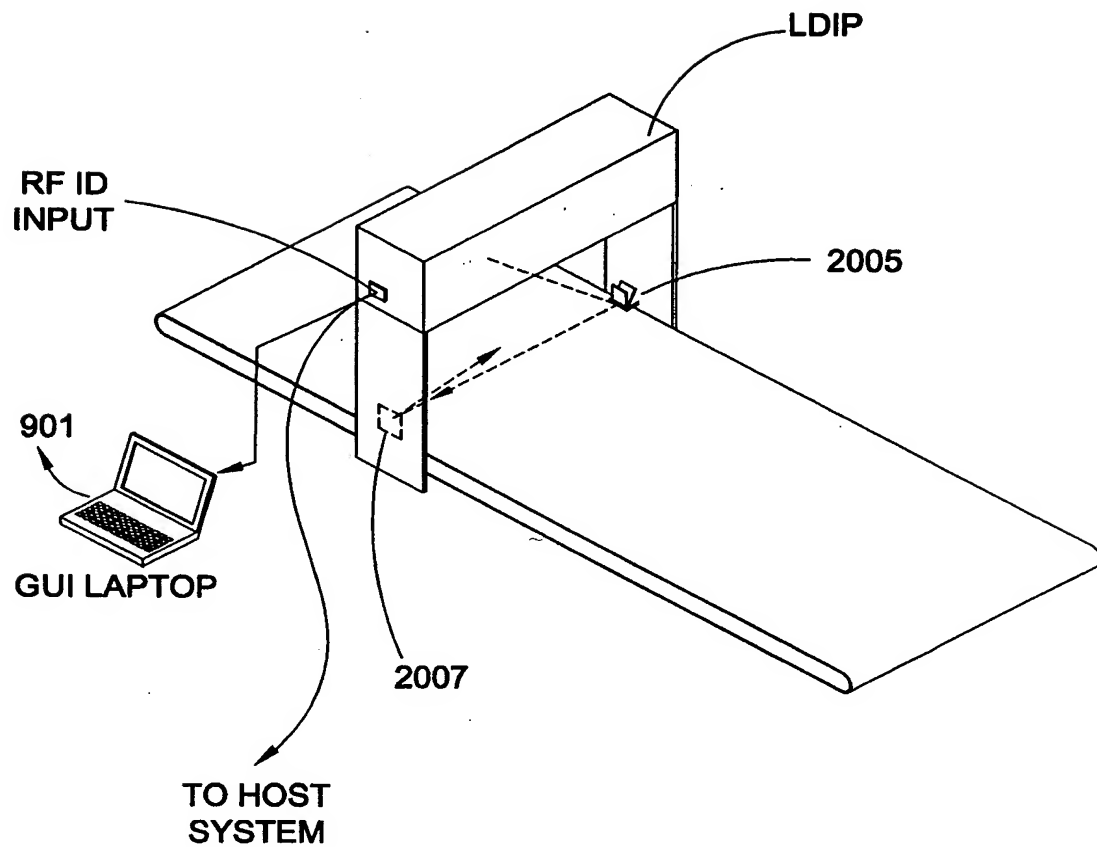


FIG. 1A

2/116

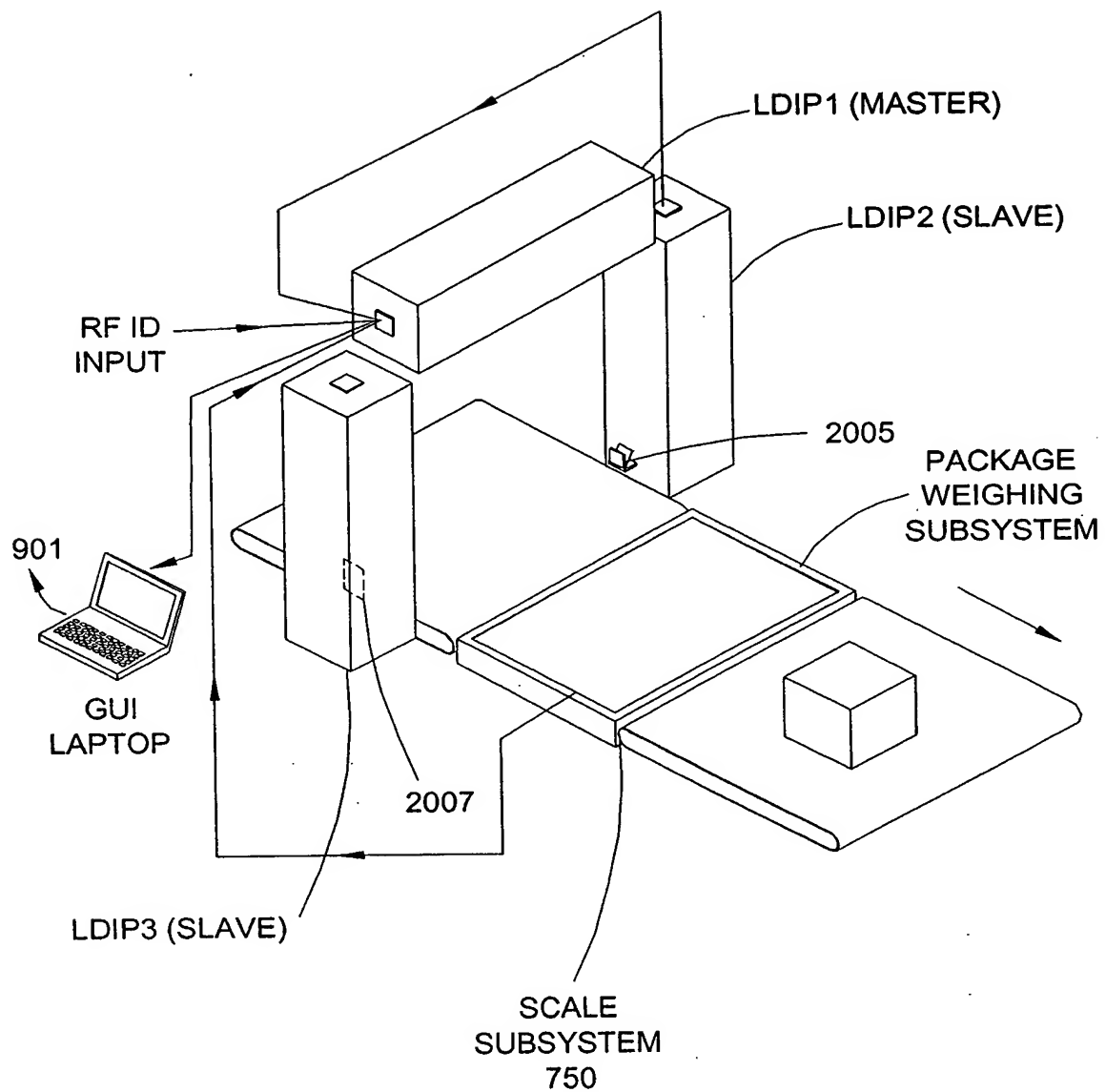
3-SIDED TUNNEL
SYSTEM

FIG. 1B

3/116

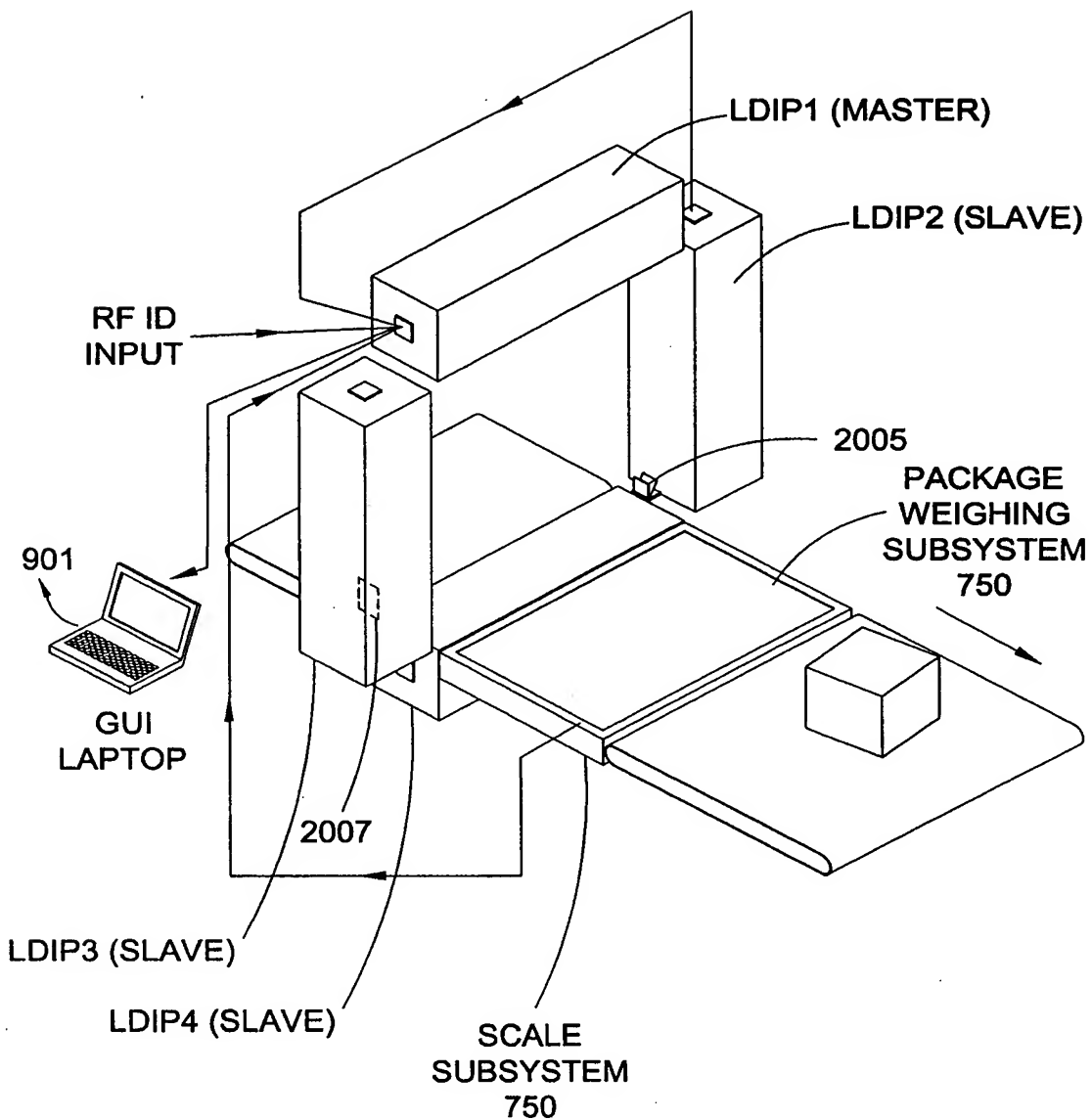
4-SIDED TUNNEL
SYSTEM

FIG. 1C

4/116

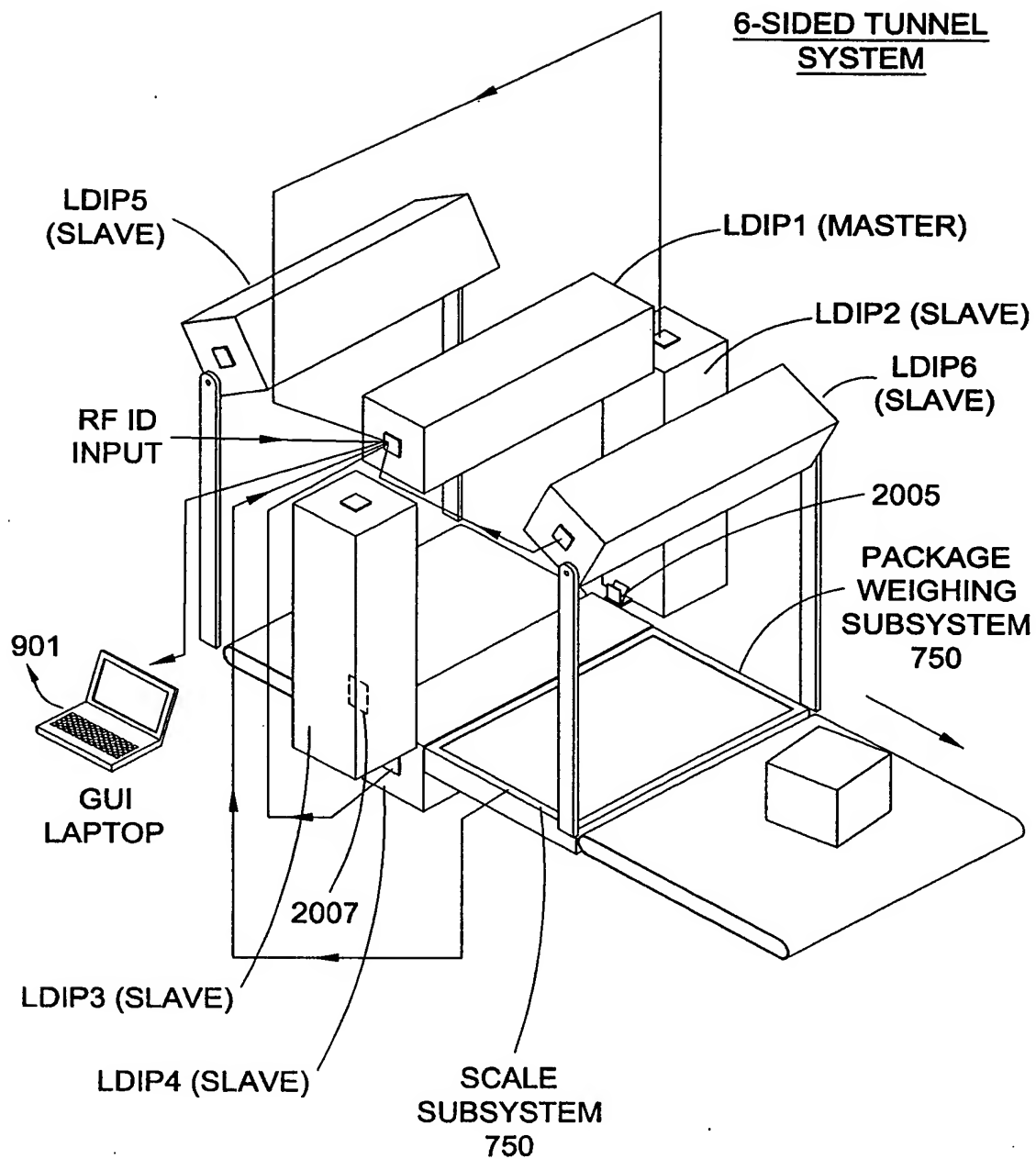


FIG. 1D

5/116

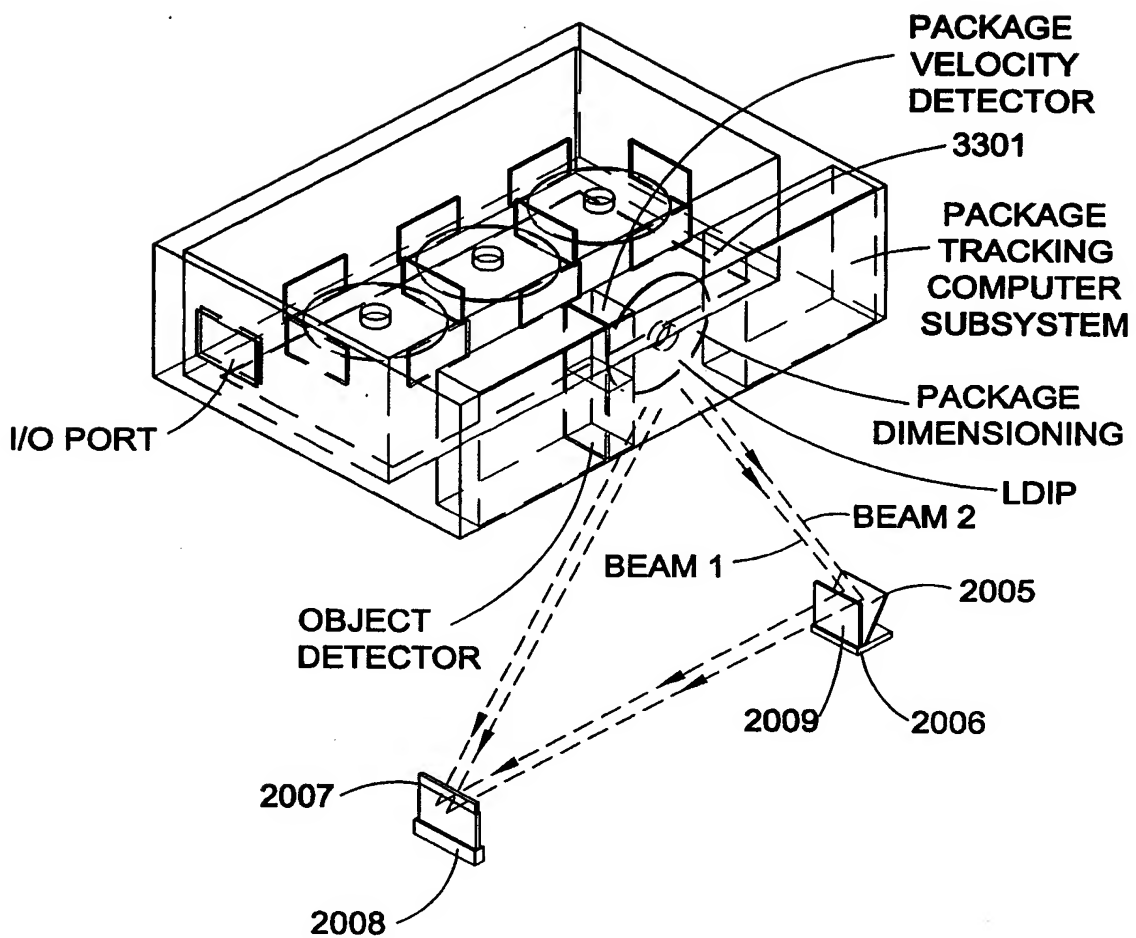


FIG. 2A

6/116

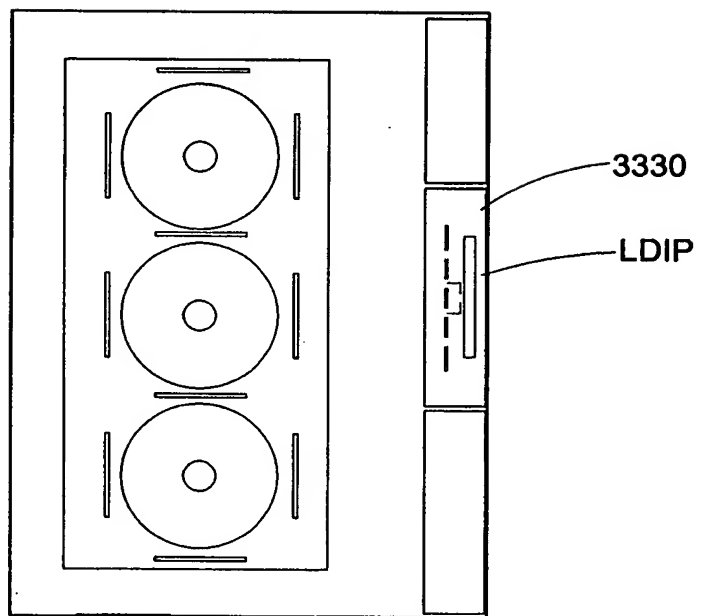


FIG. 2B

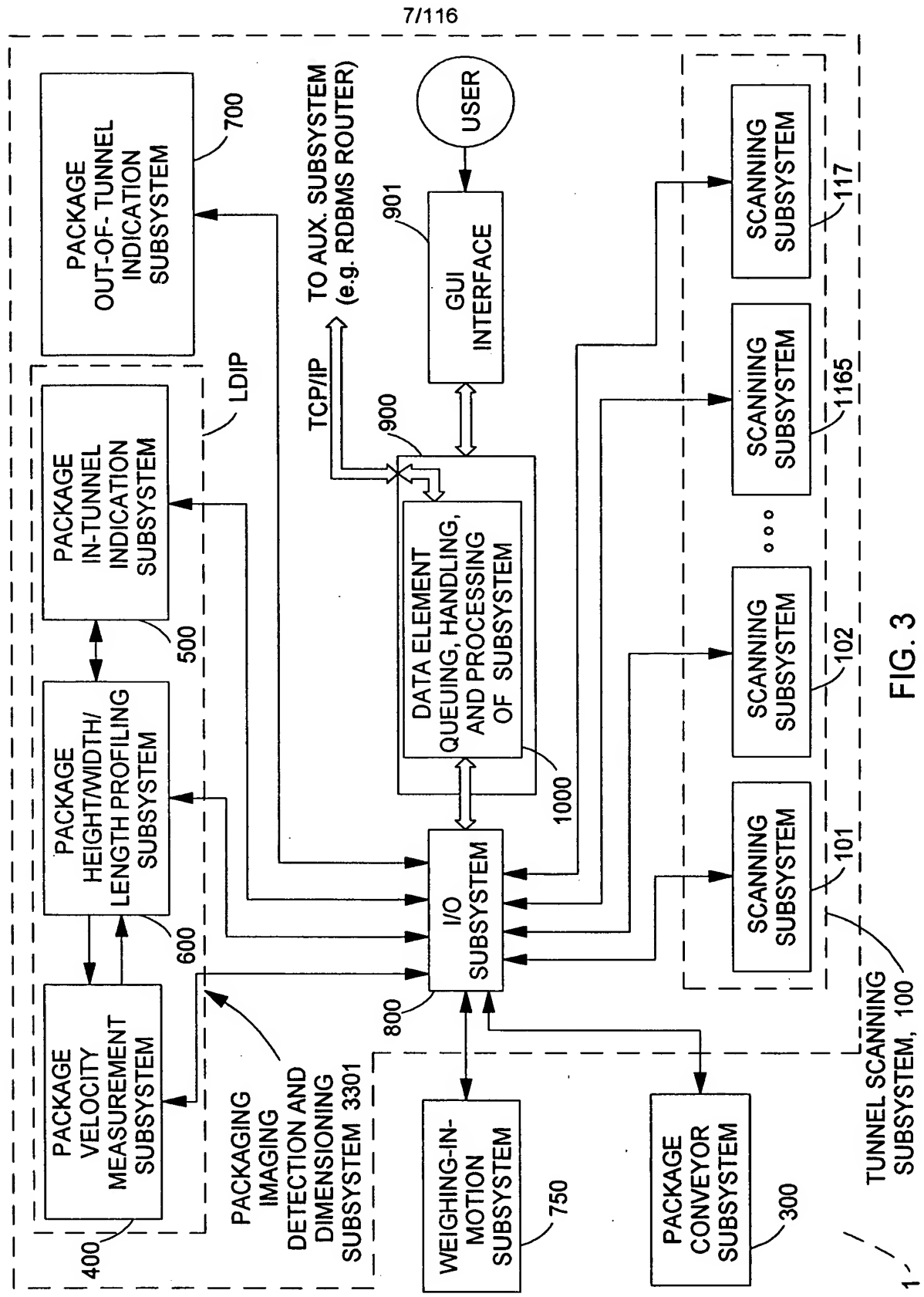


FIG. 3

8/116

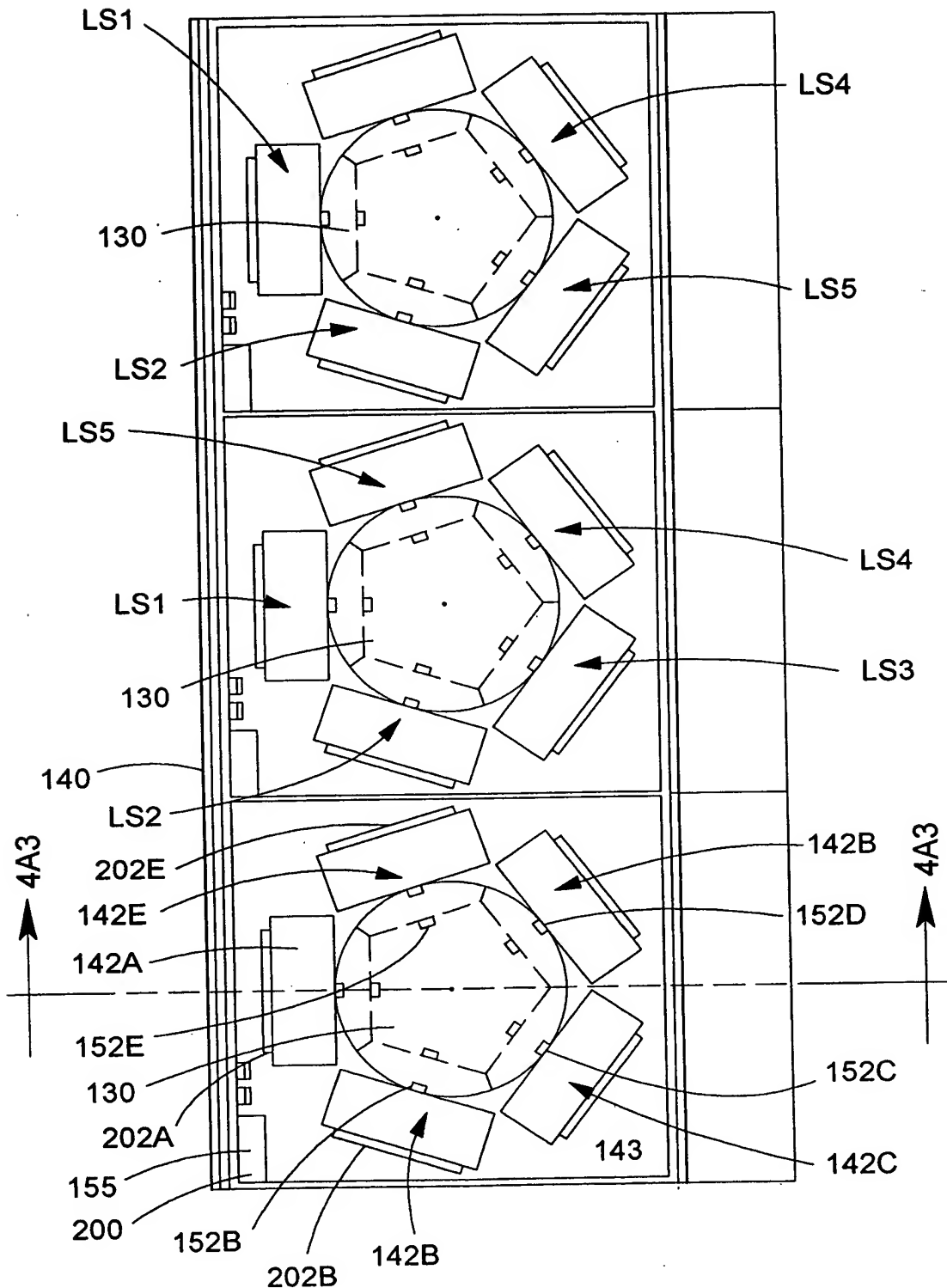


FIG. 4A1

9/116

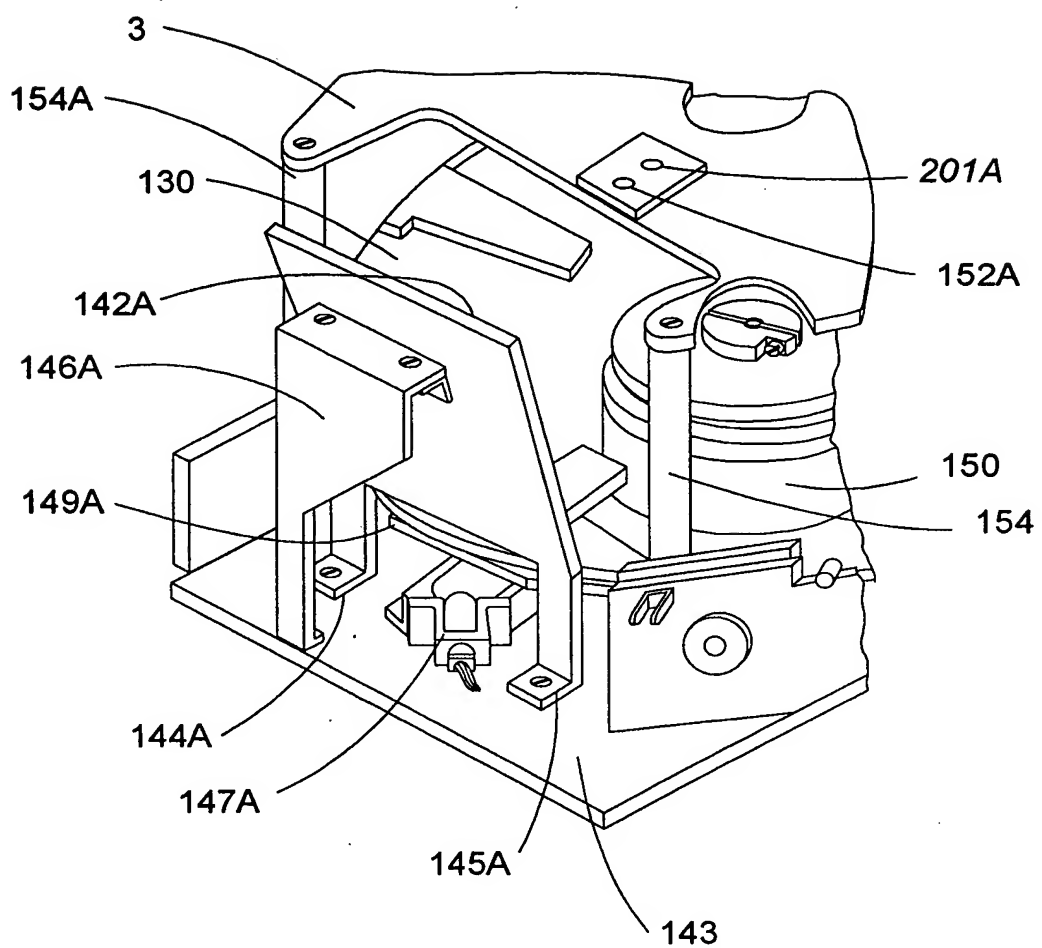


FIG. 4A2

10/116

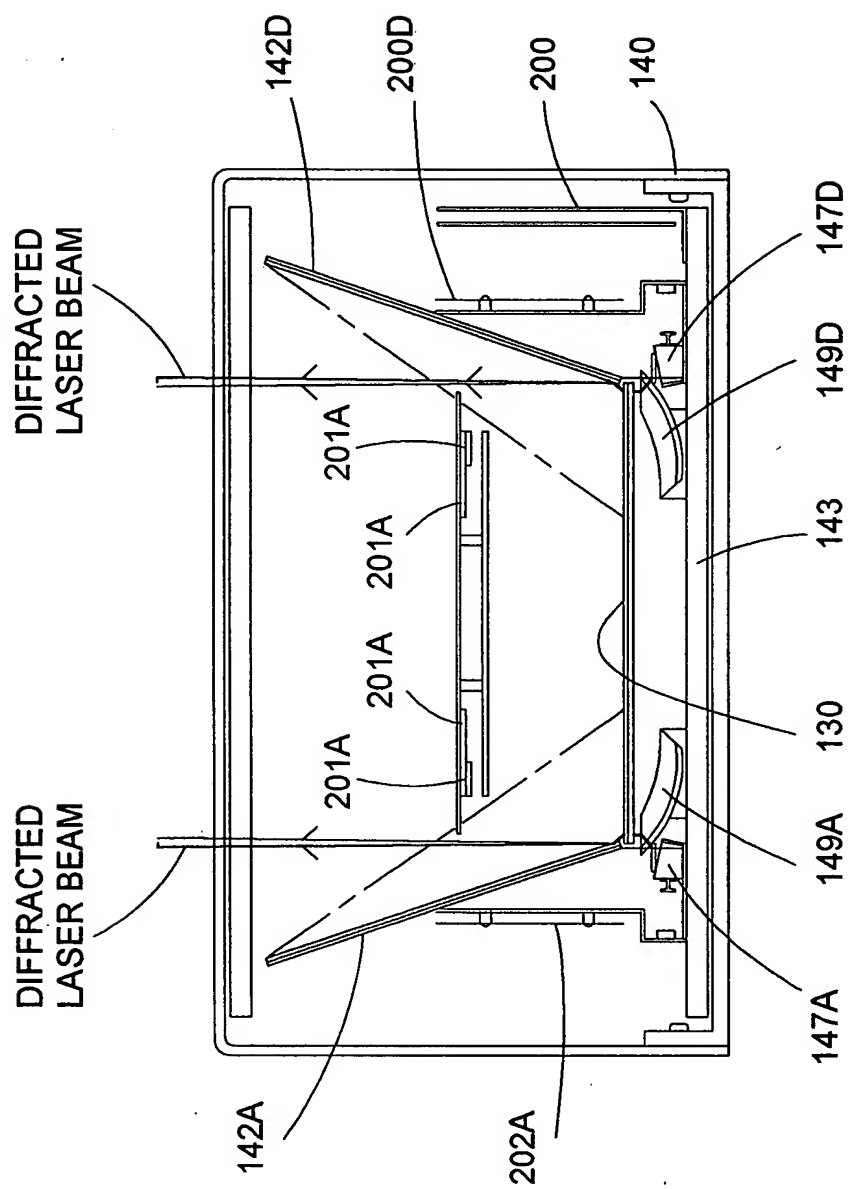


FIG. 4A3

11/116

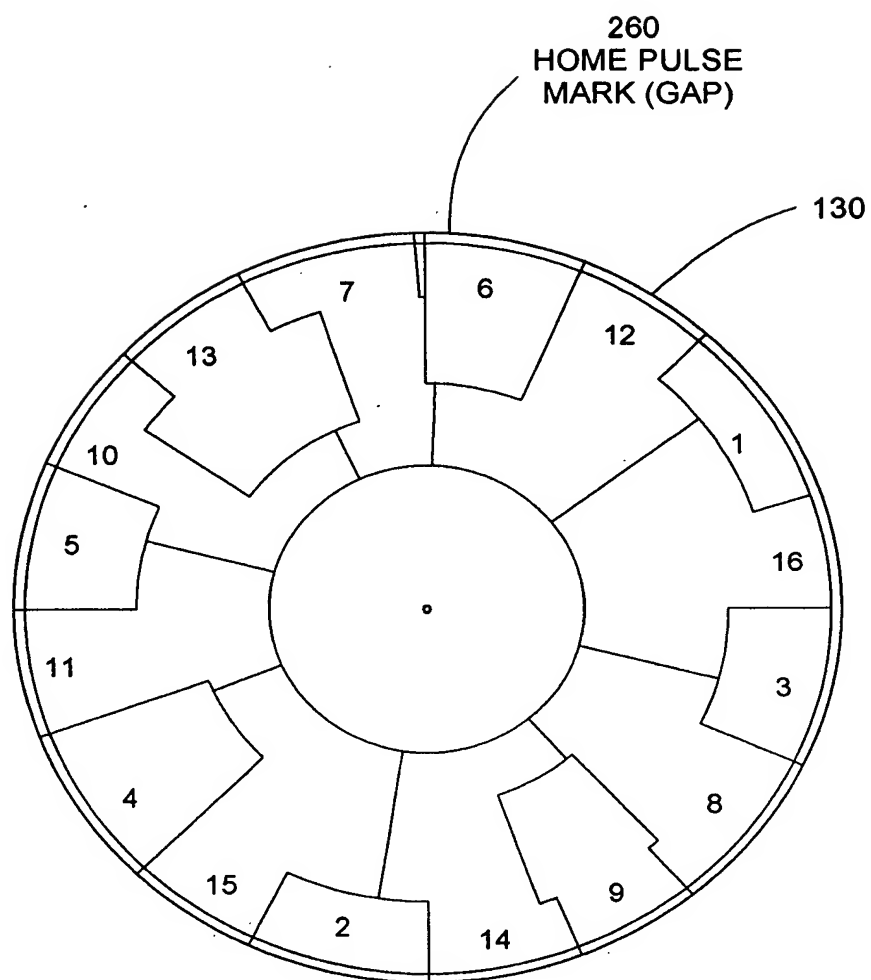


FIG. 4A4

12/116

	DIFFRACTION FACET FOCAL LENGTH (INCHES)	GEOMETRICAL FOCAL LENGTH (INCHES)	ANGLE A (DEGREE)	ANGLE B (DEGREE)	ANGLE OF DIFFRACTION (DEGREES)	ANGLE OF BEAM FROM VERTICAL (DEGREES)	SCAN ANGLE (DEGREES)	SCAN MULT. ROTATION ANGLE (DEGREES)	SCAN MULT. FACTOR (m)
1	49.57	49.76	45.9	61.06	28.94	-3.06	29.61	1.26	23.51
2	49.54	49.73	45.9	55.62	34.38	2.38	29.62	1.34	22.10
3	49.96	50.16	45.9	50.23	39.77	7.77	29.39	1.41	20.77
4	50.81	51.01	45.9	44.97	45.03	13.03	28.92	1.48	19.52
5	49.57	49.76	45.9	61.06	28.94	-3.06	29.61	1.26	23.51
6	49.54	49.73	45.9	55.62	34.38	2.38	29.62	1.34	22.10
7	49.96	50.16	45.9	50.23	39.77	7.77	29.39	1.41	20.77
8	50.81	51.01	45.9	44.97	45.03	13.03	28.92	1.48	19.52
9	59.06	59.38	45.9	60.56	29.44	-2.56	25.01	1.25	55.73
10	59.04	59.36	45.9	56.00	34.00	2.00	25.02	1.32	55.73
11	59.39	59.72	45.9	51.47	38.53	6.53	24.88	1.39	55.73
12	60.10	60.44	45.9	47.01	42.99	10.99	24.59	1.44	55.73
13	59.06	59.38	45.9	60.56	29.44	-2.56	25.01	1.25	55.89
14	59.04	59.36	45.9	56.00	34.00	2.00	25.02	1.32	55.89
15	59.39	59.72	45.9	51.47	38.53	6.53	24.88	1.39	55.89
16	60.10	60.44	45.9	47.01	42.99	10.99	24.59	1.44	55.89

FIG. 4A5

13/116

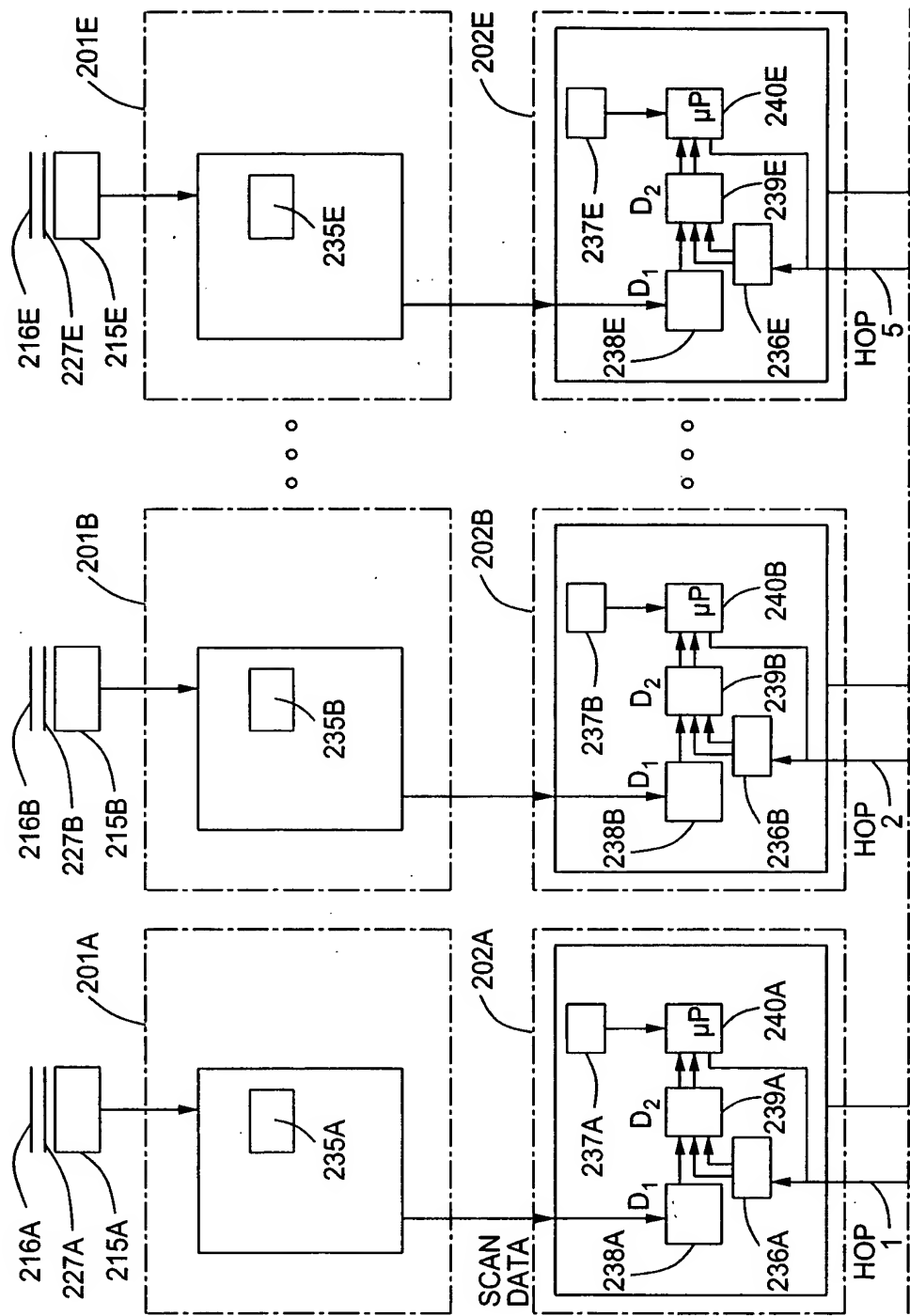


FIG. 5A

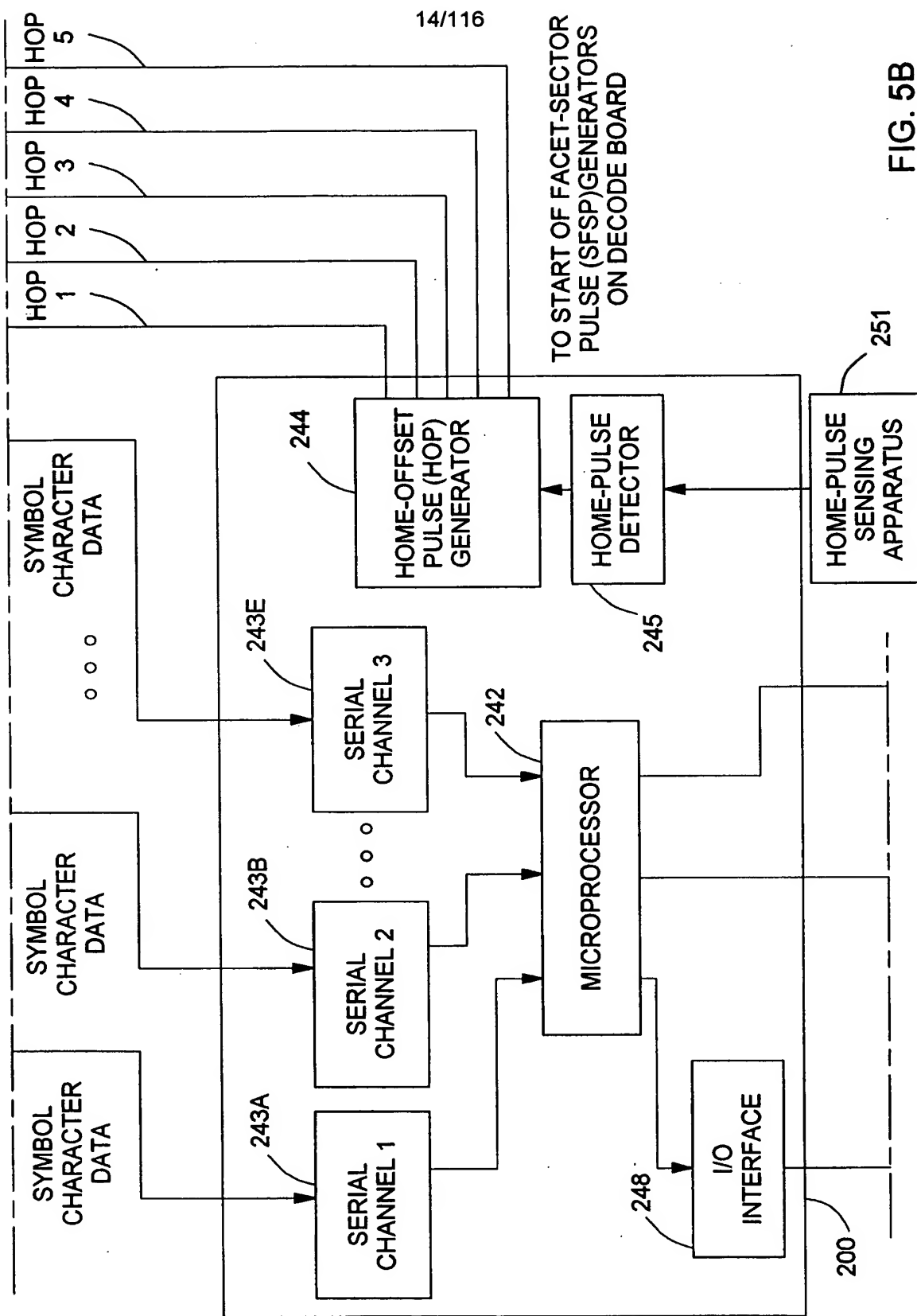


FIG. 5B

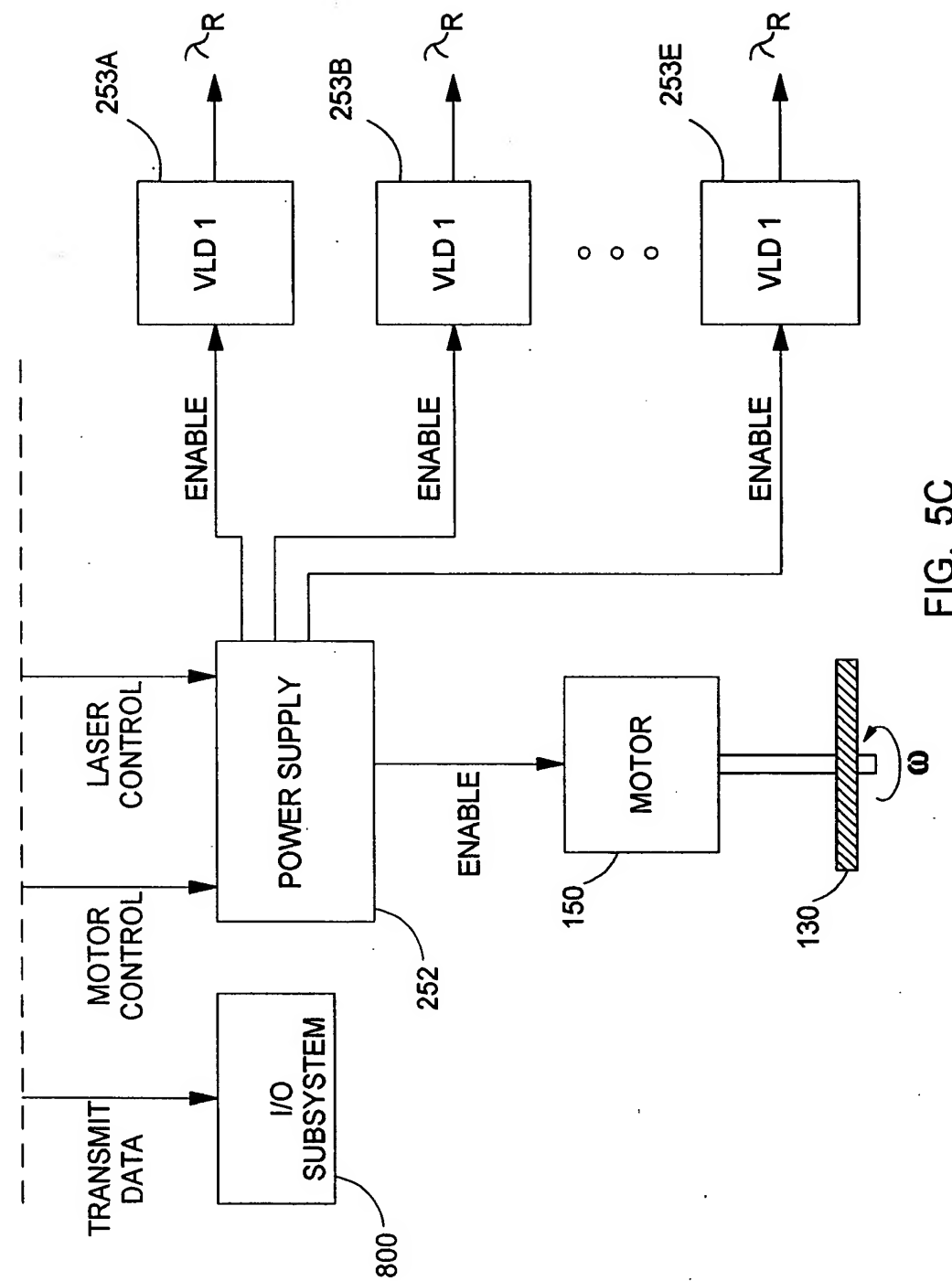


FIG. 5C

16/116

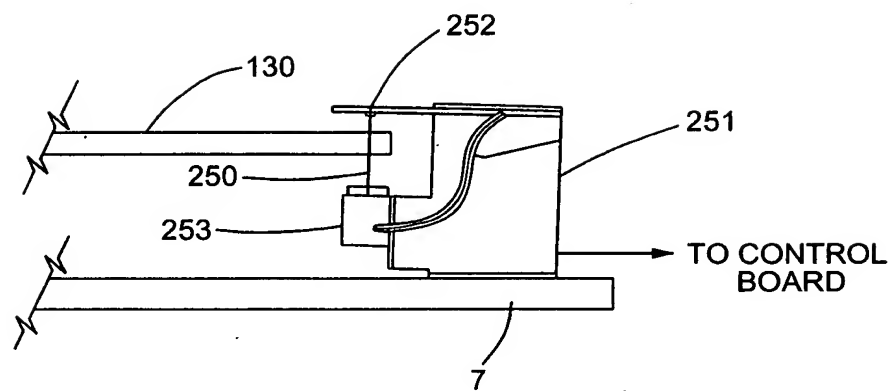


FIG. 6A

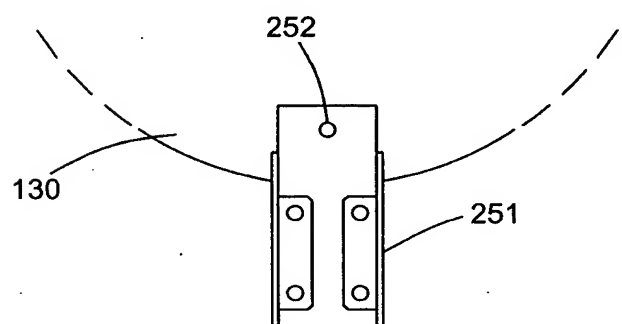


FIG. 6B

17/116

245

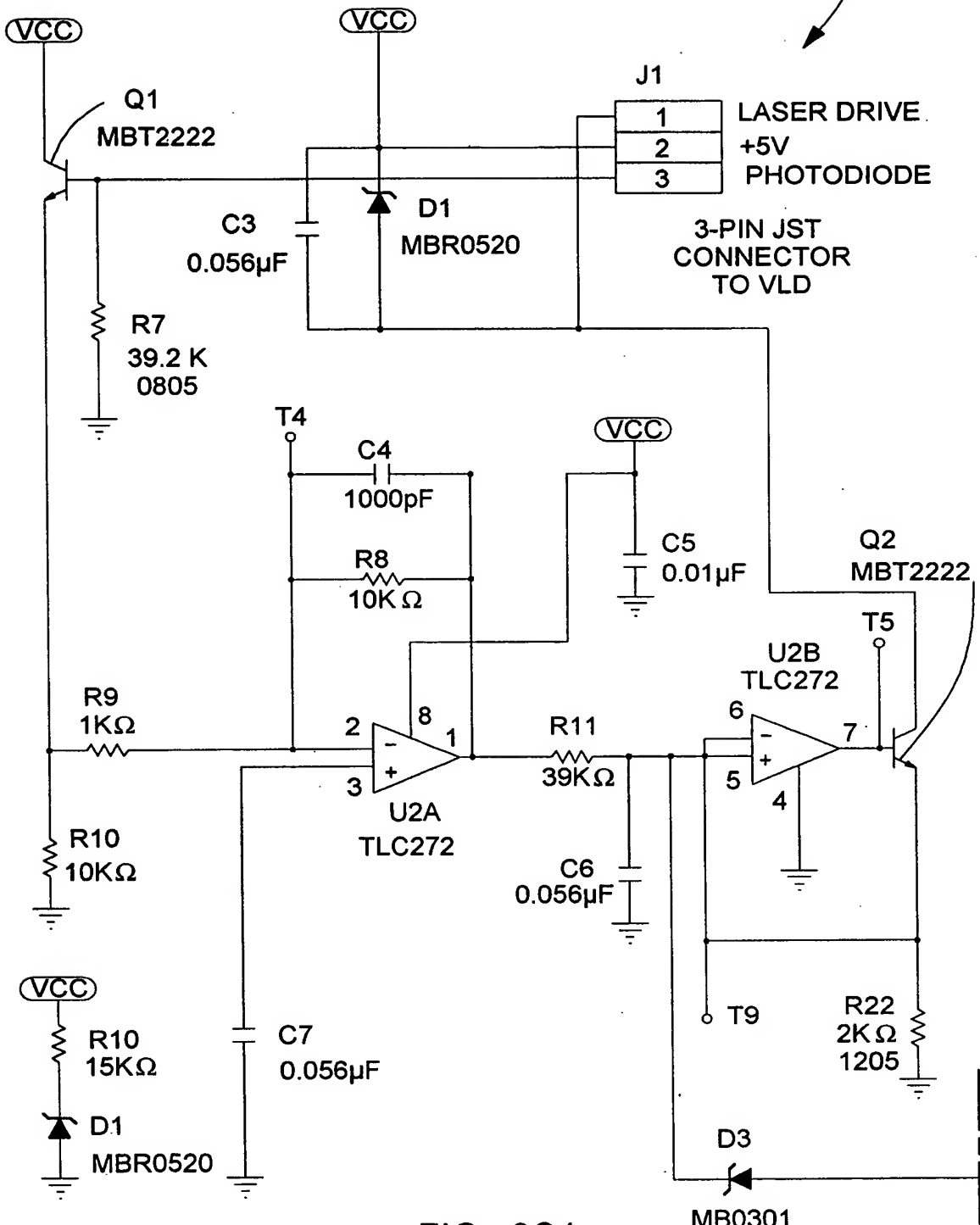


FIG. 6C1

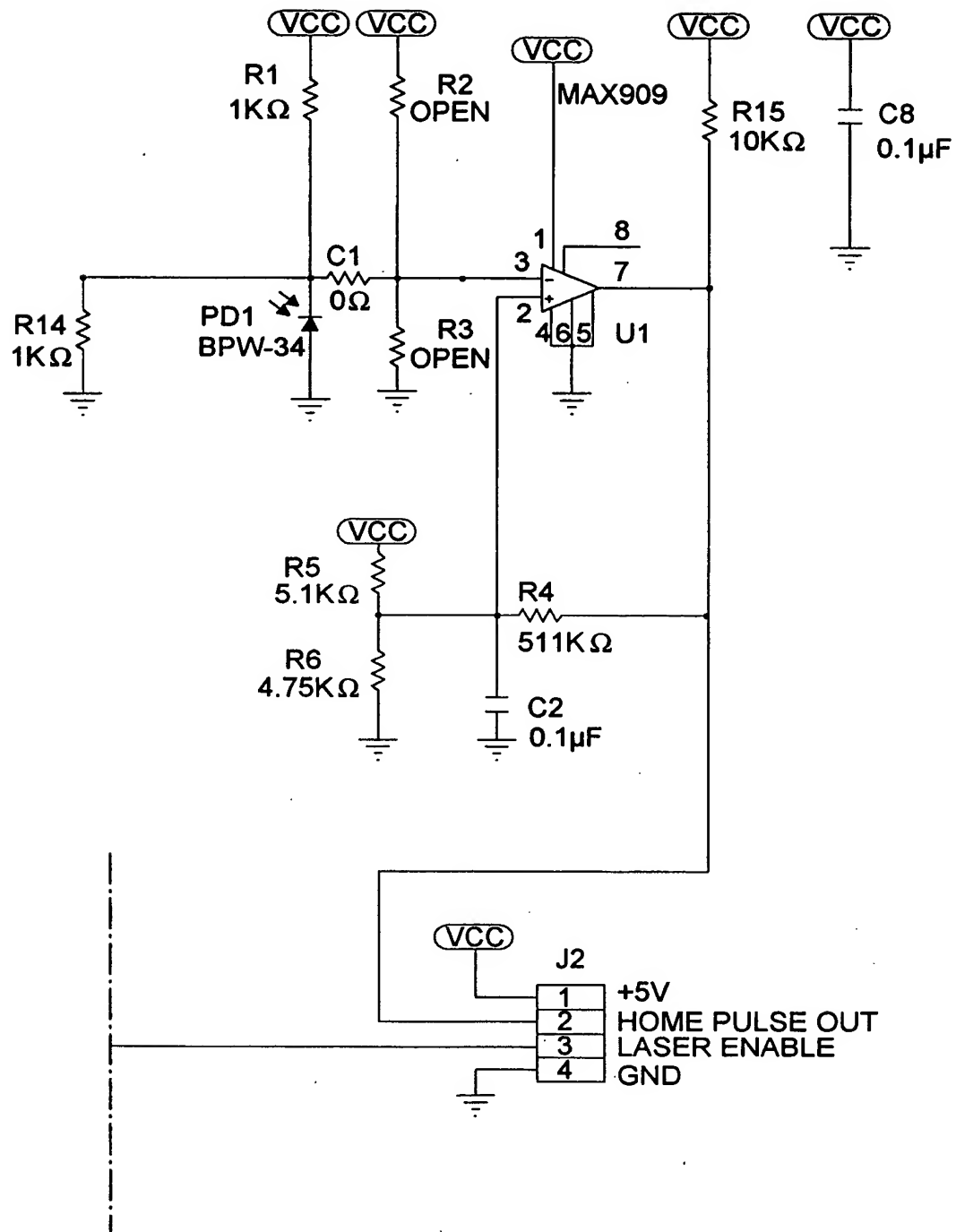


FIG. 6C2

19/116

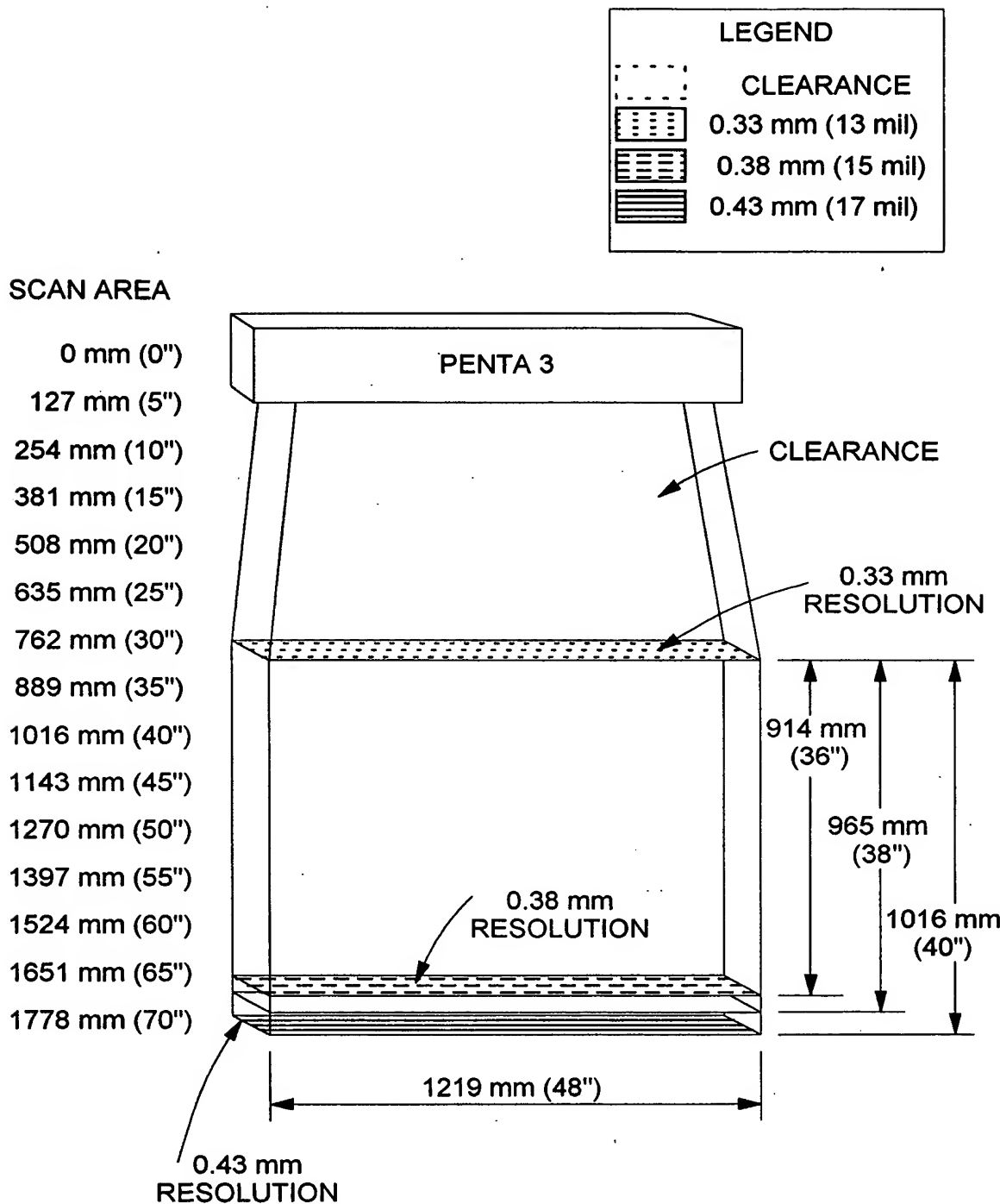


FIG. 7A

20/116

LEGEND	
	CLEARANCE
	0.33 mm (13 mil)
	0.38 mm (15 mil)
	0.43 mm (17 mil)

SCAN AREA

0 mm (0")
127 mm (5")
254 mm (10")
381 mm (15")
508 mm (20")
635 mm (25")
762 mm (30")
889 mm (35")
1016 mm (40")
1143 mm (45")
1270 mm (50")
1397 mm (55")
1524 mm (60")
1651 mm (65")
1778 mm (70")

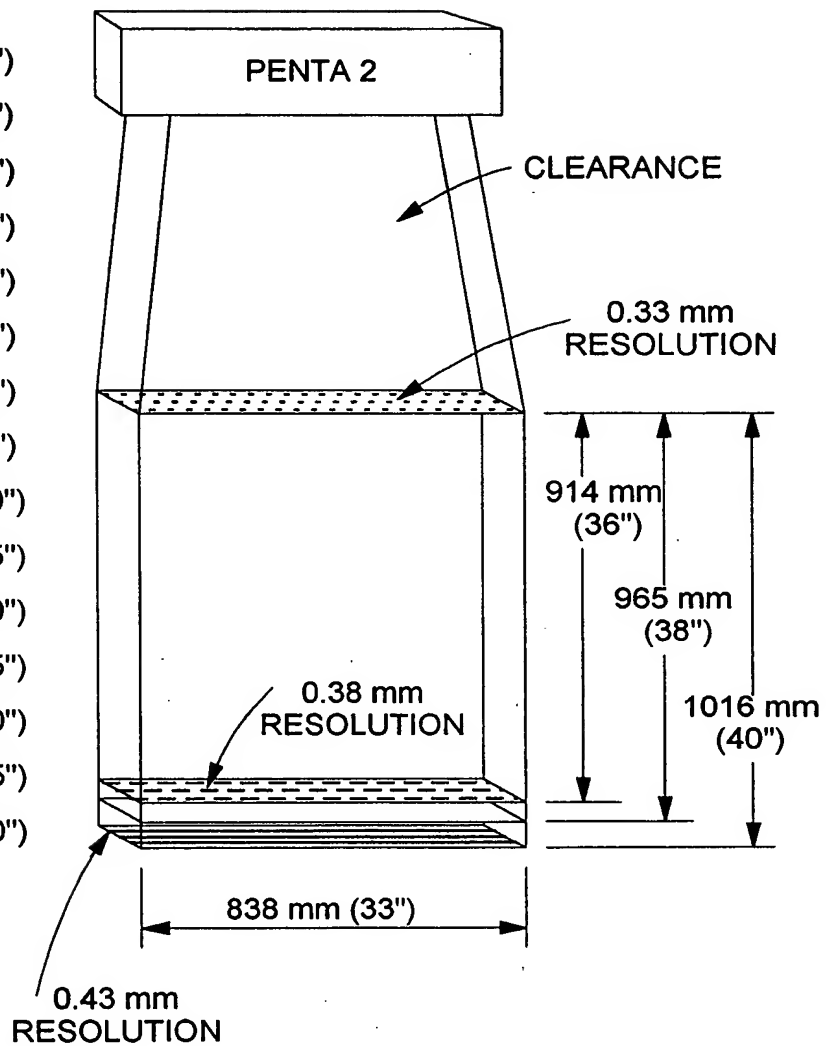


FIG. 7B

21/116

LEGEND	
	CLEARANCE
	0.33 mm (13 mil)
	0.38 mm (15 mil)
	0.43 mm (17 mil)

SCAN AREA

0 mm (0")

127 mm (5")

254 mm (10")

381 mm (15")

508 mm (20")

635 mm (25")

762 mm (30")

889 mm (35")

1016 mm (40")

1143 mm (45")

1270 mm (50")

1397 mm (55")

1524 mm (60")

1651 mm (65")

1778 mm (70")

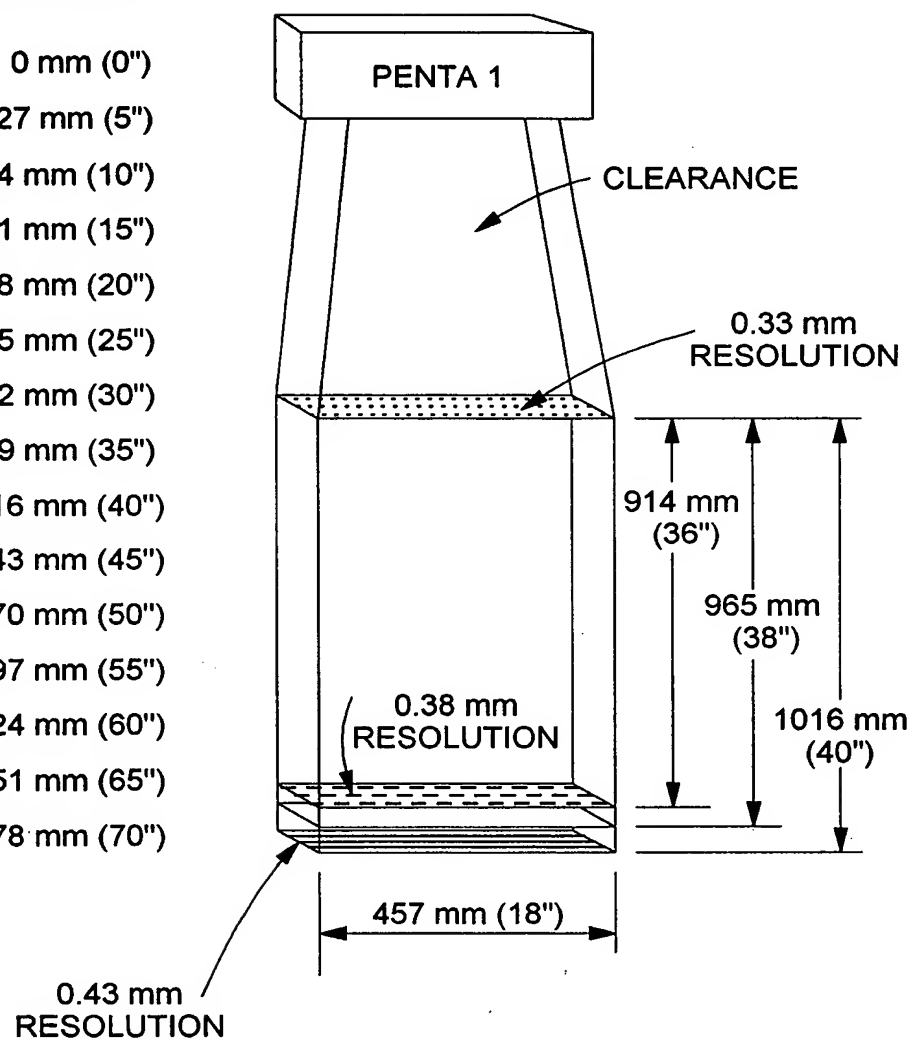


FIG. 7C

SPECIFICATIONS FOR PENTA 1, PENTA 2, PENTA 3 SCANNERS	
OPERATIONAL	
LIGHT SOURCE	5 VISIBLE LASER DIODES 858 + 5mm
LASER POWER	8.4mW (PEAK): LESS THAN 1 mW AVERAGE POWER
DEPTH OF SCAN FIELD	914mm (36") FOR 0.33 mm (13mil) BAR CODES 965mm (38") FOR 0.38 mm (15mil) BAR CODES 1,016mm (40") FOR 0.43 mm (17mil) BAR CODES
WIDTH OF SCAN FIELD	PENTA 1 : 457mm (18") PENTA 2 : 838mm (33") PENTA 3: 1219mm (48")
SCAN SPEED	PENTA 1 : 6,930 SCAN LINES PER SECOND PENTA 2 : 13,860 SCAN LINES PER SECOND PENTA 3 : 20,790 SCAN LINES PER SECOND
SCAN PATTERN	OMNIDIRECTIONAL 5-SIDED PENTAGON SCAN PATTERN PENTA 1: 20 SCAN LINES REPEATED AT FOUR DISTANCES (80 TOTAL) PENTA 2: 40 SCAN LINES REPEATED AT FOUR DISTANCES (160 TOTAL) PENTA 3: 60 SCAN LINES REPEATED AT FOUR DISTANCES (240 TOTAL)
MINIMUM BAR WIDTH	0.33 mm (13mil)
DECODE CAPABILITY	AUTODISCRIMINATES ALL STANDARD BAR CODES
SYSTEM INTERFACES	RS 232. POINT TO POINT. RS422. LIGHT PEN EMULATION
PRINT CONTRAST	35% MINIMUM REFLECTANCE DIFFERENCE
NUMBER OF CHARACTERS READ	UP TO 60 DATA CHARACTERS. (MAXIMUM NUMBER OF CHARACTERS WILL VARY BASED ON SYMBOLOGY AND DENSITY)
ASPECT RATIO	UP TO 2.6 TO 1

FIG. 8

23/156

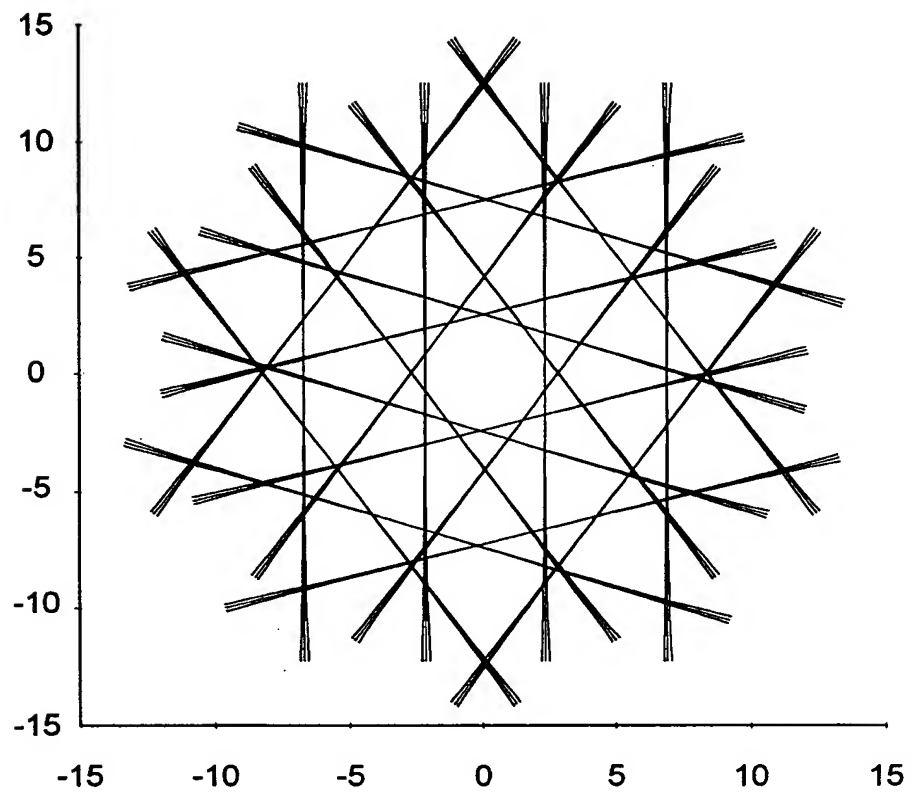


FIG. 9A

24/116

PENTA TRIPLE SCANNER FOCAL PLANE SCAN PATTERN

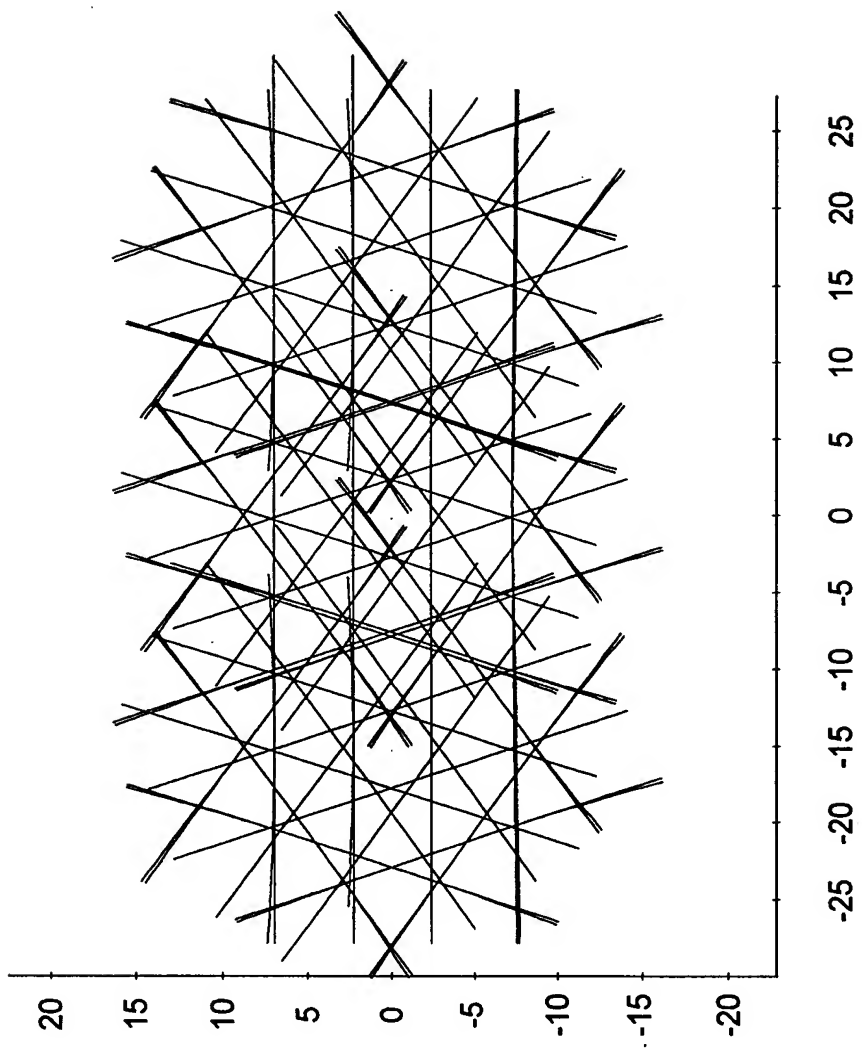


FIG. 9B

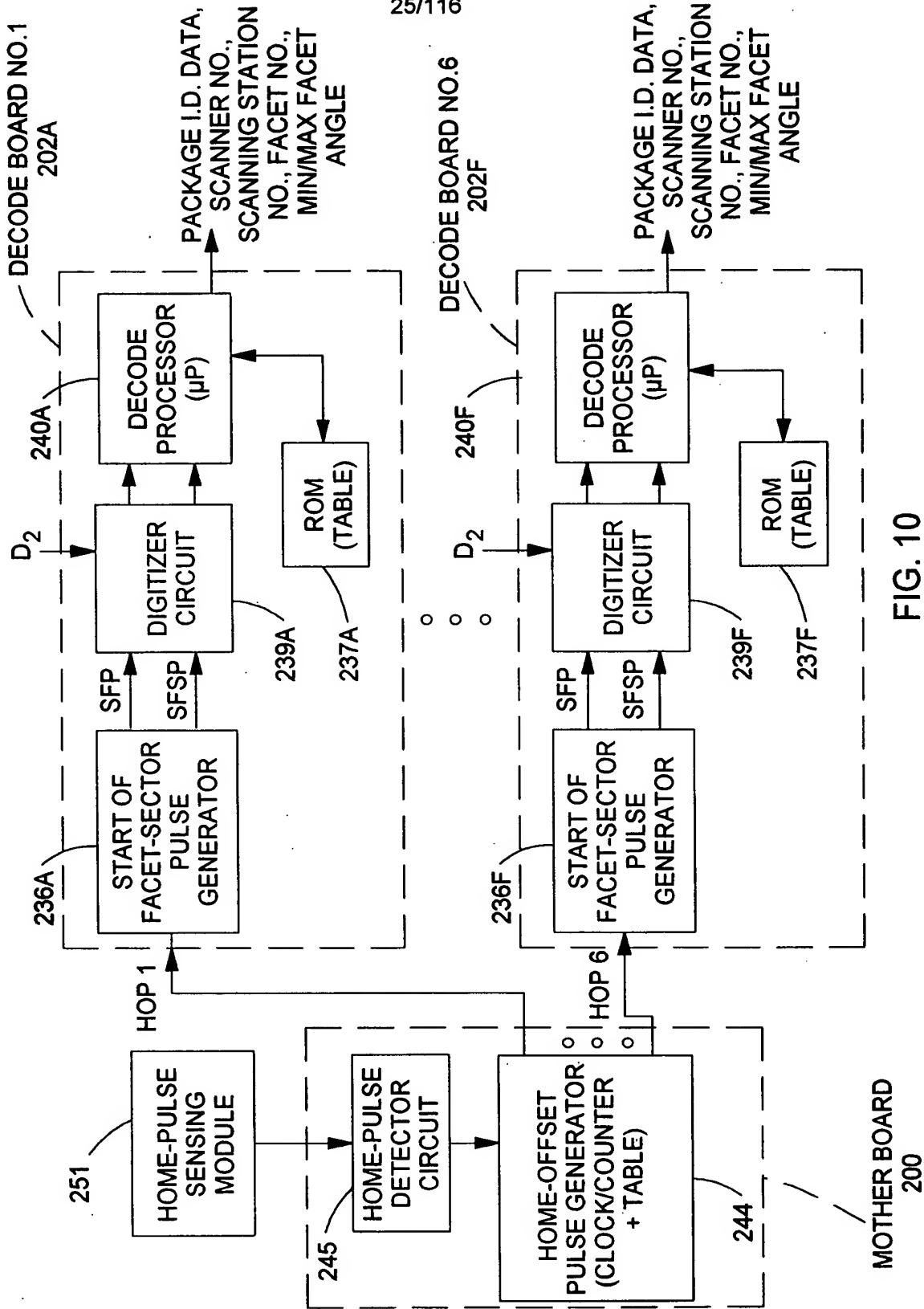


FIG. 10

200

26/116

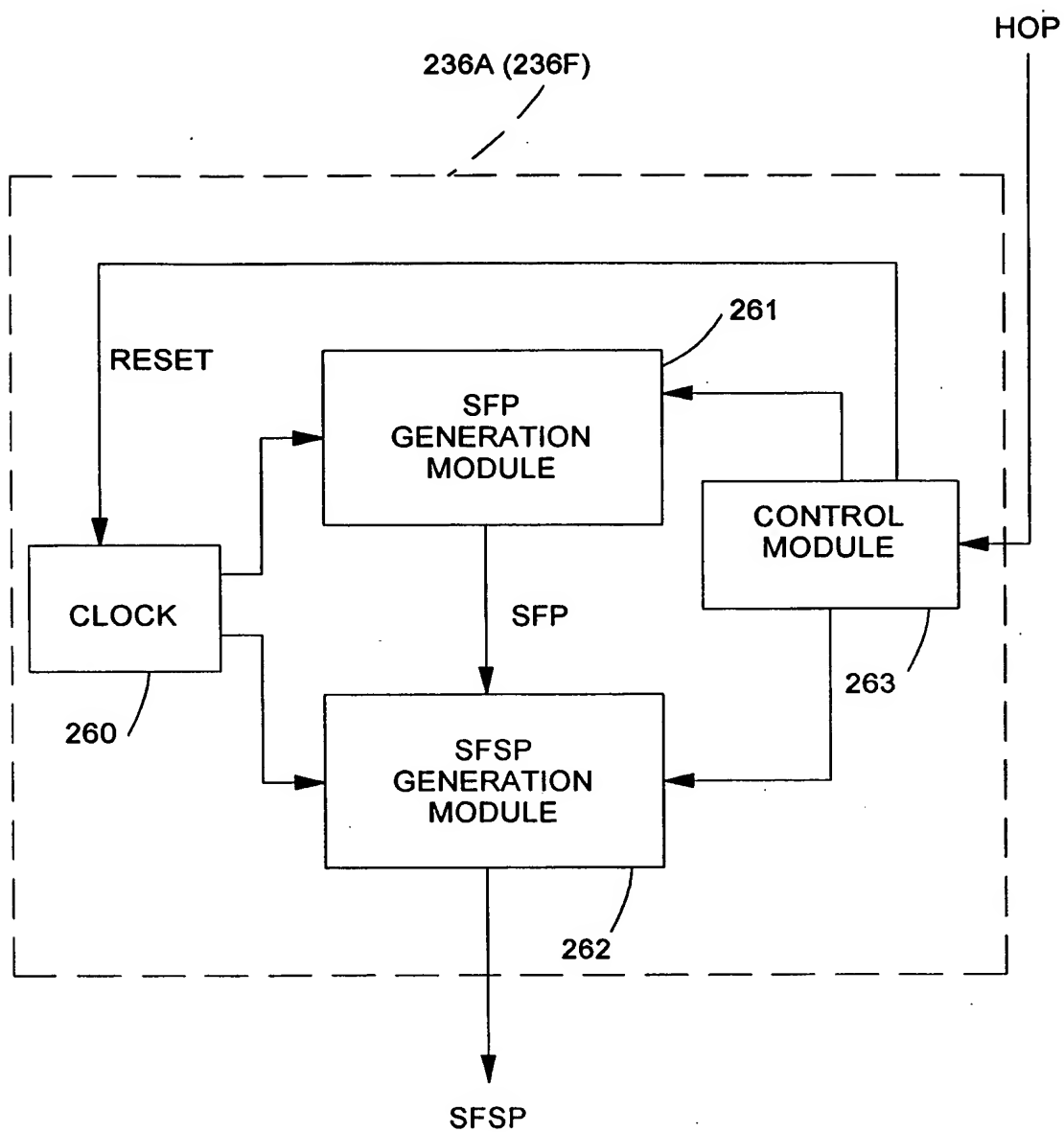


FIG. 10A

27/116

DATA TABLE EMBODIED IN SFP GENERATOR ON DECODE
PROCESSOR BOARD

SCANNING FACET NO.	TRIGGERING EVENT WHEN THE CLOCK PULSE COUNT ATTAINS THE VALUE EQUAL TO THE COUNT VALUE SET FORTH BELOW	PULSE EVENT FROM SFP MODULE
12	7	SF12P
16	146	SF16P
4	271	SF4P
20	4467	SF20P
8	561	SF8P
11	716	SF11P
15	855	SF15P
3	980	SF3P
19	1155	SF19P
7	1270	SF7P
10	1425	SF10P
14	1564	SF14P
2	1689	SF2P
18	1864	SF18P
6	1979	SF6P
9	2134	SF9P
13	2273	SF13P
1	2398	SF1P
17	2573	SF17P
5	2688	SF5P

W = 5200 RPM

CLOCK PULSE WIDTH = 4 μ SEC

FIG. 10B

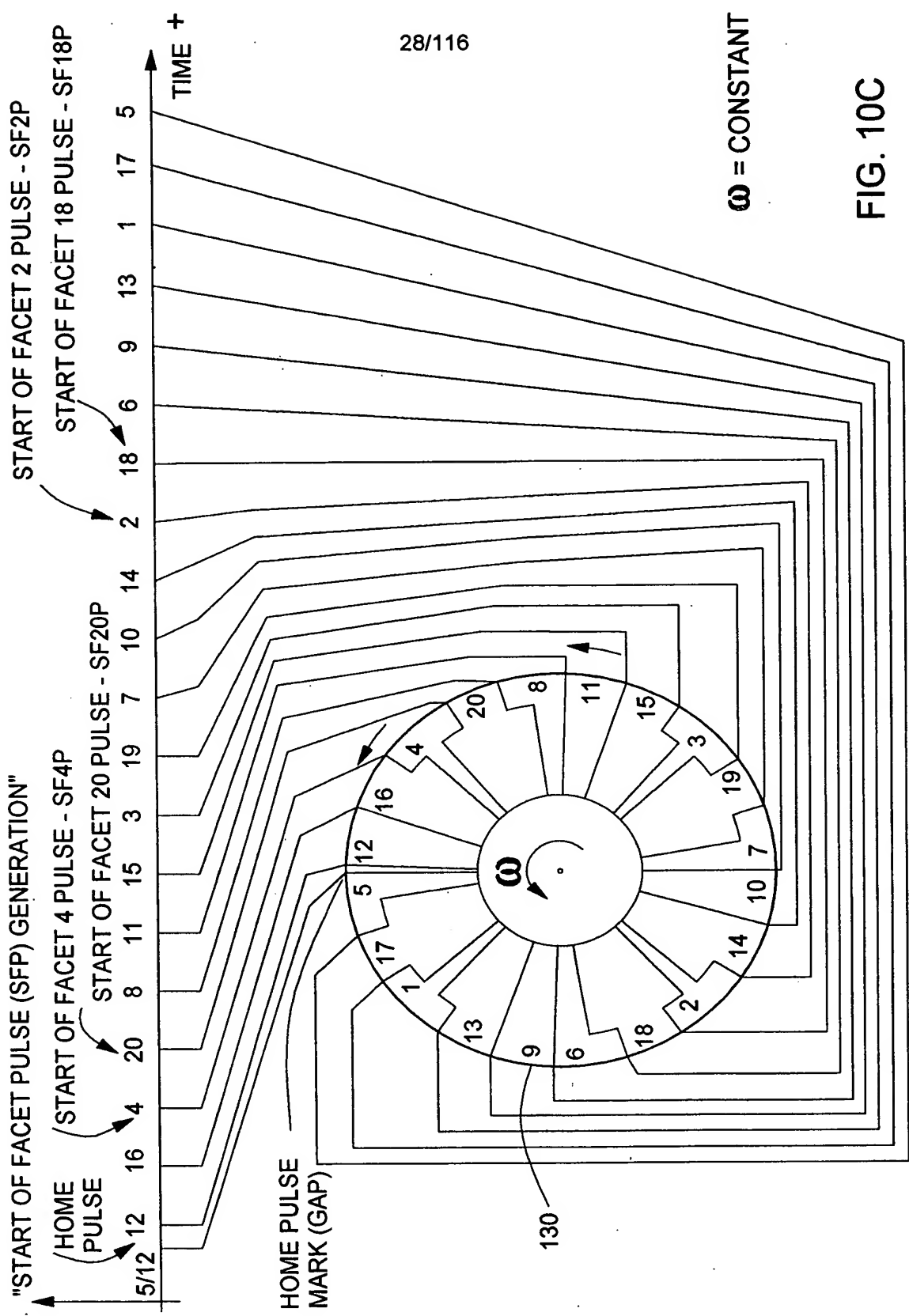


FIG. 10C

29/116

**TABLE EMBODIED IN SFSP GENERATOR DECODE
PROCESSOR BOARD**

SCANNING FACET NO.	SFSP TRIGGERING EVENT	PULSE EVENT FROM SFSP MODULE .
12	RULES 1 - 4 IN FIGS.	SFSP 12/1P SFSP 12/2P SFSP 12/3P SFSP 12/4P
16	RULES 1 - 4 IN FIGS.	SFSP 16/1P SFSP 16/2P SFSP 16/3P SFSP 16/4P
4	RULES 1 - 4 IN FIGS.	SFSP 4/1P SFSP 4/2P SFSP 4/3P SFSP 4/4P
20	RULES 1 - 4 IN FIGS.	SFSP 20/1P SFSP 20/2P SFSP 20/3P SFSP 20/4P
8	RULES 1 - 4 IN FIGS.	SFSP 8/1P SFSP 8/2P SFSP 8/3P SFSP 8/4P
11	RULES 1 - 4 IN FIGS.	SFSP 11/1P SFSP 11/2P SFSP 11/3P SFSP 11/4P
○ ○ ○		
17	RULES 1 - 4 IN FIGS.	SFSP 17/1P SFSP 17/2P SFSP 17/3P SFSP 17/4P
5	RULES 1 - 4 IN FIGS.	SFSP 5/1P SFSP 5/2P SFSP 5/3P SFSP 5/4P

FIG. 10D

30/116

RULE 1: FOR GENERATING SFSP/1P TYPE PULSES

FOR EACH FACET X BEFORE WHICH IS LOCATED FACET X-1 AND BEYOND WHICH IS LOCATED FACET X+1 (ABOUT THE SCANNING DISC), THE SFSP GENERATION MODULE GENERATES SFSX/1P TYPE PULSES WHEN THE COUNT IS EQUAL TO:

COUNT (SFSP)

RULE 2: FOR GENERATING SFSX/2P TYPE PULSES

FOR EACH FACET X BEFORE WHICH IS LOCATED FACET X-1 AND BEYOND WHICH IS LOCATED FACET X+1 (ABOUT THE SCANNING DISC), THE SFSP GENERATION MODULE GENERATES SFSX/2P TYPE PULSES WHEN THE COUNT IS EQUAL TO:

COUNT (SFSP) +1

$$\frac{\text{COUNT (SFX+1P)} - \text{COUNT (SFXP)}}{4}$$

FIG. 10E1

31/116

RULE 3: FOR GENERATING SFSP/3P TYPE PULSES

FOR EACH FACET X BEFORE WHICH IS LOCATED FACET X-1 AND BEYOND WHICH IS LOCATED FACET X+1 (ABOUT THE SCANNING DISC), THE SFSP GENERATION MODULE GENERATES

SFSX/3 TYPE PULSES WHEN THE COUNT IS EQUAL TO:

$$\text{COUNT (SFSP) } + 2 \left[\frac{\text{COUNT (SFX+1P)} - \text{COUNT (SFXP)}}{4} \right]$$

RULE4: FOR GENERATING SFSX/4P TYPE PULSES

FOR EACH FACET X BEFORE WHICH IS LOCATED FACET X-1 AND BEYOND WHICH IS LOCATED FACET X+1 (ABOUT THE SCANNING DISC), THE SFSP GENERATION MODULE GENERATES SFSX/4 TYPE PULSES WHEN THE COUNT IS EQUAL TO:

$$\text{COUNT (SFSP) } + 3 \left[\frac{\text{COUNT (SFX+1P)} - \text{COUNT (SFXP)}}{4} \right]$$

FIG. 10E2

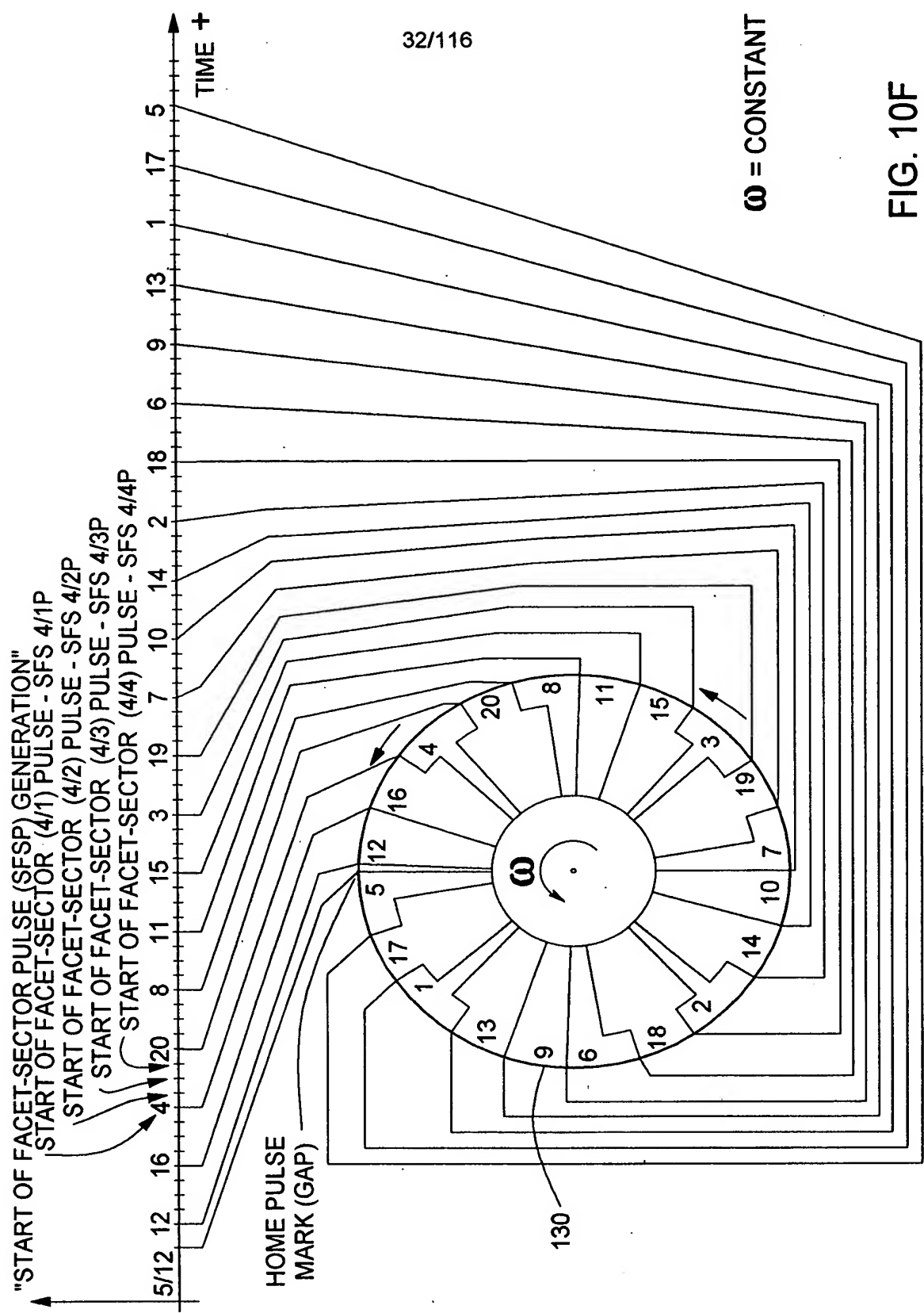
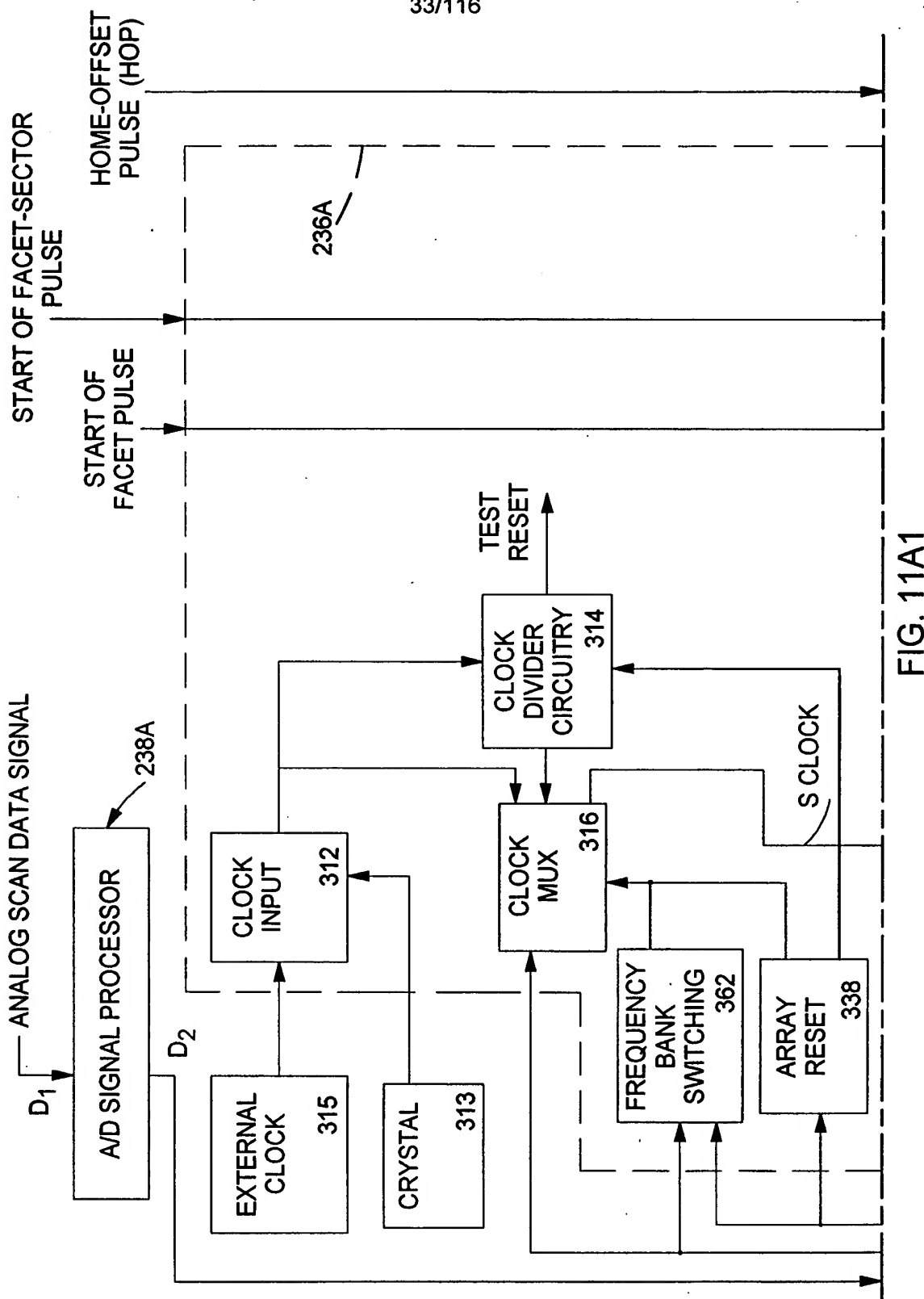


FIG. 10F

33/116



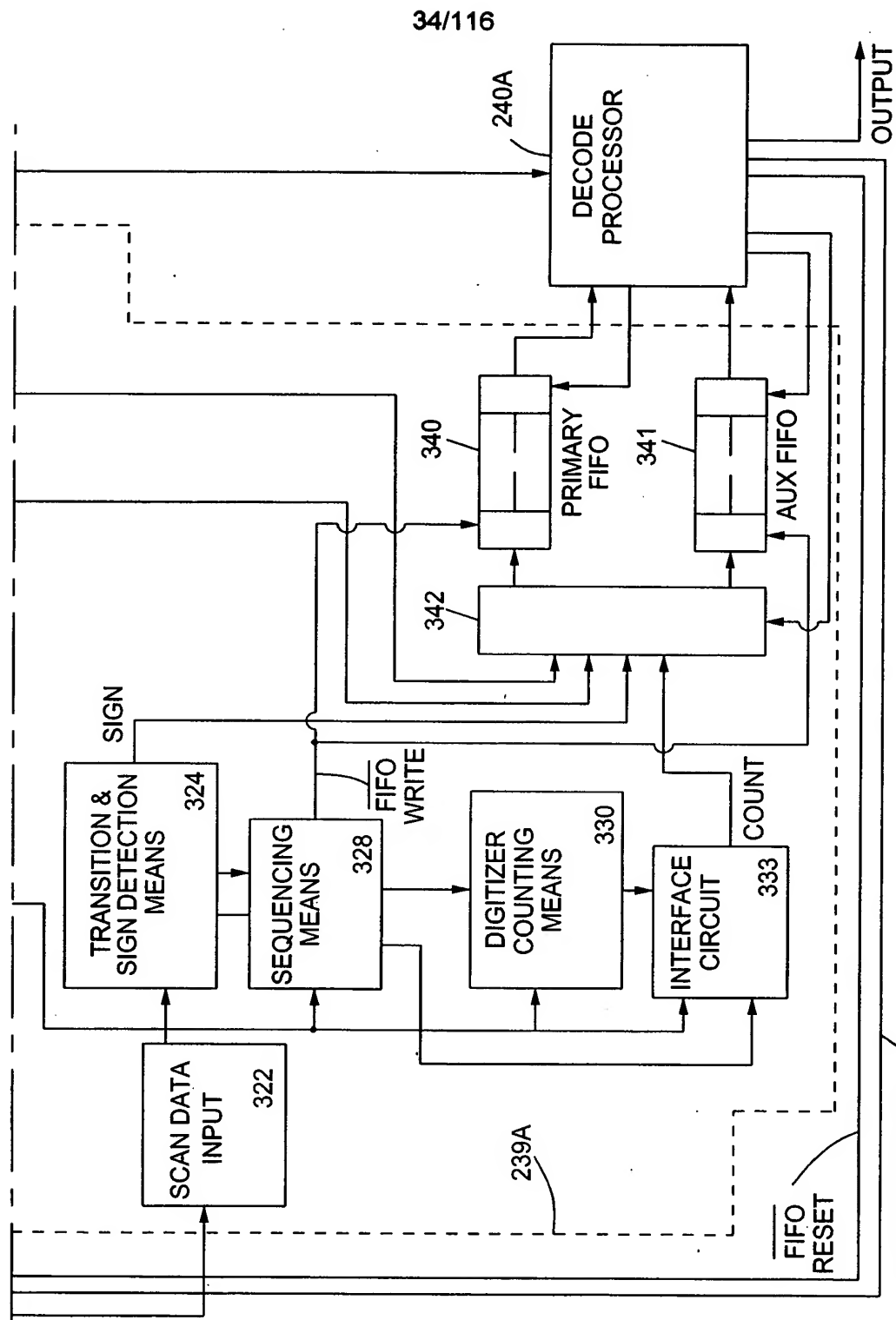
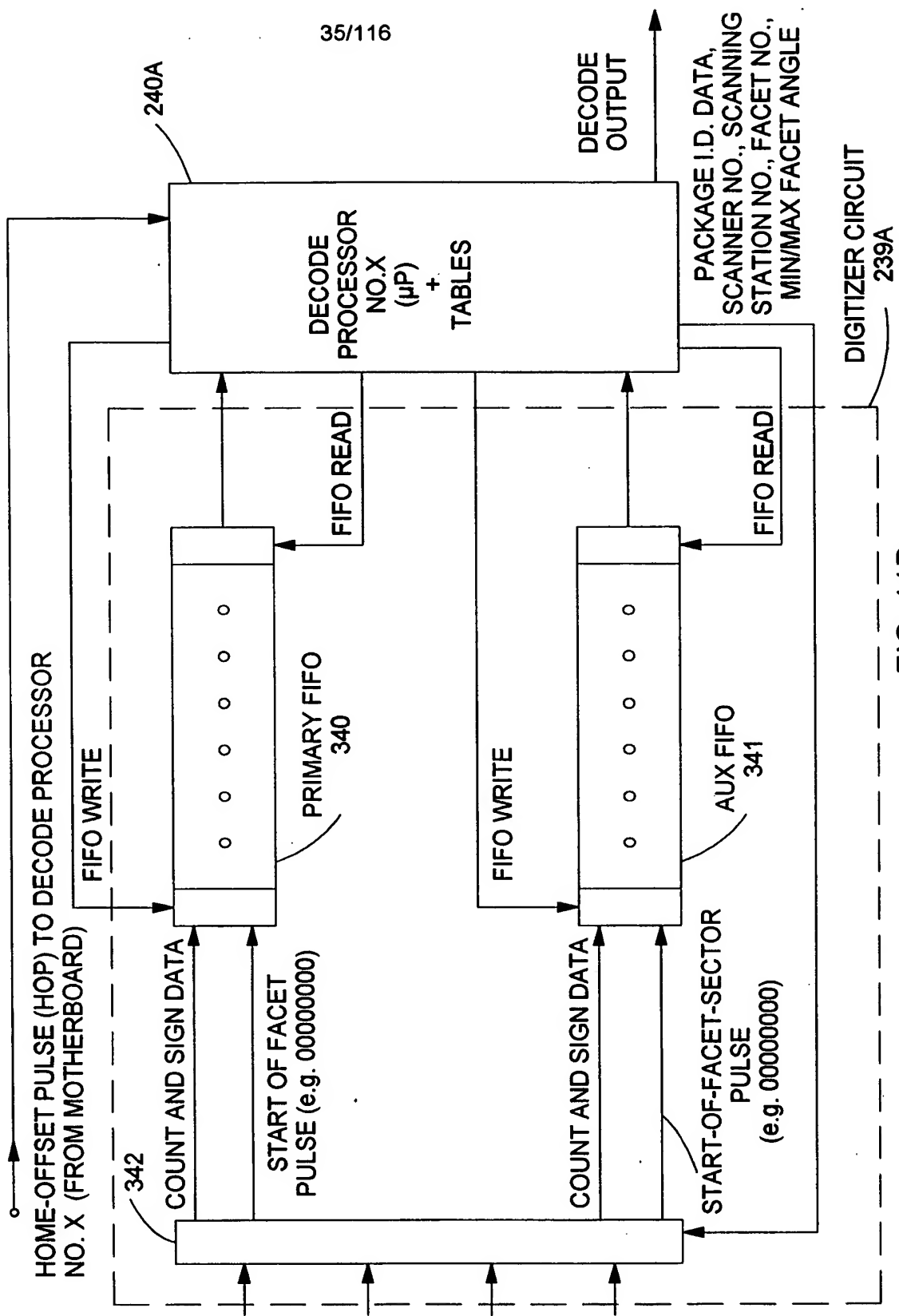


FIG. 11A2



36/116

SCANNER NO.	TOTAL NO. OF FACETS ON DISC
NO. OF SECTORS / FACET	SCANNING STATION NO.

FIG. 11C1

SCANNING FACET NO.	TRIGGERING EVENT WHEN THE CLOCK PULSE COUNT ATTAINS THE VALUE EQUAL TO THE COUNT VALUE SET FORTH BELOW	PULSE EVENT FROM SFP MODULE
12	7	SF12P
16	146	SF16P
4	271	SF4P
20	4467	SF20P
8	561	SF8P
11	716	SF11P
15	855	SF15P
3	980	SF3P
19	1155	SF19P
7	1270	SF7P
10	1425	SF10P
14	1564	SF14P
2	1689	SF2P
18	1864	SF18P
6	1979	SF6P
9	2134	SF9P
13	2273	SF13P
1	2398	SF1P
17	2573	SF17P
5	2688	SF5P

TABLES EMBODIED IN DECODE PROCESSOR

CLOCK PULSE WIDTH = 4 μ SEC

W = 5200 RPM

FIG. 11C2

37/116

TABLE EMBODIED IN DECODE PROCESSOR

			MINIMUM AND MAXIMUM FACET ANGLES CORRESPONDING TO FACET-SECTOR IDENTIFIED BY SFSP EVENT
SCANNING FACET NO.	SFS TRIGGERING EVENT	PULSE EVENT FROM SFSP MODULE .	
12	RULES 1 - 4 IN FIGS.	SFSP 12/1P	$\theta_{ROT\ MIN}, \theta_{ROT\ MAX}$
		SFSP 12/2P	
		SFSP 12/3P	
		SFSP 12/4P	
16	RULES 1 - 4 IN FIGS.	SFSP 16/1P	
		SFSP 16/2P	
		SFSP 16/3P	
		SFSP 16/4P	
4	RULES 1 - 4 IN FIGS.	SFSP 4/1P	
		SFSP 4/2P	
		SFSP 4/3P	
		SFSP 4/4P	
20	RULES 1 - 4 IN FIGS.	SFSP 20/1P	
		SFSP 20/2P	
		SFSP 20/3P	
		SFSP 20/4P	
8	RULES 1 - 4 IN FIGS.	SFSP 8/1P	
		SFSP 8/2P	
		SFSP 8/3P	
		SFSP 8/4P	
11	RULES 1 - 4 IN FIGS.	SFSP 11/1P	
		SFSP 11/2P	
		SFSP 11/3P	
		SFSP 11/4P	
o o o			
17	RULES 1 - 4 IN FIGS.	SFSP 17/1P	
		SFSP 17/2P	
		SFSP 17/3P	
		SFSP 17/4P	
5	RULES 1 - 4 IN FIGS.	SFSP 5/1P	
		SFSP 5/2P	
		SFSP 5/3P	
		SFSP 5/4P	

FIG. 11D

38/116

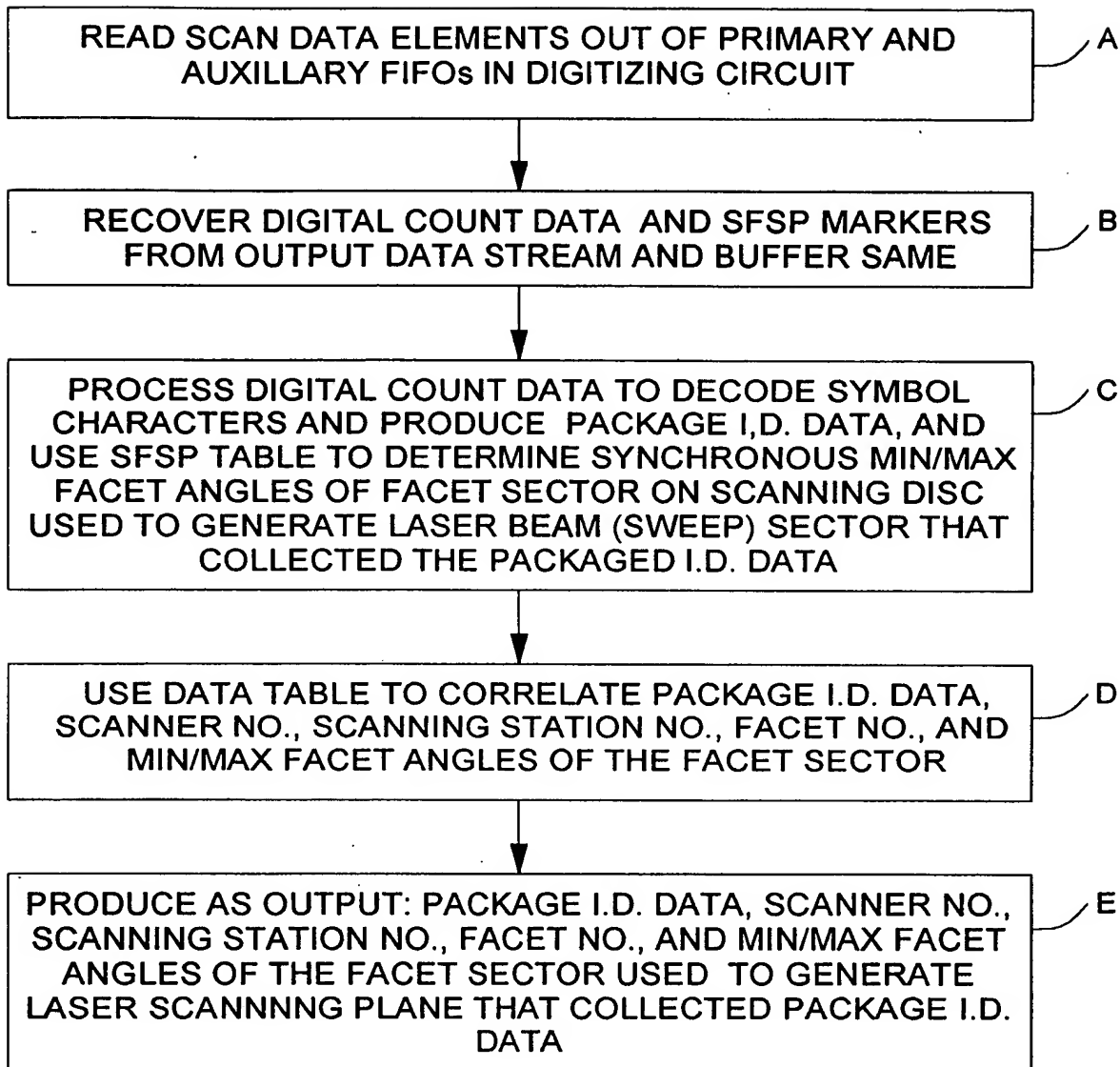


FIG. 11E

39/116

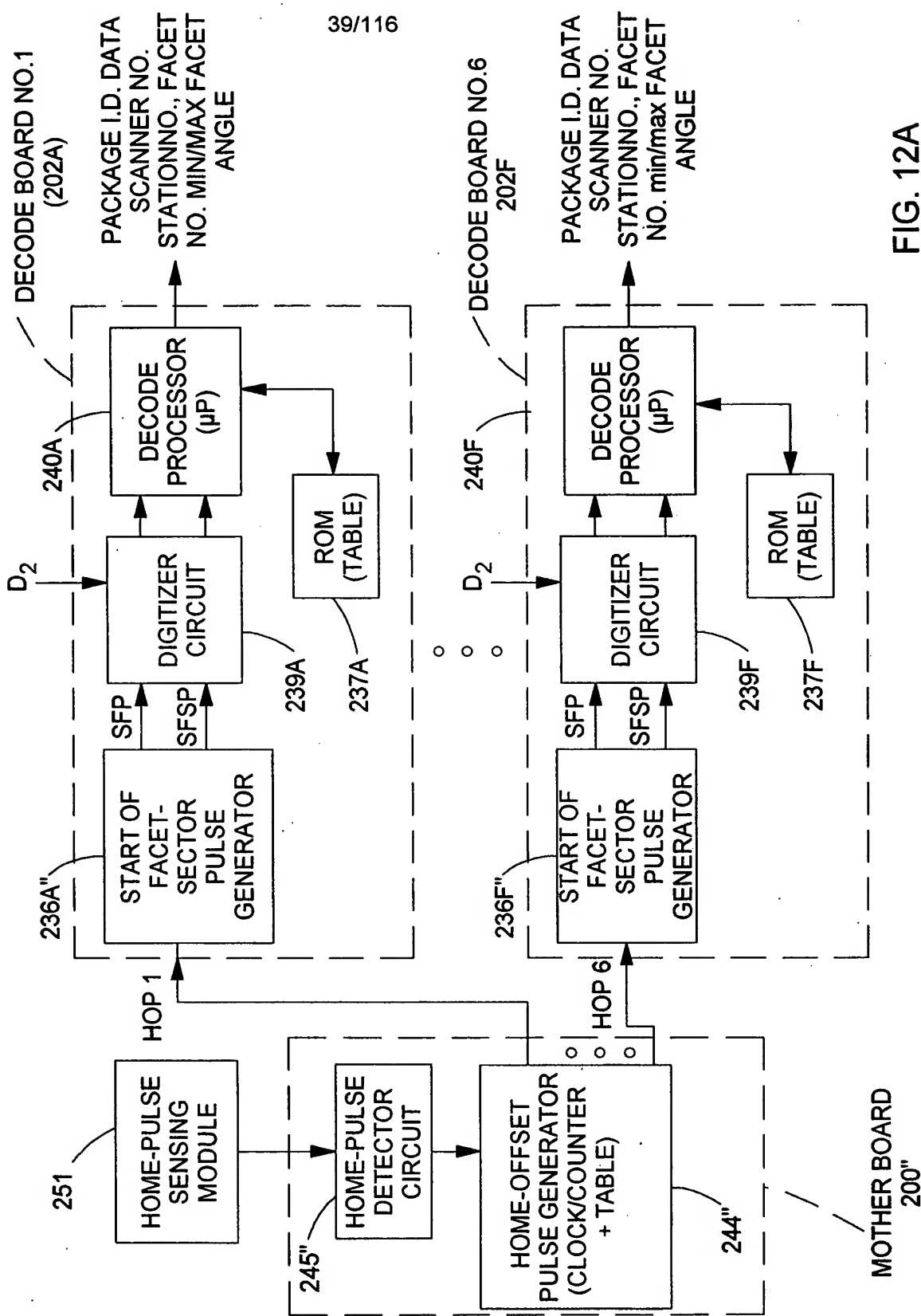


FIG. 12A

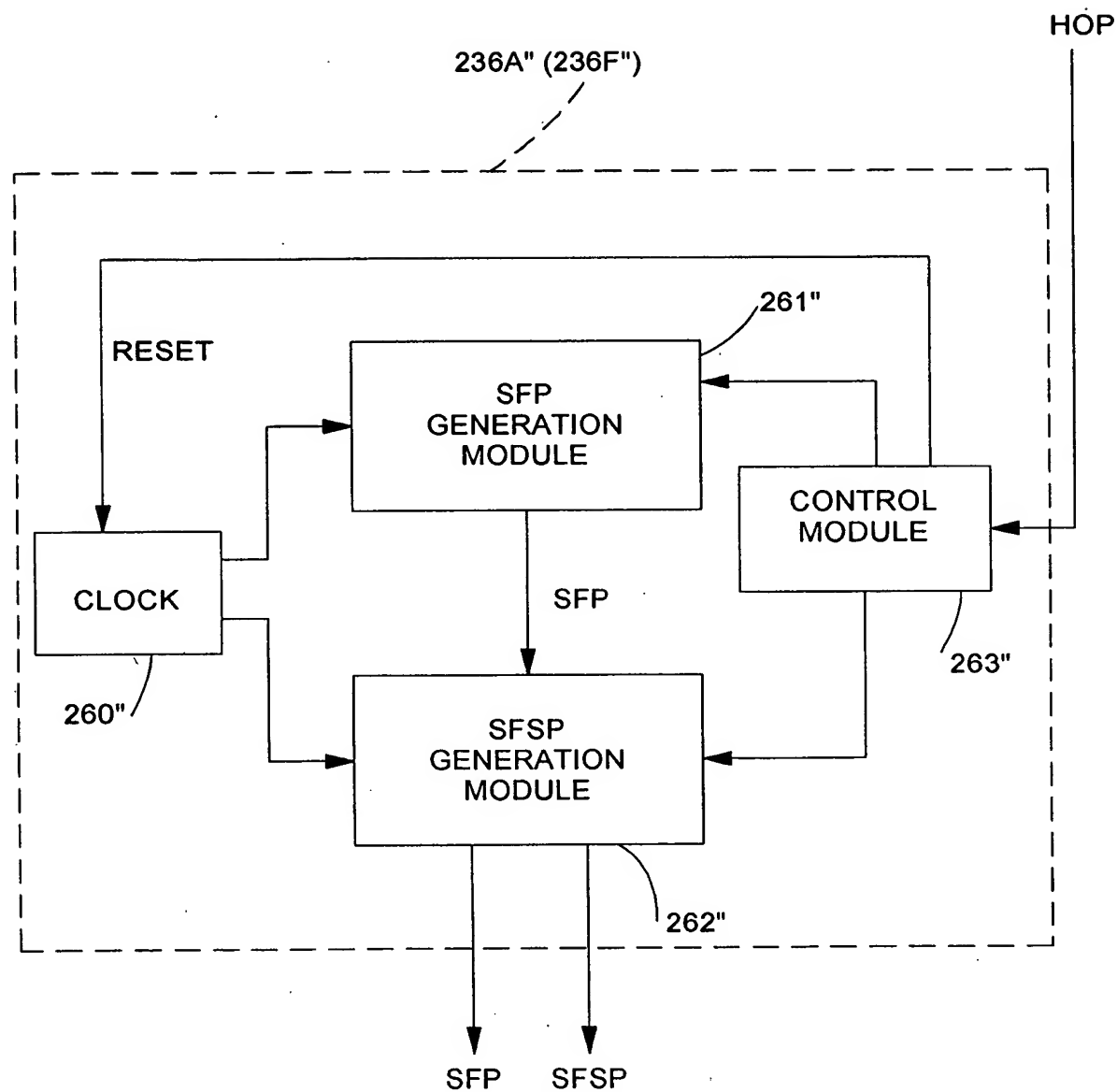


FIG. 12B

41/116

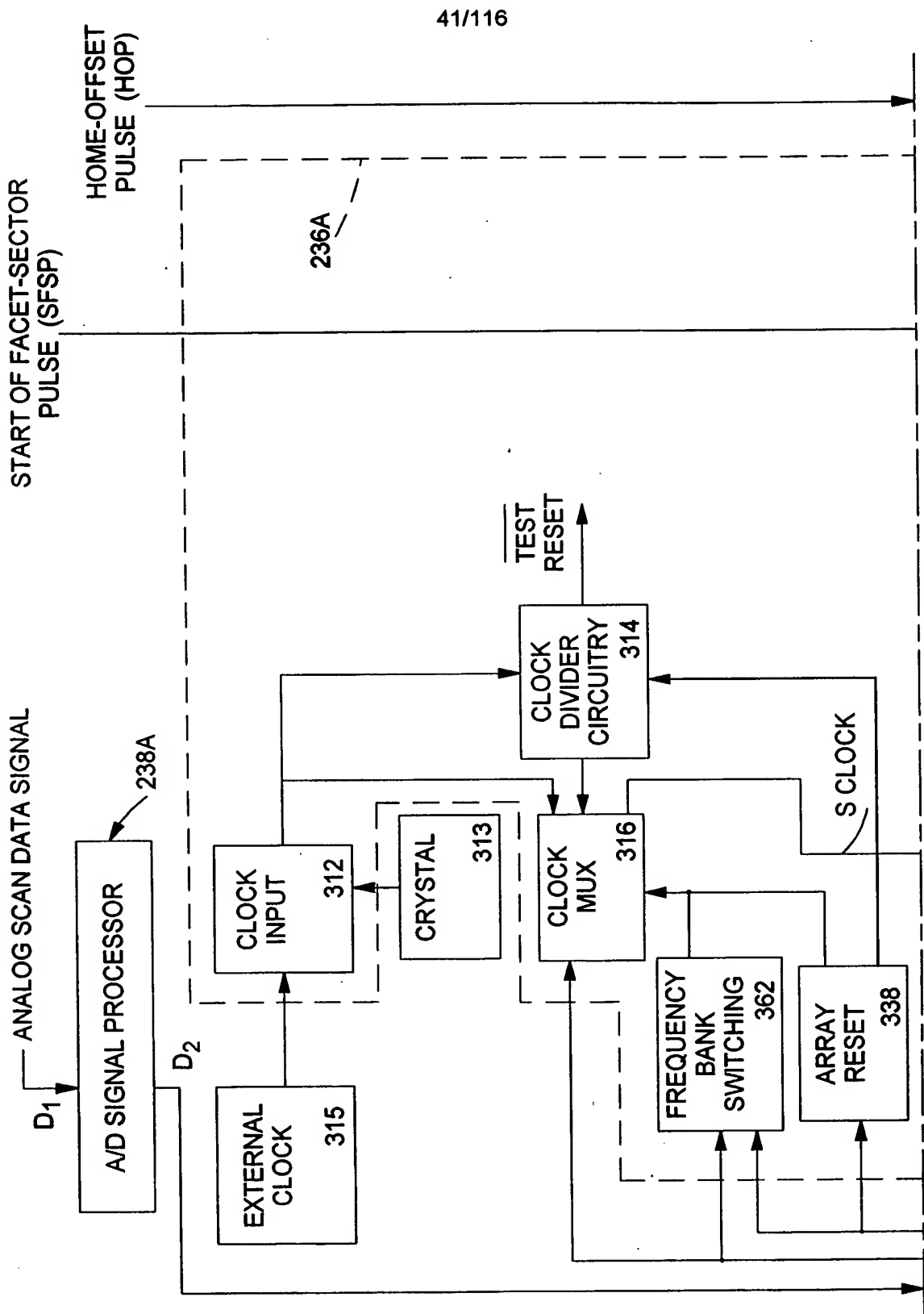


FIG. 13A1

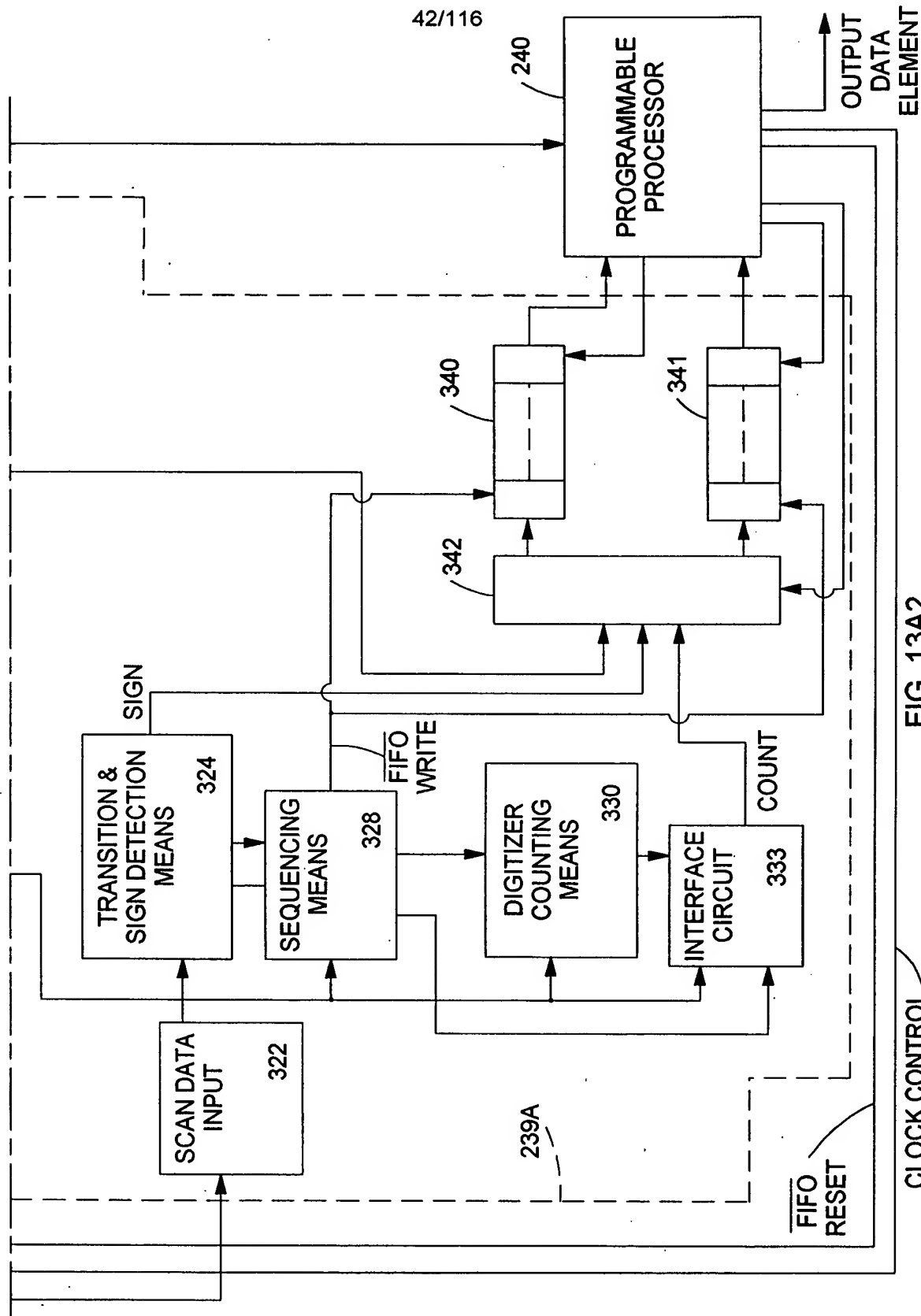


FIG. 13A2

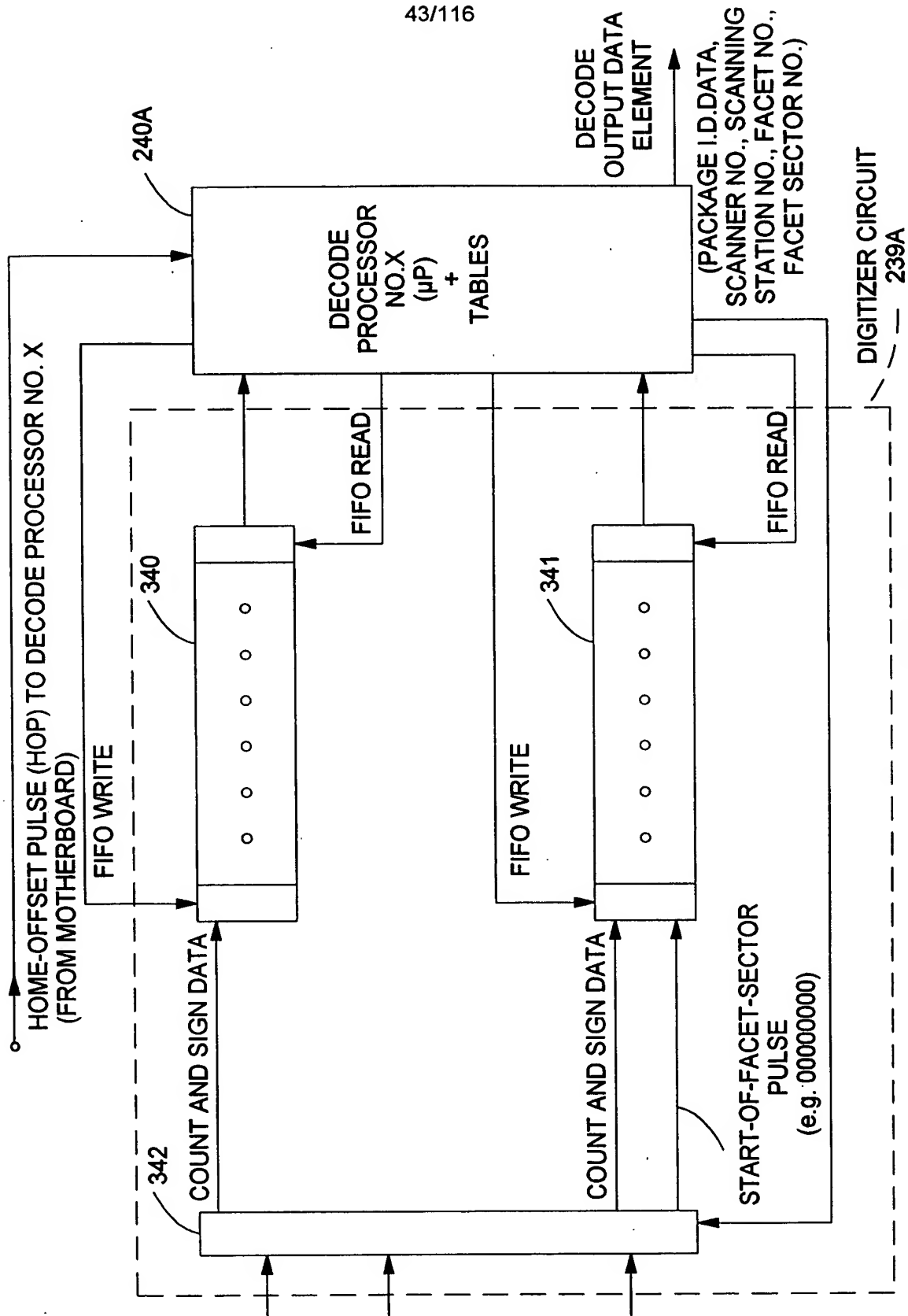


FIG. 13B

44/116

HOP GENERATION ALGORITHM

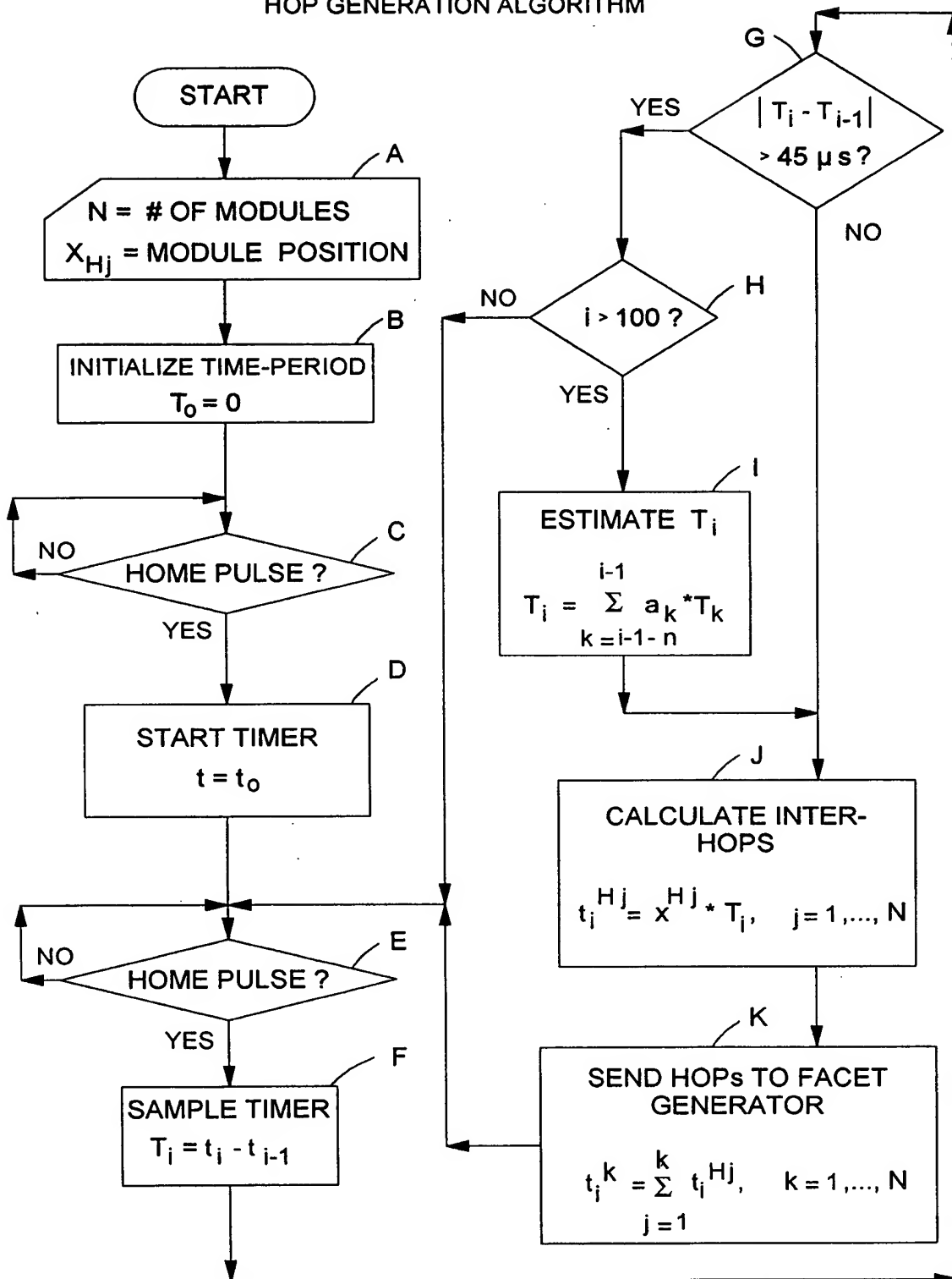


FIG. 14A

45/116

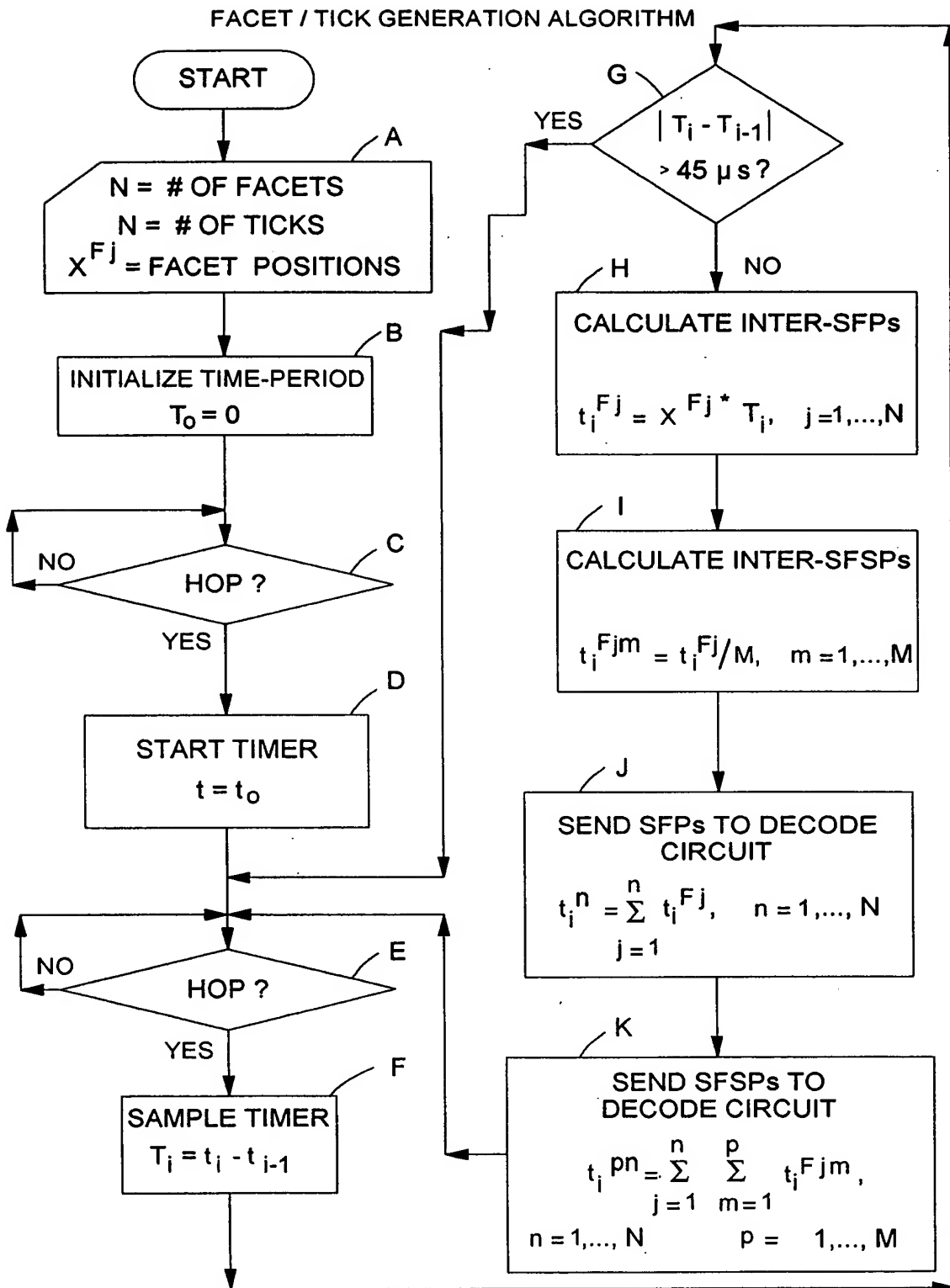
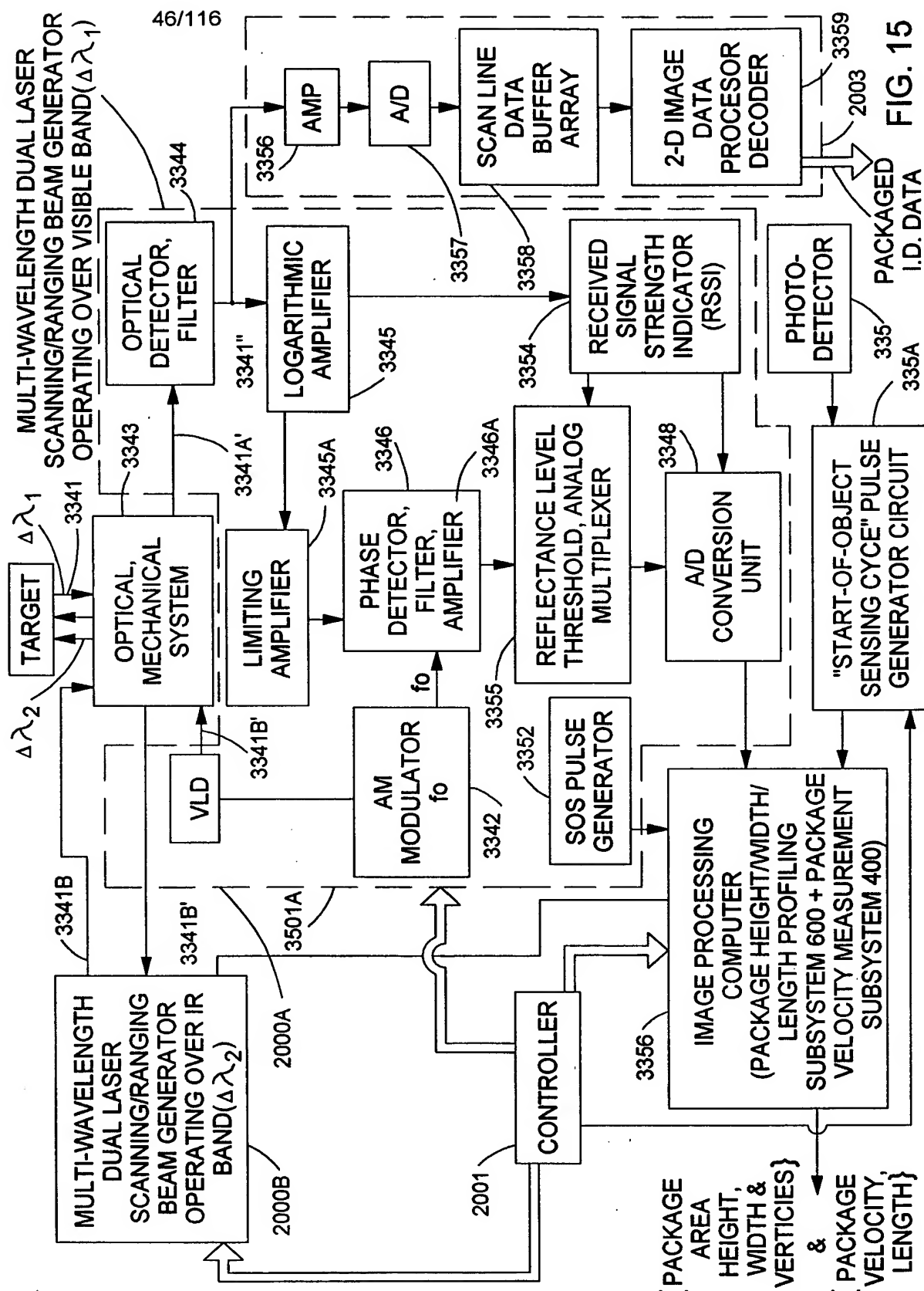


FIG. 14B



47/116

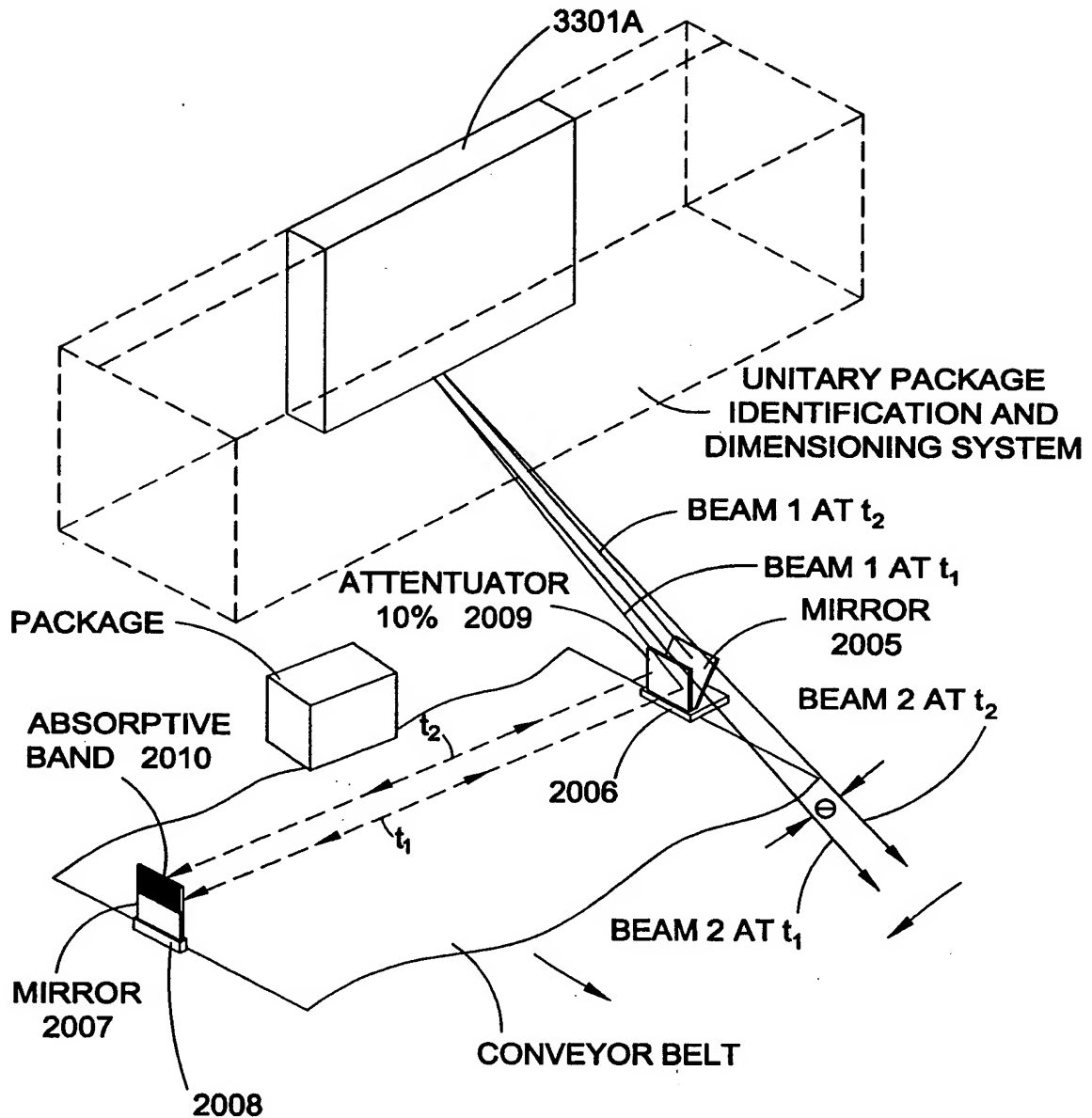


FIG. 15A

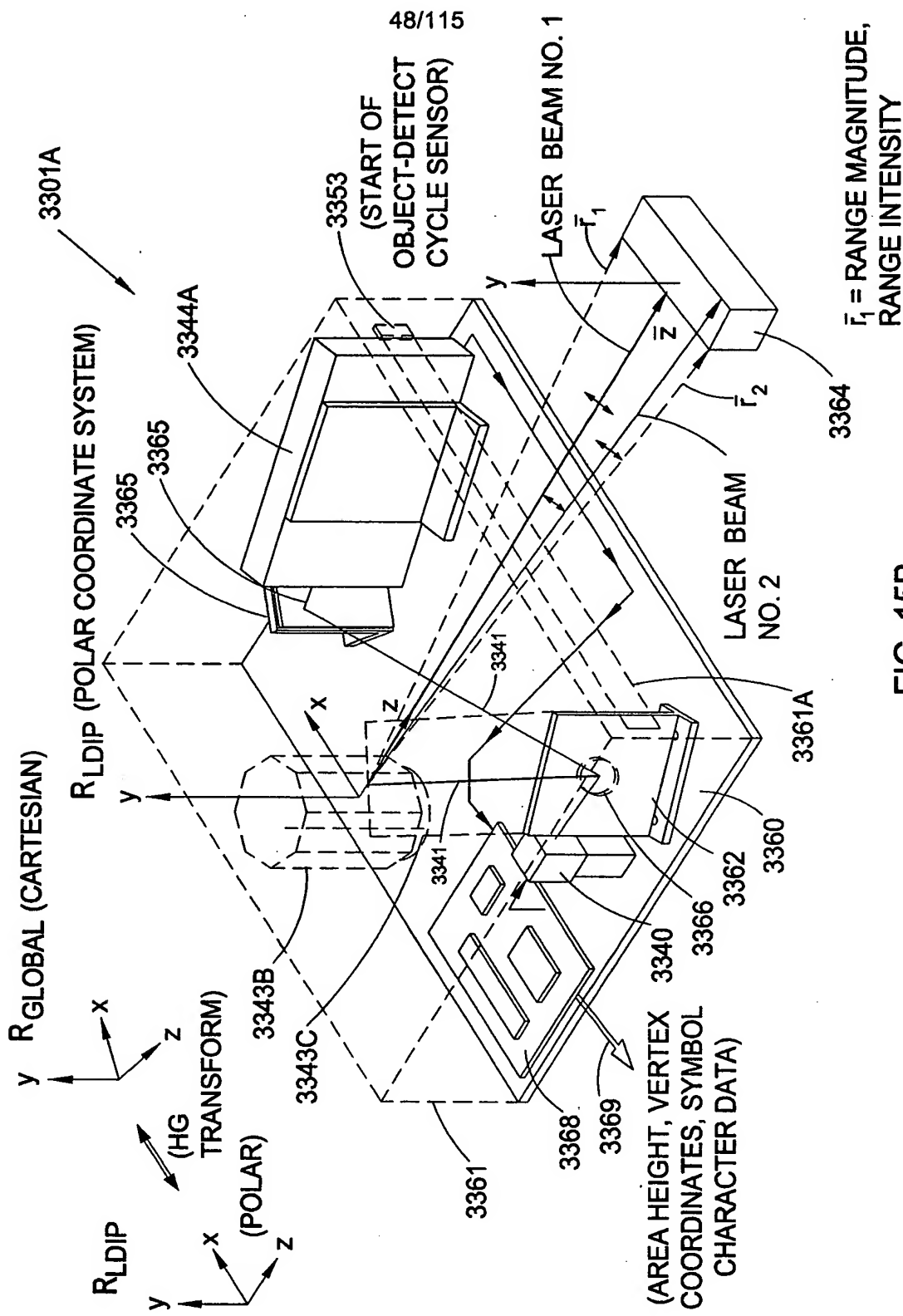


FIG. 15B

49/116

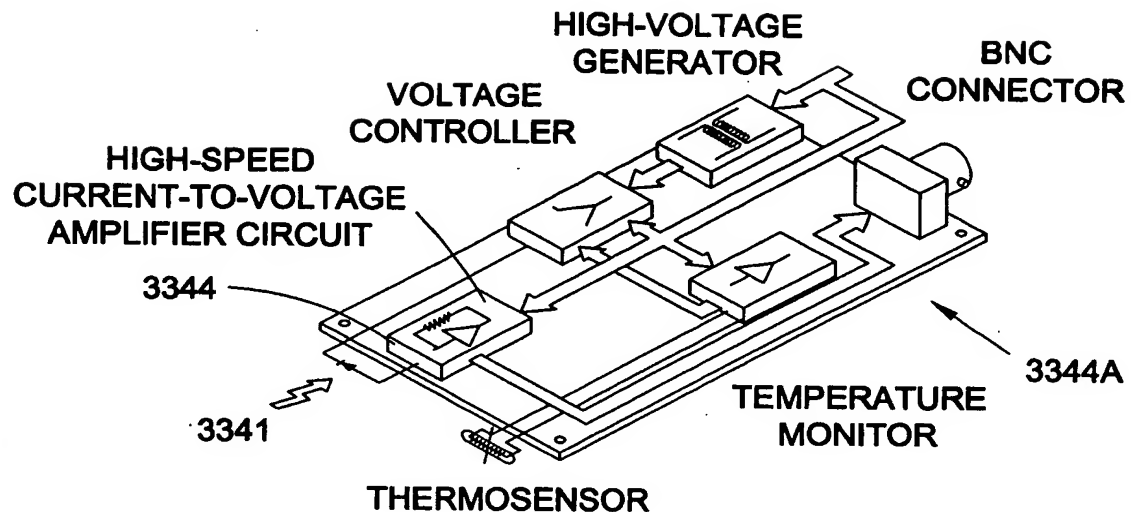


FIG. 15C

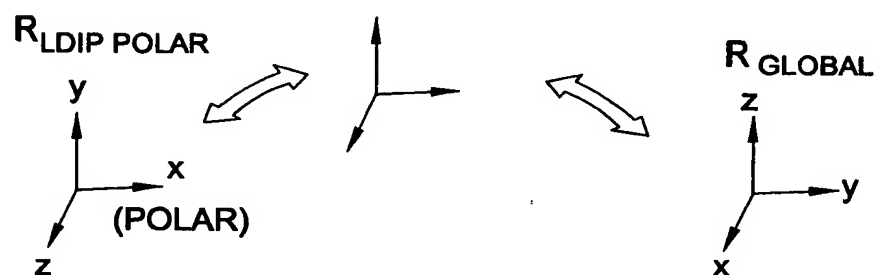
 R_{LDIP} CARTESIAN

FIG. 15D

50/116

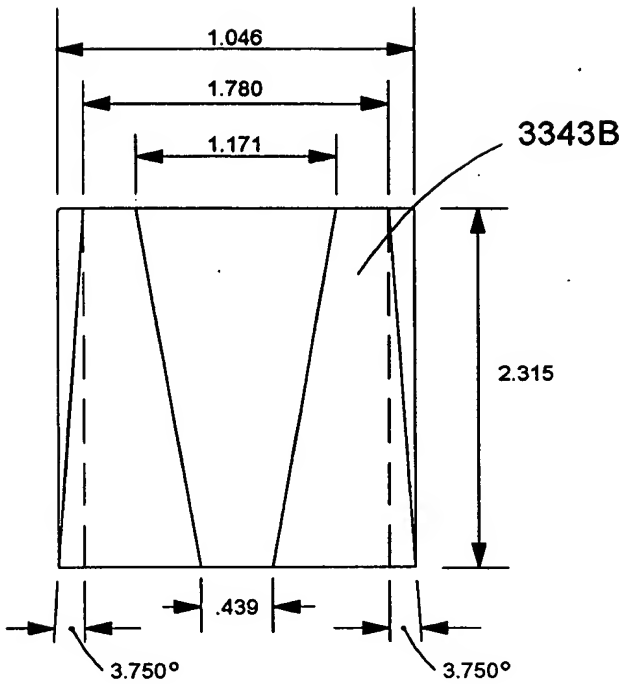


FIG. 15E1

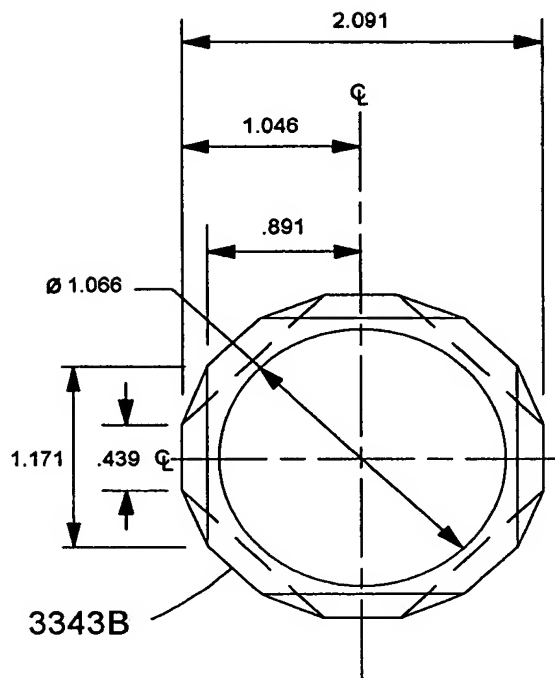


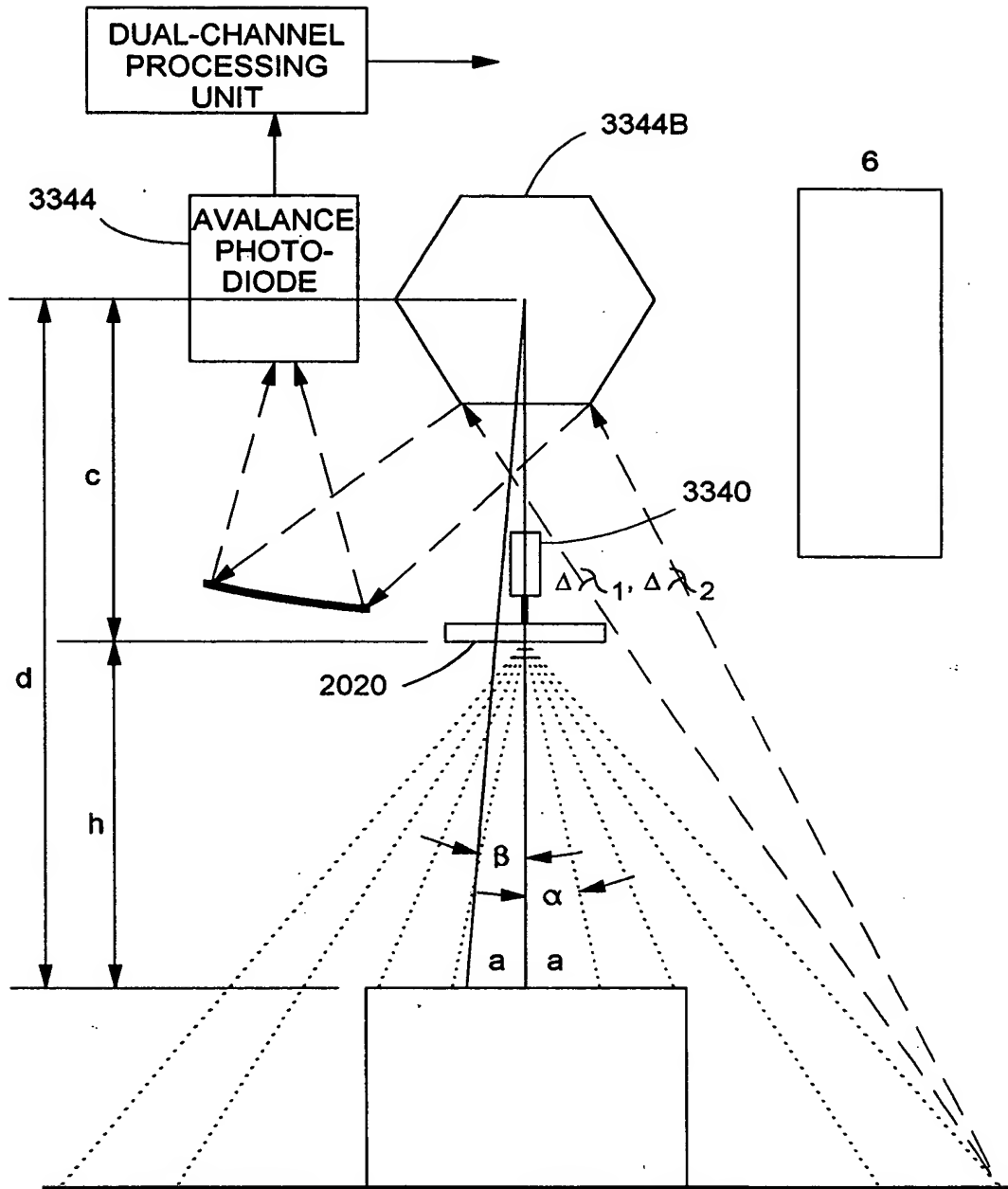
FIG. 15E2

FACE #	ANGLE (DEGREES)
1	3.75
2	-3.75
3	3.75
4	-3.75
5	3.75
6	-3.75
7	3.75
8	-3.75

FIG. 15E3

BEAM NO. 1	1	$\Delta \lambda_1$ $\Delta \lambda_2$
	3	
	5	
	7	
BEAM NO. 2	2	$\Delta \lambda_1$ $\Delta \lambda_2$
	4	
	6	
	8	

FIG. 15E4



THE EQUATION FOR THE CALCULATION OF THE DISTANCE FROM THE DEVICE TO THE OBJECT:

$$a = h \tan \alpha, \quad a = d \tan \beta, \quad d = h - c$$

$$h = (c \tan \beta) (\tan \alpha - \tan \beta)$$

FIG. 15F

52/116

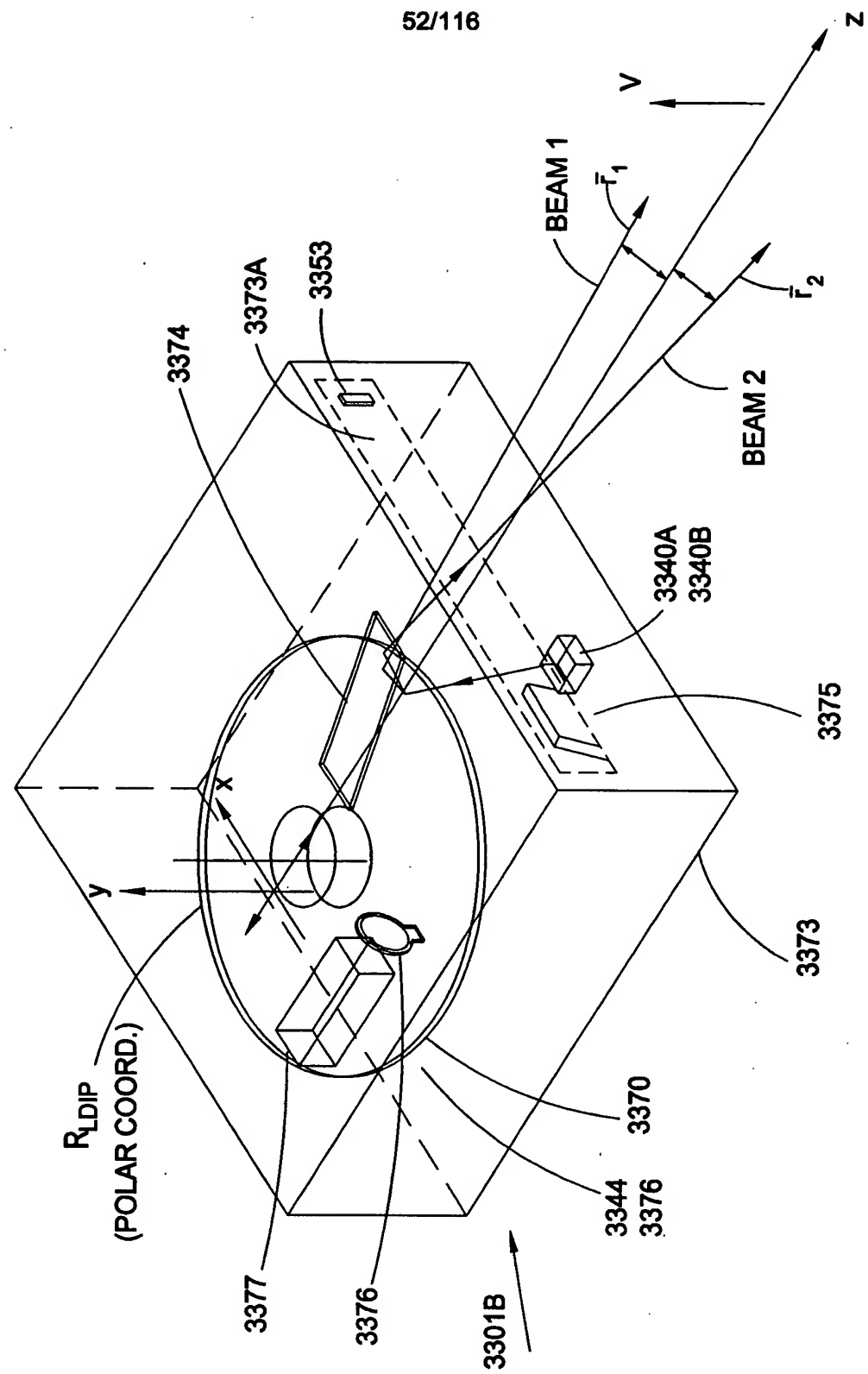


FIG. 15G

53/116

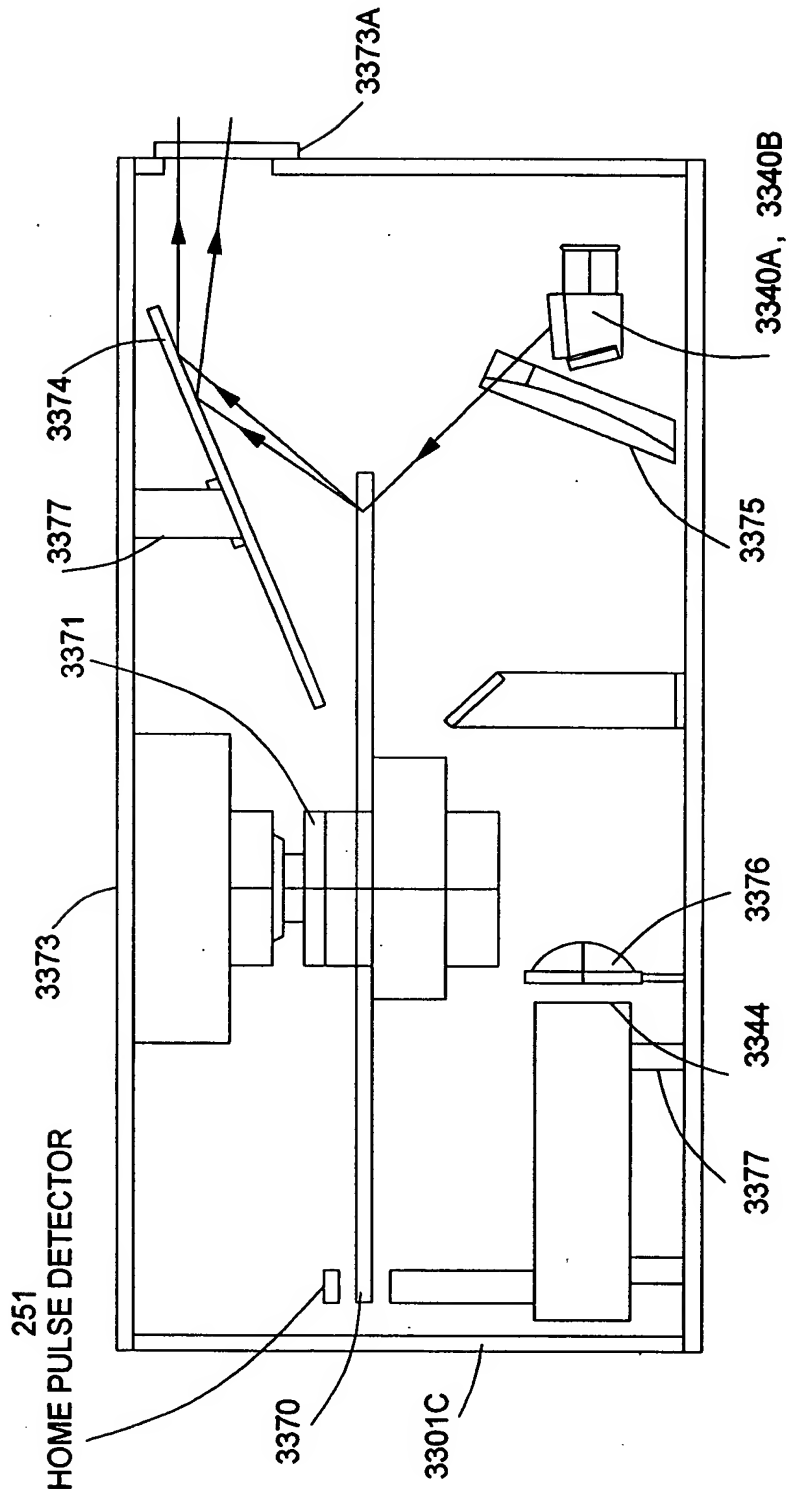


FIG. 15H

54/116

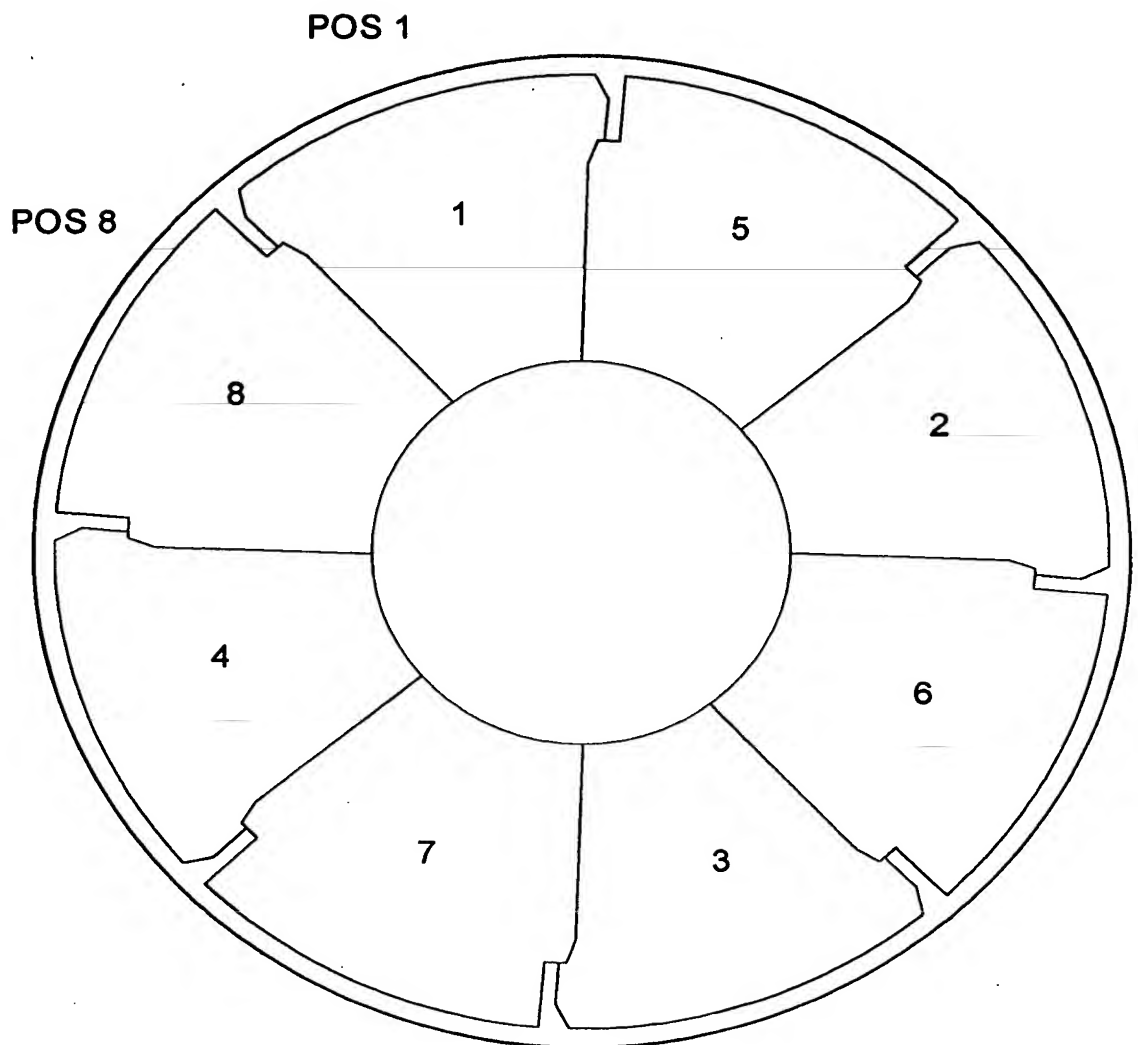


FIG. 15I

55/116

ROTATIONAL SPEED OF DISK (RPM)				658 nm			
FACET DIFFRACTION FOCAL LENGTH (INCHES)	GEOMETRICAL FOCAL LENGTH (INCHES)	ANGLE A (DEGREES)	ANGLE B (DEGREES)	ANGLE OF DIFFRACTION BEAM FROM VERTICAL (DEGREES)	ANGLE OF DIFFRACTION BEAM FROM VERTICAL (DEGREES)	SCAN MULTI. (DEGREES)	SCAN MULTI. (DEGREES)
		(INCHES)	(INCHES)	(DEGREES)	(DEGREES)	(m)	(m)
1	65.41	5000.00	45.9	53.00	37.00	5.00	54.93
2	65.41	5000.00	45.9	53.00	37.00	5.00	54.93
3	65.41	5000.00	45.9	53.00	37.00	5.00	54.93
4	65.41	5000.00	45.9	53.00	37.00	5.00	54.93
5	65.41	5000.00	45.9	48.00	42.00	10.00	54.93
6	65.41	5000.00	45.9	48.00	42.00	10.00	54.93
7	65.41	5000.00	45.9	48.00	42.00	10.00	54.93
8	65.41	5000.00	45.9	48.00	42.00	10.00	54.93

FIG. 15J1

56/116

ROTATION ANGLE (DEGREES)	ACCOUNTING FOR DEAD TIME FOR LASER BEAM	LIGHT COLLECTION FACTOR	MAXIMUM COLLECTION AREA	DESIGN (INCLUDES NOTCH)	BEAM SPEED AT CENTER NOTCH LOSS OF 0.15 SQ. LINE	BEAM SPEED AT MAX. DEPTH OF FIELD OF FIELD	BEAM SPEED AT MIN. DEPTH OF FIELD OF FIELD	BEAM SPEED AT FIELD (INCHES INCHES) (INCHES /SEC)	BEAM SPEED AT FIELD (INCHES /SEC)	BEAM SPEED AT FIELD (INCHES /SEC)
42.30	44.30	1.00	5.29	5.30	46251	51021	41302	0	0	0
42.30	44.30	1.00	5.29	5.30	46251	51021	41302	0	0	0
42.30	44.30	1.00	5.29	5.30	46251	51021	41302	0	0	0
42.30	44.30	1.00	5.29	5.30	46251	51021	41302	0	0	0
39.82	41.82	1.19	6.30	6.28	48649	53855	43443	0	0	0
39.82	41.82	1.19	6.30	6.28	48649	53855	43443	0	0	0
39.82	41.82	1.19	6.30	6.28	48649	53855	43443	0	0	0
39.82	41.82	1.19	6.30	6.28	48649	53855	43443	0	0	0

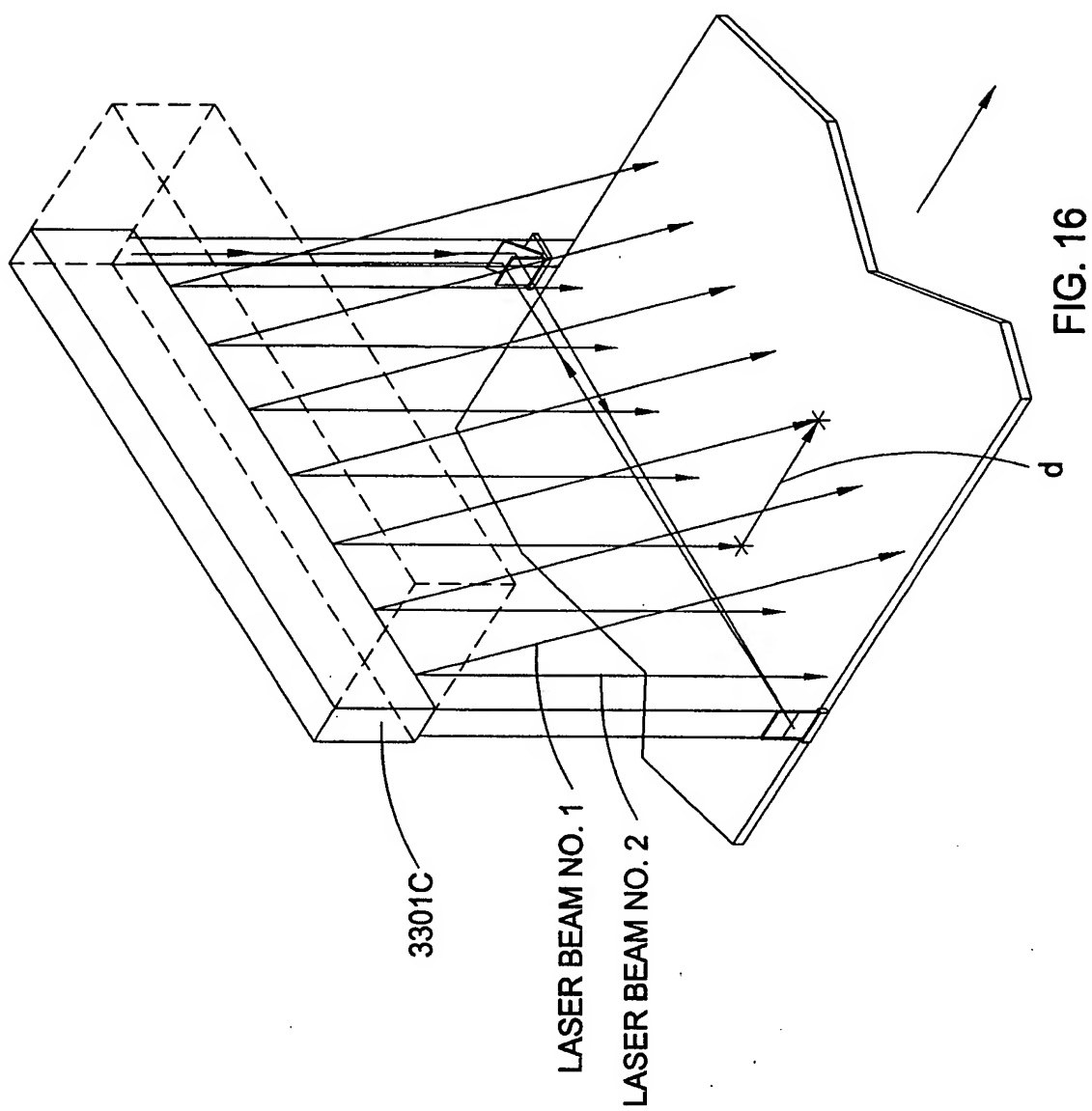
FIG. 15J2

57/116

BEAM NO.	FACET NOS.	
1	1	$\Delta\lambda_1, \Delta\lambda_2$
	2	
	3	
	4	
2	5	$\Delta\lambda_1, \Delta\lambda_2$
	6	
	7	
	8	

FIG. 15K

58/116



59/116

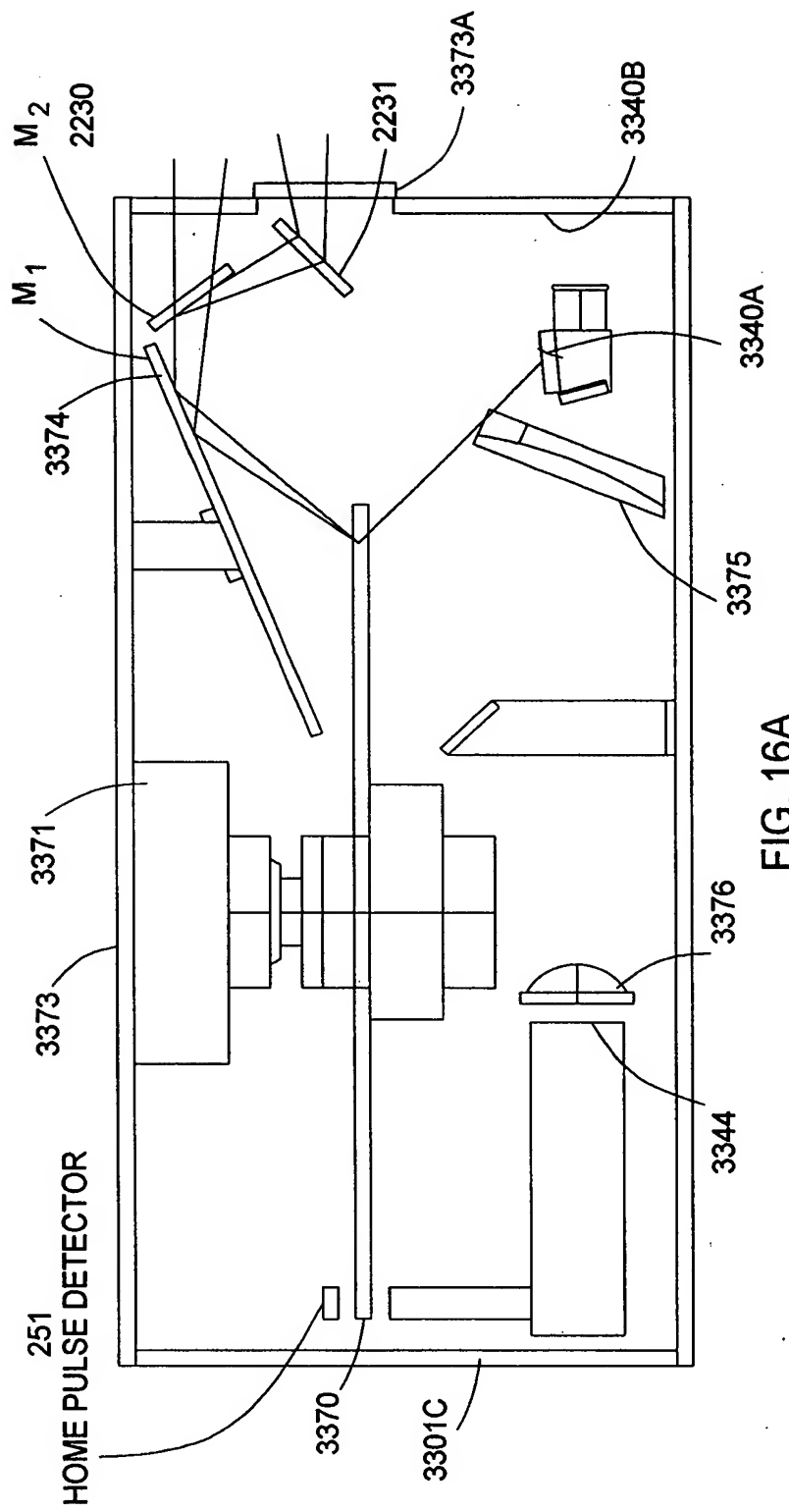


FIG. 16A

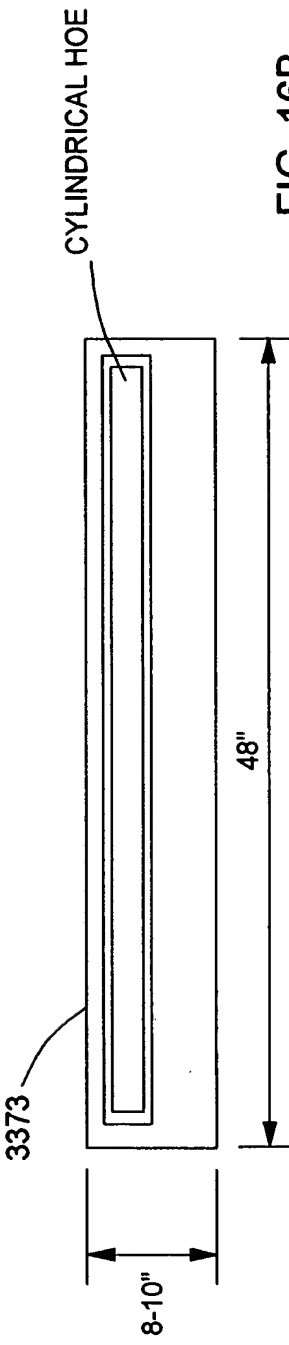


FIG. 16B

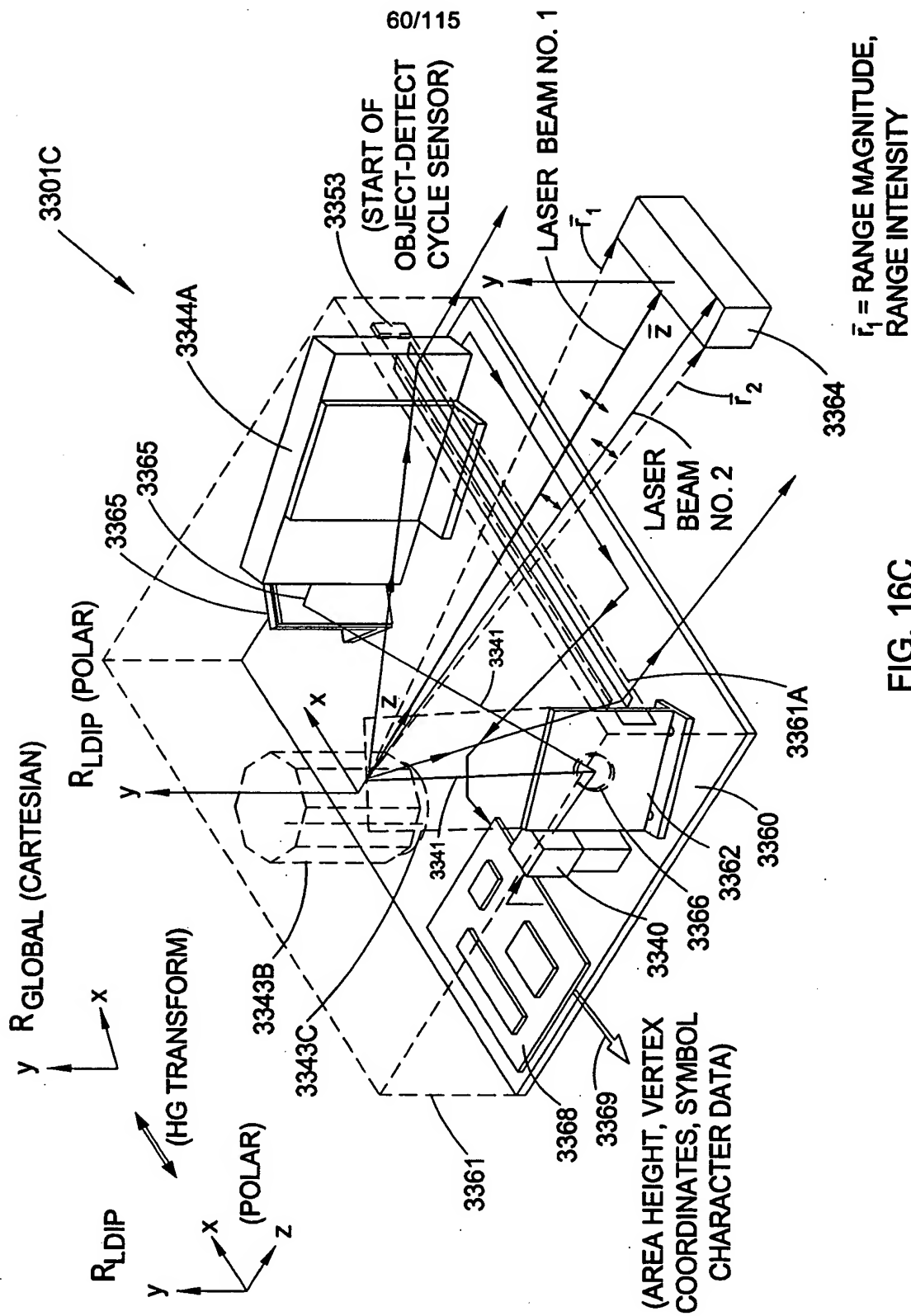


FIG. 16C

61/116

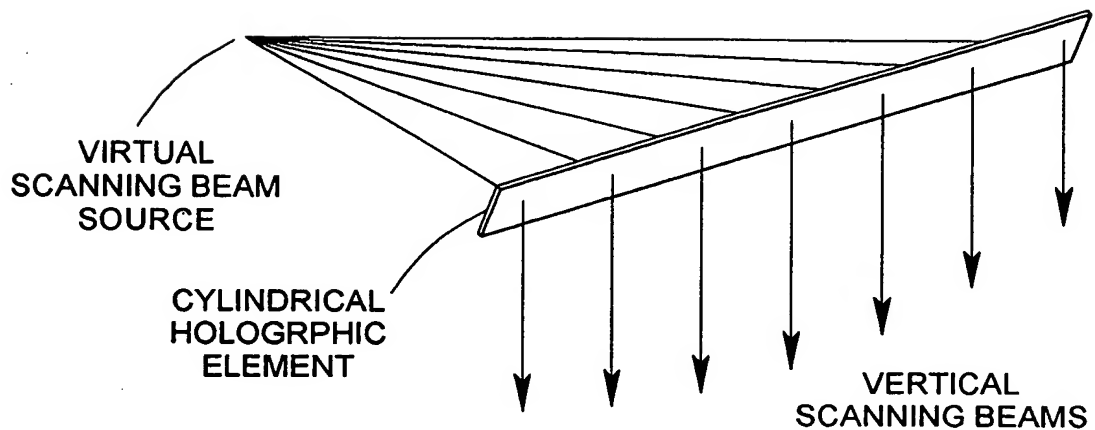


FIG. 16D

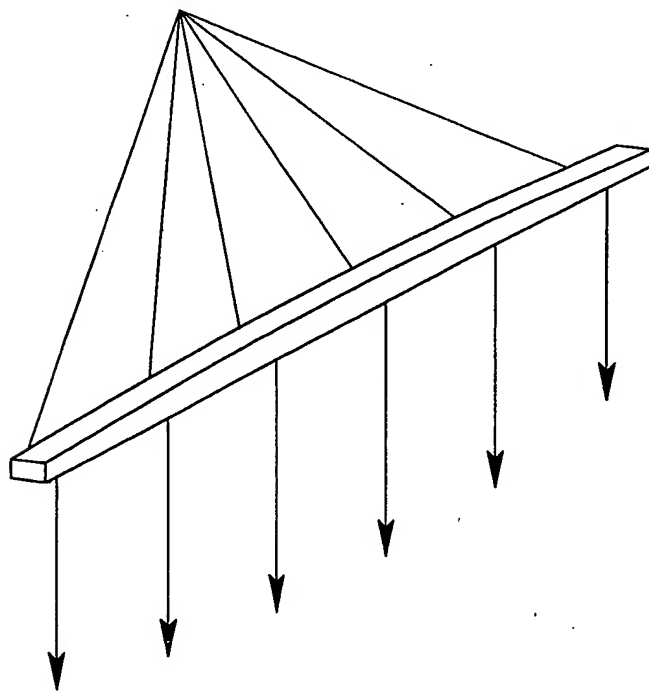


FIG. 16E

62/116

**HEIGHT/WIDTH/PROFILING
PACKAGE DIMENSIONING SUBSYSTEM**

(600) FIGS. 17 - 29B

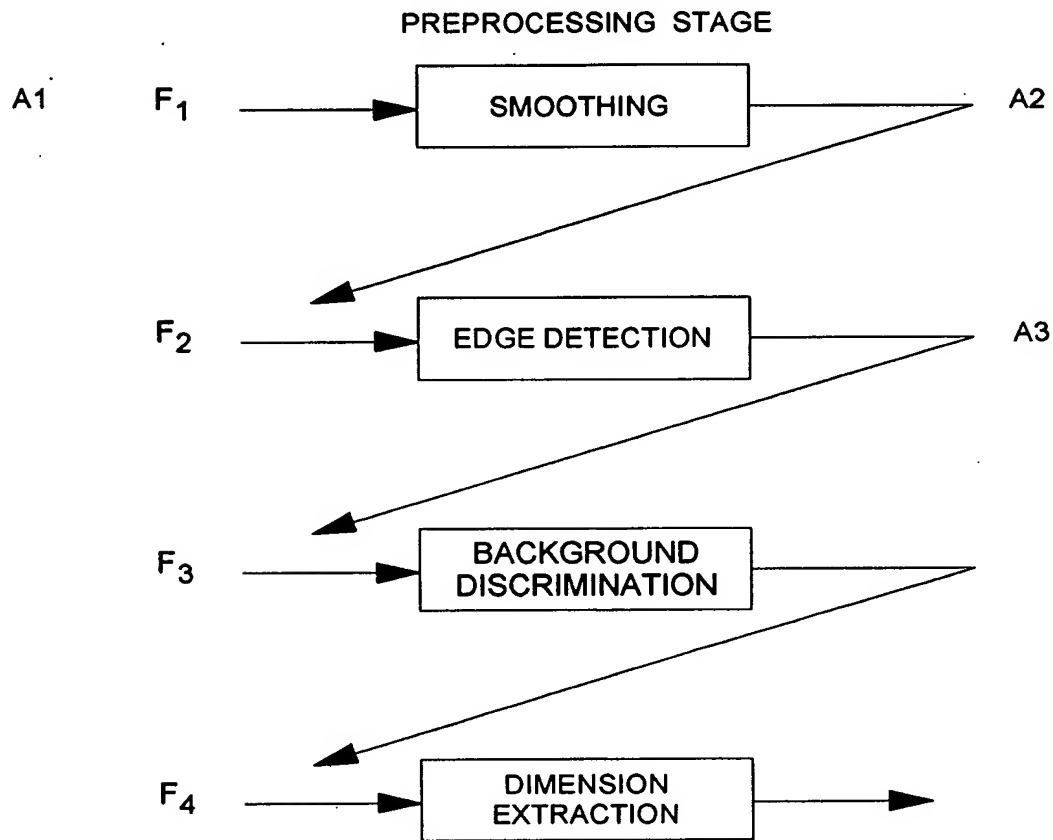
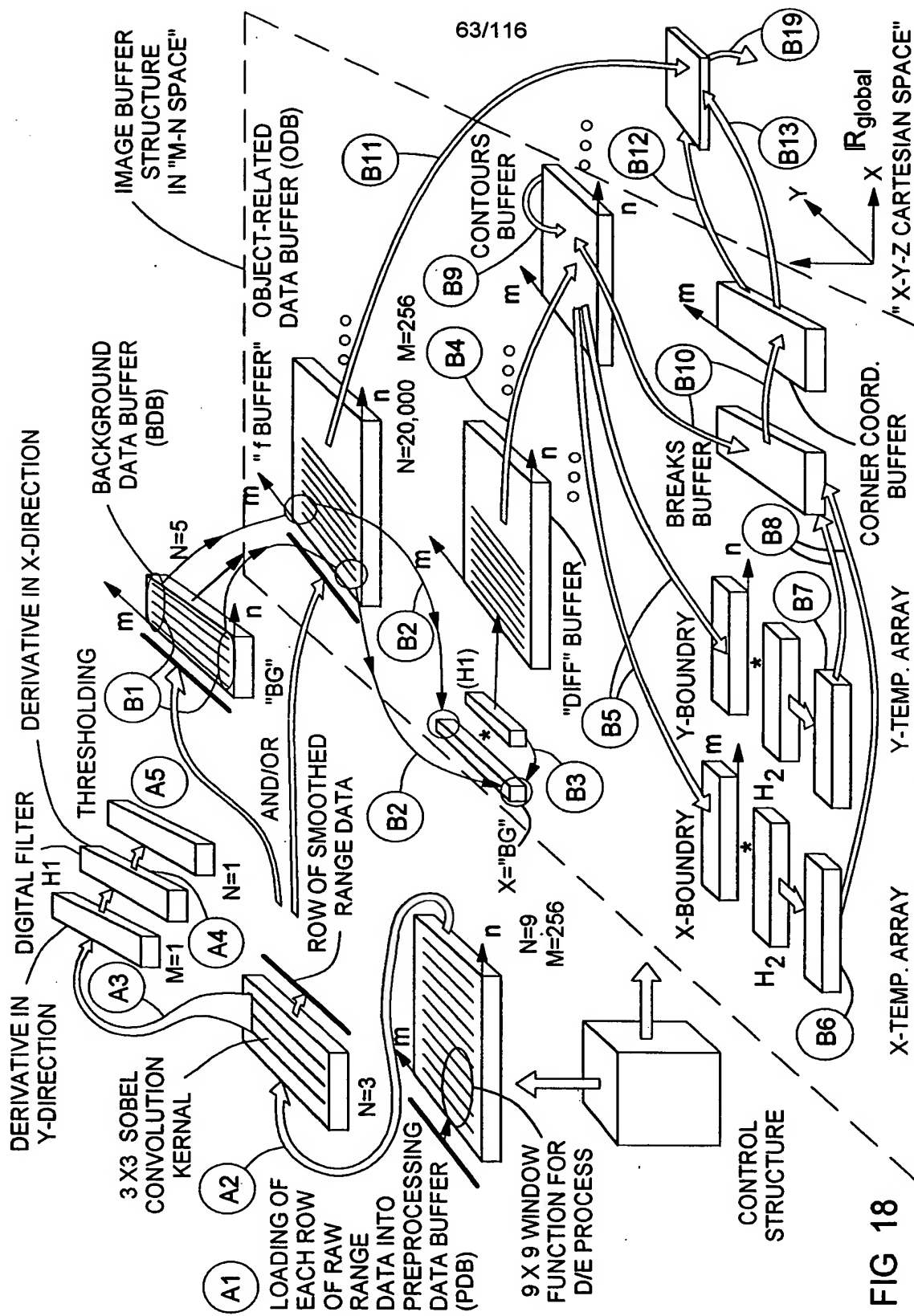
F₁ = RAW IMAGEF₂ = SMOOTH IMAGEF₃ = EDGE IMAGEF₄ = OBJECT IMAGEF₅ = AREA HEIGHT, AND CORNER COORDINATES

FIG. 17



64/116

CONTROL STRUCTURES

INPUT OF OPERATOR PARAMETERS AND INITIALIZATIONS

```

FOR z := 1 TO n DO
  READ ROW z OF f INTO THE IMAGE ROW STORE
  BUF(1...M, IND(z));
FOR y := k + 1 to N - k DO BEGIN
  FOR x := k + 1 TO M - k DO BEGIN
    FOR z := 1 TO a DO
      F(z) := BUF(x + xind(z), ind(k + 1 + yind(z)));

```

PROCESSING OF THE PICTURE WINDOW $F(f, (x, y))$ WITH A SPECIFIC OPERATOR KERNEL ARGUMENTS: $F(z)$, WITH $1 \leq z \leq a$, OR $F(i, j)$, WITH $-k \leq i, j \leq k$

RESULT: GRAY VALUE v

```

⊕ IF (PARSEQ = 0) THEN
  BUFOUT(x) := v
⊕ ELSE BUF(x, IND(k+1)) := v
  END{for};
⊕ IF (PARSEQ = 0) THEN
  WRITE ROW BUFFER STORE BUFOUT(1...M) INTO
  ROW y OF THE RESULTANT IMAGE FILE OUT
⊕ ELSE
⊕ WRITE IMAGE ROW STORE BUF(1...M, IND(K+ 1)) INTO
  ROW y OF THE RESULTANT IMAGE FILE OUT;
⊕ IF (y < N - k) THEN BEGIN
  READ ROW y + k + 1 OF THE INPUT IMAGE FILE INTO
  THE IMAGE ROW STORE BUF(1...M, IND(1));
  LINK := IND(1);
  FOR z := 1 TO n - 1 DO IND(z) := IND(z + 1)
  IND(n) := LINK
  END {if}
END {for}

```

CONTROL STRUCTURE FOR THE COMPUTATION OF LOCAL OPERATORS, USING ROW-WISE BUFFERING, THE CENTERED ij-COORDINATE SYSTEM, AND THE SPATIAL ARRANGEMENT FOR THE WINDOW CONTENT IF THE ONE-DIMENSIONAL ARRAY $F(z)$ IS USED. PROGRAM LINES LABELED WITH \oplus ARE SUPERFLUOUS IF A PARALLEL OPERATOR HAS TO BE IMPLEMENTED

FIG. 19

STEP A1 INVOLVES CAPTURING LINES (ROWS) OF DIGITIZED RANGE DATA PRODUCED BY THE LASER SCANNING/RANGING UNIT DURING EACH SWEEP OF THE AMPLITUDE MODULATED LASER BEAM ACROSS THE WIDTH OF THE CONVEYER BELT. EACH ROW OF RAW RANGE DATA HAS A PREDETERMINED NUMBER OF RANGE VALUE SAMPLES (E.G. M=256) TAKEN DURING EACH SCAN ACROSS THE CONVEYOR BELT. EACH SUCH RANGE DATA SAMPLE REPRESENTS THE MAGNITUDE OF THE POSITION VECTOR POINTING TO THE CORRESPONDING SAMPLE POINT ON THE SCANNED PACKAGE, REFERENCED WITH RESPECT TO A POLAR-TYPE COORDINATE SYSTEM SYMBOLICALLY EMBEDDED WITHIN THE LADAR-BASED IMAGING AND DIMENSIONING SUBSYSTEM. STEP A1 ALSO INVOLVES LOADING A PREDETERMINED NUMBER OF RAW RANGE DATA SAMPLES INTO A FIFO-TYPE PREPROCESSING DATA BUFFER (e.g. M=9) FOR BUFFERING 9 ROWS OF RANGE DATA AT ANY INSTANT OF TIME.

STEP A2 INVOLVES USING, AT EACH PROCESSING CYCLE AND SYNCHRONIZED WITH THE CAPTURE OF EACH NEW ROW OF RAW RANGE DATA, A 2-D (9X9) WINDOW FUNCTION EMBEDDED INTO A GENERAL CONTROL STRUCTURE (e.g. PIXEL PROGRAM LOOP), TO SMOOTH EACH LINE (OR ROW) OF RAW RANGE DATA BUFFERED IN THE PROCESSING DATA BUFFER USING DILUTION AND EROSION (D/E) PROCESS BASED ON NON-LINEAR TYPE MIN/MAX METHODS. THE OUTPUT FROM THIS NON-LINEAR OPERATION IS A SINGLE ROW OF SMOOTH RANGE DATA OF LENGTH M=256 WHICH IS INPUT TO A THREE ROW FIFO BUFFER, AS SHOWN IN FIG. 44G.

STEP 3A INVOLVES USING, AT EACH PROCESSING CYCLE, A 2-D (3X3) CONVOLUTION KERNEL BASED ON THE SOBEL OPERATOR, AND EMBEDDED INTO A GENERAL CONTROL STRUCTURE (e.g. PIXEL PROGRAM LOOP), TO EDGE-DETECT EACH BUFFERED ROW OF SMOOTH EDGE DATA OF LENGTH M=256 WHICH IS INPUT TO A FIRST ONE ROW (N=1) FIFO BUFFER AS SHOWN IN FIG. 44G. THE OUTPUT ROW OF "EDGE DETECTED" RANGE DATA REPRESENTS THE FIRST SPATIAL DERIVATIVE A OF THE BUFFERED ROWS OF RANGE DATA ALONG THE n DIRECTION OF THE N=9 FIFO (CORRESPONDING TO THE FIRST SPATIAL DERIVITIVE OF THE RANGE DATA CAPTURED ALONG THE Y DIRECTION OF THE CONVEYER BELT.

A

FIG. 20A

66/116

STEP A4 INVOLVES USING, AT EACH PROCESSING CYCLE, A 7-TAP FIR-TYPE DIGITAL FILTER (H1) TO COMPUTE THE FIRST SPATIAL DERIVATIVE OF THE BUFFERED ROW OF EDGE-DETECTED RANGE DATA ALONG THE m DIRECTION OF THE N=9 FIFO (CORRESPONDING TO THE FIRST SPATIAL DERIVATIVE OR THE RANGE DATA CAPTURED ALONG THE x DIRECTION OF THE CONVEYOR BELT). THE OUTPUT OF THIS OPERATION IS STORED IN A SECOND ONE ROW (N=1) FIFO, AS SHOWN IN FIG. 44G.

STEP A5 INVOLVES ANALYZING, AT EACH PROCESSING CYCLE, THE EDGE -DETECTED DERIVATIVE STORED IN THE SECOND ONE ROW FIFO IN ORDER TO (1) FIND THE MAXIMUM VALUE THEREOF, AND THEN (2) COMPARE THE MAXIMUM DERIVATIVE VALUE TO A PREDETERMINED THRESHOLD VALUE. IF ANY OF THE MAXIMUM FIRST DERIVATIVE VALUES IS LARGER THAN THE PREDETERMINED THRESHOLD VALUE, THEN THE UNLOADED ROW OF SMOOTHED RANGE DATA (FROM OUTPUT PORT OF THE THREE ROW FIFO) IS LABELED AS CONTAINING OBJECT DATA, AND IS LOADED INTO THE INPUT PORT OF THE FIFO-TYPE OBJECT-RELATED DATA BUFFER (ODB), ALSO REFERRED TO AS THE "f" BUFFER, FOR FUTURE USE. OTHERWISE, THE UNLOADED ROW OF SMOOTHED RANGE DATA FROM THE THREE ROW FIFO IS LABELED AS CONTAINING BACKGROUND DATA AND IS LOADED INTO THE INPUT PORT OF THE FIFO-TYPE BACKGROUND DATA BUFFER (BDB), AND POSSIBLY THE ODB, FOR FUTURE USE.

STEP B1: AT EACH PROCESSING CYCLE, AND FOR EACH COLUMN POSITION IN THE ROWS BACKGROUND DATA IN THE BDB (REFERENCED BY INDEX m), COMPUTE THE "MEDIAN VALUE" BASED ON THE CURRENT ROWS OF BACKGROUND DATA BUFFERED THEREIN.

STEP B2: AT EACH PROCESSING CYCLE, AND FOR EACH ROW OF OBJECT-RELATED DATA IN THE ODB, SUBTRACT THE PRECOMPUTED MEDIAN VALUE (BG) FROM THE CORRESPONDING RANGE VALUE ($f=x$), TO PRODUCE A DIFFERENCE VALUE ($x-BG$) FOR EACH OF THE 256 COLUMN POSITIONS IN THE CORRESPONDING ROW OF OBJECT-RELATED DATA BEING BUFFERED IN THE ODB (ALSO INDICATED AS THE "f BUFFER"), THEREBY PRODUCING A VERTICAL FIRST DISCRETE DERIVATIVE THEREOF (HAVING A COLUMN LENGTH $M=256$).

FIG. 20B

67/116

A

H

STEP B3: AT EACH PROCESSING CYCLE, SMOOTH THE COMPUTED VERTICAL FIRST DISCRETE DERIVATIVE BY CONVOLVING THE SAME WITH A 5-TAP FIR SMOOTHING FILTER AND TRUNCATING THE RESULTANT ROW OF SMOOTHED DISCRETE DERIVATIVE DATA TO LENGTH $M=256$, AND THEREAFTER LOAD THE ROW OF SMOOTHED DISCRETE DERIVATIVE DATA IN THE "DIFF" (i.e. DERIVATIVE) DATA BUFFER HAVING $m=256$ COLUMNS AND $n=10,000$ OR MORE ROWS (AS REQUIRED BY THE COLLECTED RANGE DATA MAP). THE OUTPUT ROW OF DISCRETE DERIVATIVE DATA CONTAINS OBJECT-RELATED DATA ONLY, AND MOST BACKGROUND NOISE WILL BE ELIMINATED.



I

STEP B4: AT EACH PROCESSING CYCLE, PERFORM A 2-D IMAGE-BASED CONTOUR TRACING OPERATION ON THE DISCRETE DERIVATIVE DATA CURRENTLY BUFFERED IN THE DIFF DATA BUFFER IN ORDER TO PRODUCE AN ARRAY OF m,n CONTOUR POINTS IN $M-N$ SPACE (AND CORRESPONDING TO x,y CONTOUR POINTS IN X-Y CARTESIAN SPACE) TYPICALLY, THE ARRAY OF CONTOUR POINTS m,n WILL CORRESPOND TO THE SIDES OF THE POLYGONAL OBJECT EMBODIED IN THE ROWS OF OBJECT DATA CURRENTLY BUFFERED WITHIN THE OBJECT DATA BUFFER, AND THE OUTPUT DATA SET PRODUCED FROM THIS STEP OF THE METHOD CONTAINS EXTRANEOUS CORNER POINTS WHICH NEED TO BE REMOVED FROM THE PRODUCED ARRAY OF CONTOUR POINTS.



J

STEP B5: AT EACH PROCESSING CYCLE, STORE THE m,n INDICES (ASSOCIATED WITH THE CORNER POINTS OF THE TRACED CONTOURS) IN THE x -BOUNDARY AND y -BOUNDARY BUFFERS, RESPECTIVELY. NOTABLY, THE x -BOUNDARY AND y -BOUNDARY BUFFER IS $M=256$, AND THE LENGTH OF THE y -BOUNDARY BUFFER IS ALSO $M=256$



K

STEP B6: AT EACH PROCESSING CYCLE, DETECT THE m INDICES ASSOCIATED WITH "CORNER POINTS" IN THE TRACED CONTOURS BY CONVOLVING THE CURRENT DISCRETE DATA SET STORED IN THE x -BOUNDARY BUFFER (OF LENGTH $M=256$) WITH THE 11-TAP FIRFILTER (i.e. LOW-PASS 1st DIFFERENTIATOR) AND STORING THE RESULTANT DISCRETE m INDICE DATA SET IN THE x -TEMP ARRAY.

B

FIG. 20C

68/116

(B)

STEP B7: AT EACH PROCESSING CYCLE, DETECT THE n INDICES ASSOCIATED WITH THE "CORNER POINTS" IN THE TRACED CONTOURS BY CONVOLVING THE DISCRETE DATA SET STORED IN THE y-BOUNDARY BUFFER (OF LENGTH n) WITH THE 11-TAP FIR FILTER (i.e. LOW-PASS 1st DIFFERENTIATOR) AND THEN STORING THE RESULTANT DISCRETE n INDICE DATA SET IN THE y-TEMP-ARRAY.

L

STEP B8: AT EACH PROCESSING CYCLE, FIND THE "BREAK POINTS" AMONG THE DETECTED CORNER POINTS STORED IN THE x-TEMP-ARRAY AND y-TEMP-ARRAYS, AND BUFFER THE m AND n INDICES ASSOCIATED WITH THESE BREAK POINTS IN THE IN THE BREAKS BUFFER.

M

STEP B9: AT EACH PROCESSING CYCLE, PERFORMING LINEAR CURVE FITTING BETWEEN EVERY TWO CONSECUTIVE BREAK POINTS STORED IN THE BREAKS BUFFER, TO PRODUCE A SINGLE LINE REPRESENTATION THEREOF. EACH LINE CONSTITUTES A SIDE OF A POLYGON REPRESENTATION OF THE OBJECT REPRESENTED IN THE RANGE DATA MAP BUFFERED IN THE ODB OR f DATA BUFFER. FOR EVERY TWO CONSECUTIVE SIDES OF THE POLYGON REPRESENTATION, THE INTERSECTION POINT IS DETERMINED, AND DEEMED A CORNER VERTEX OF THE POLYGON.

N

STEP B10: AT PROCESSING CYCLE, ONCE ALL CORNER COORDINATES (VERTICES) ARE OBTAINED, THE CORNER VERTICES ARE FURTHER REDUCDED USING A SHARP/DULL ANGLE ELIMINATION ALGORITHM AND CLOSE CORNER ELIMINATION OPERATORS. TYPICALLY, THE FINAL RESULT IS A SET OF m AND n INDICES CORRESPONDING TO THE x AND y COORDINATES ASSOCIATED WITH THE FOUR CORNERS COORDINATES OF A CUBIC BOX, WHICH SET IS THEREAFTER STORED IN A CORNER COORDINATE (OR INDICE) ARRAY.

O

(C)

FIG. 20D

69/116

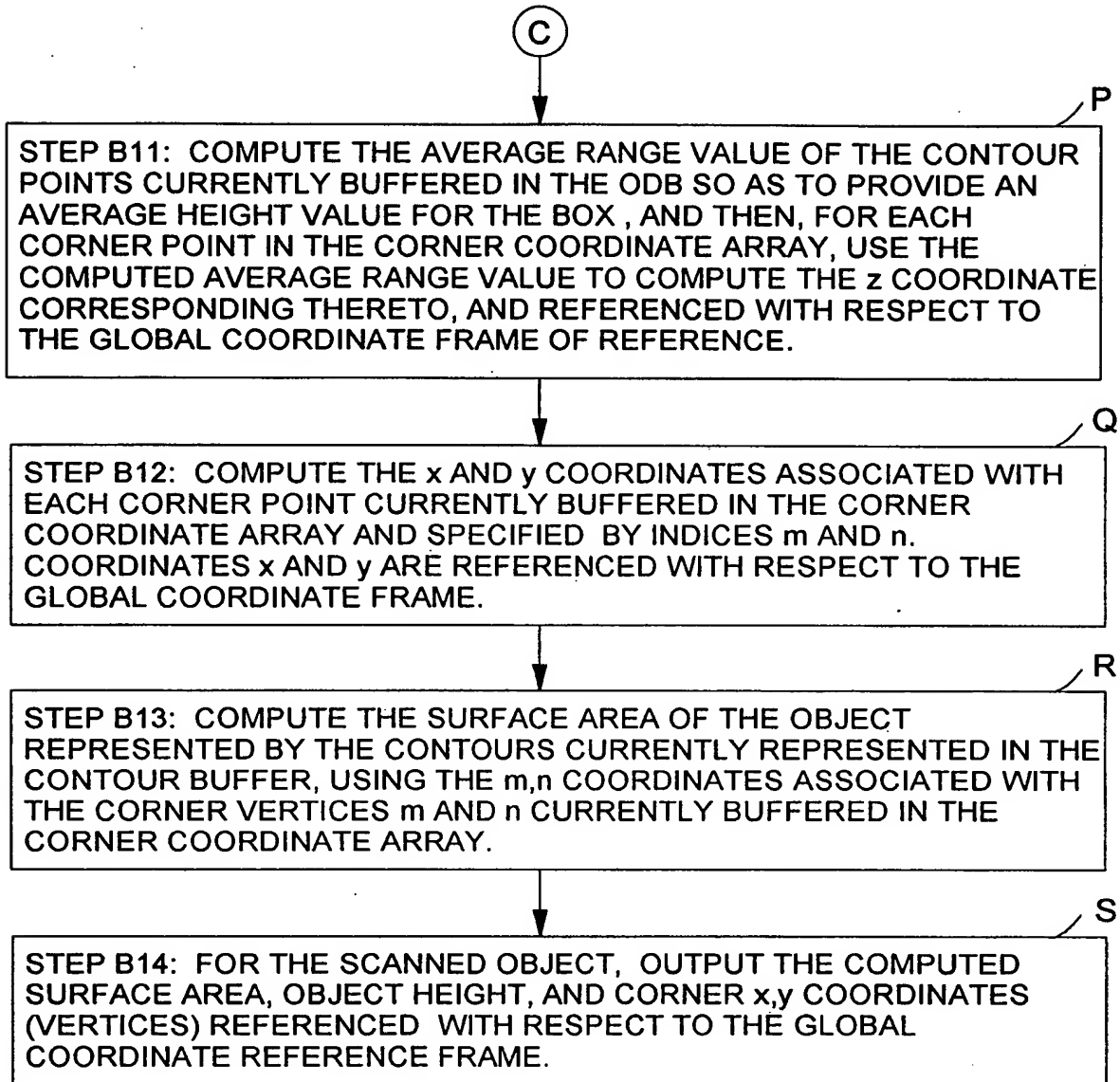


FIG. 20E

70/116

RAW RANGE DATA

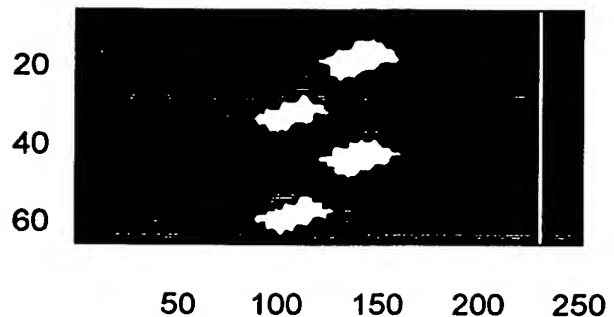


FIG. 21A

SMOOTHED RANGE DATA

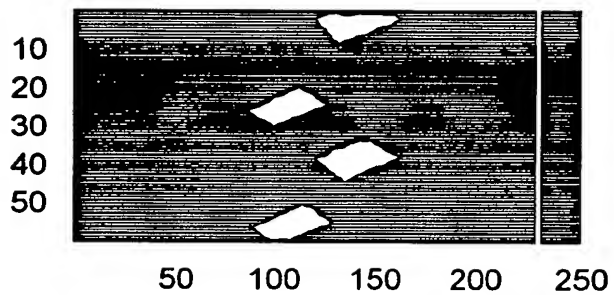


FIG. 21B

VERTICAL EDGE

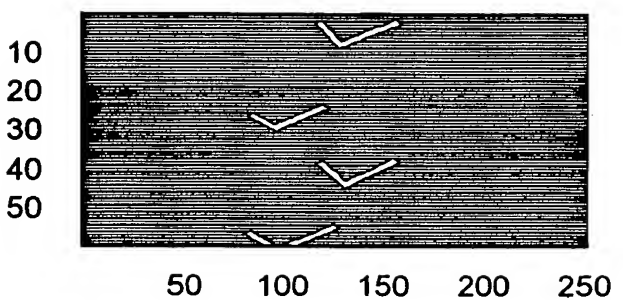


FIG. 21C

71/116

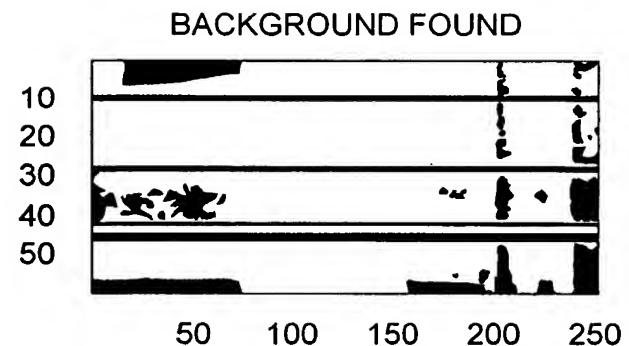


FIG. 21D

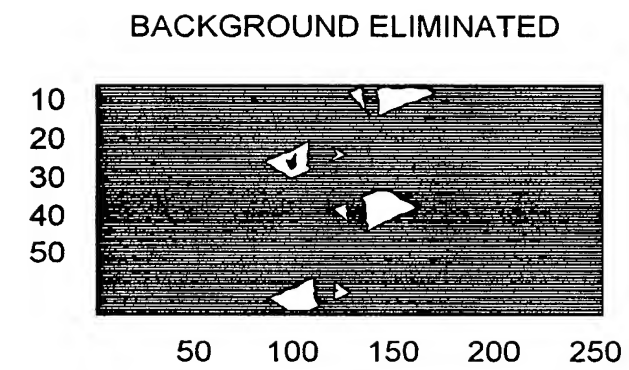
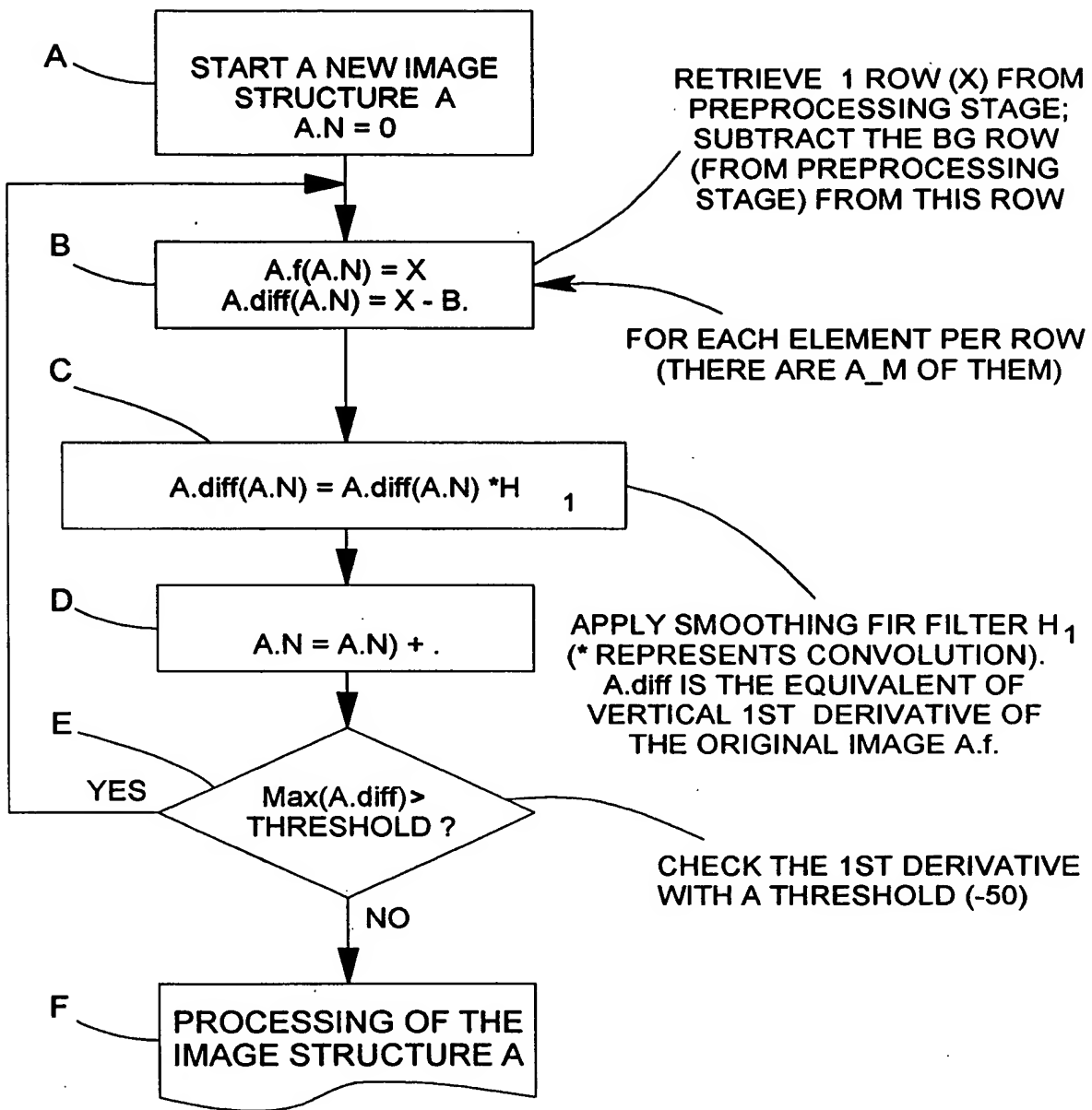


FIG. 21E



$$H_1 = (0.15 \ 0.25 \ 0.2 \ 0.25 \ 0.15)$$

THIS FUNCTIONAL BLOCK RETRIEVES DATA ALREADY PRE-PROCESSED, COMPUTES VERTICAL FIRST DERIVATIVE, AND STORES THE RESULTS IN AN IMAGE STRUCTURE FOR FURTHER PROCESSING, SUCH AS COMPUTER TRACING, ETC.

FIG. 22

73/116

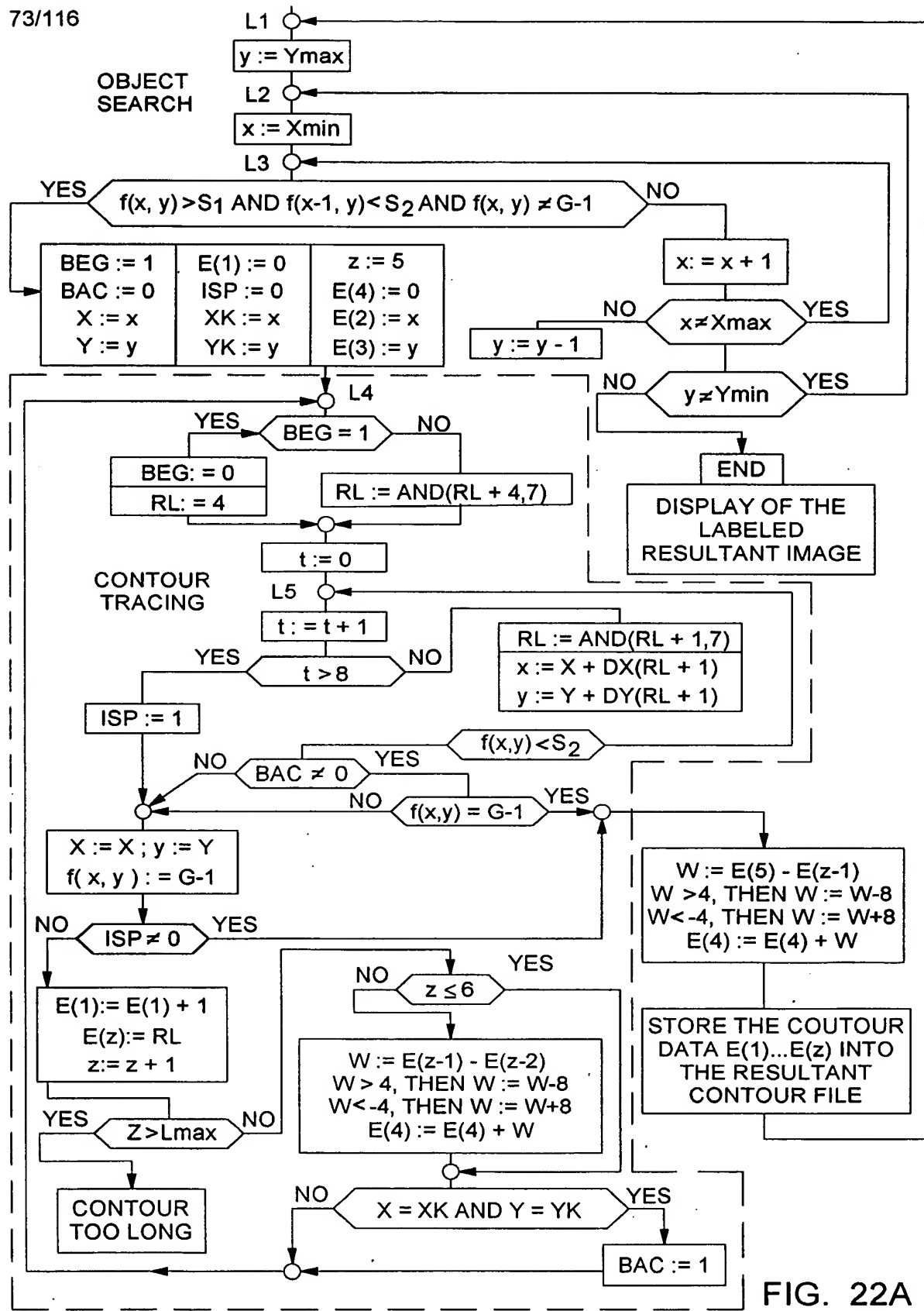
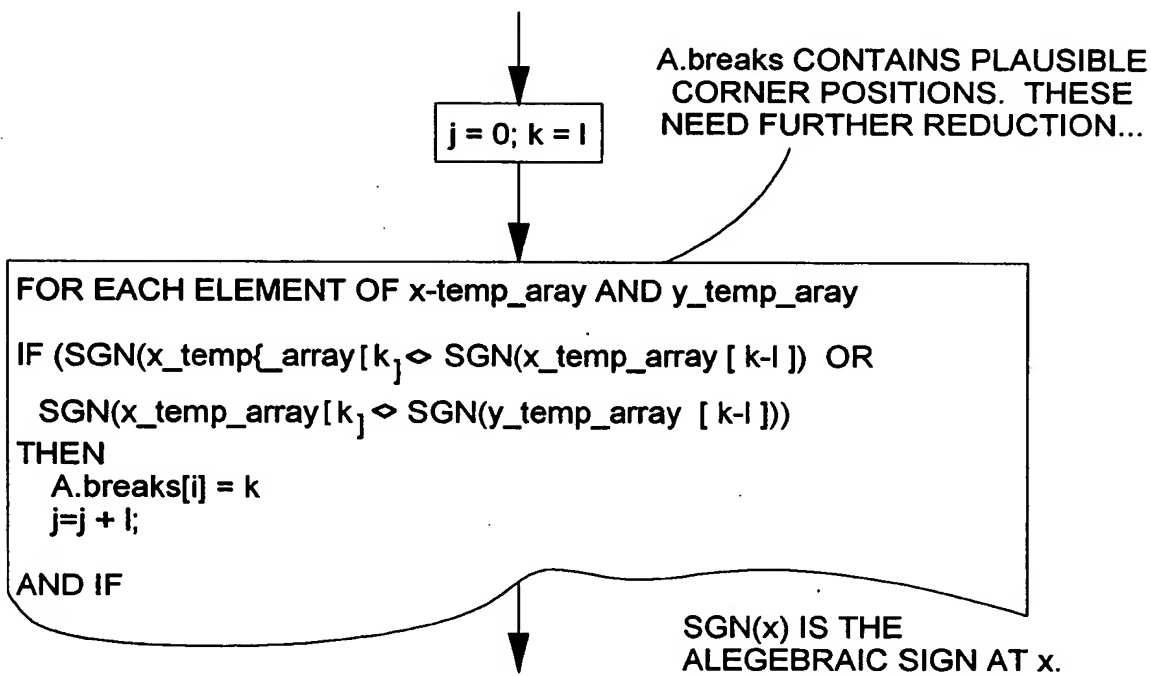
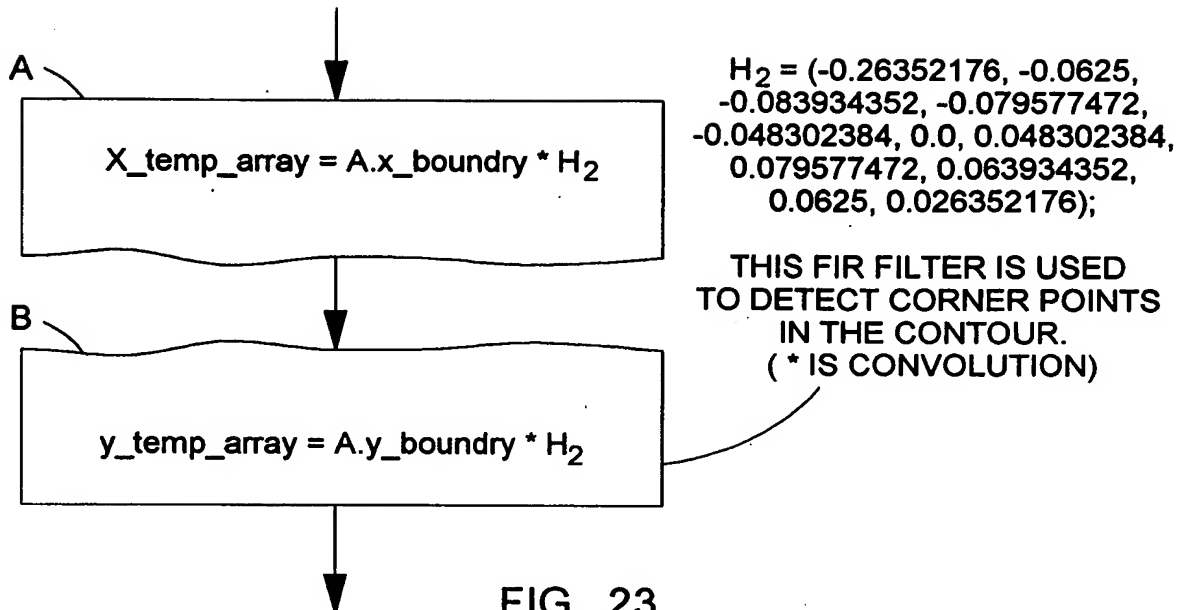


FIG. 22A

74/116



75/116

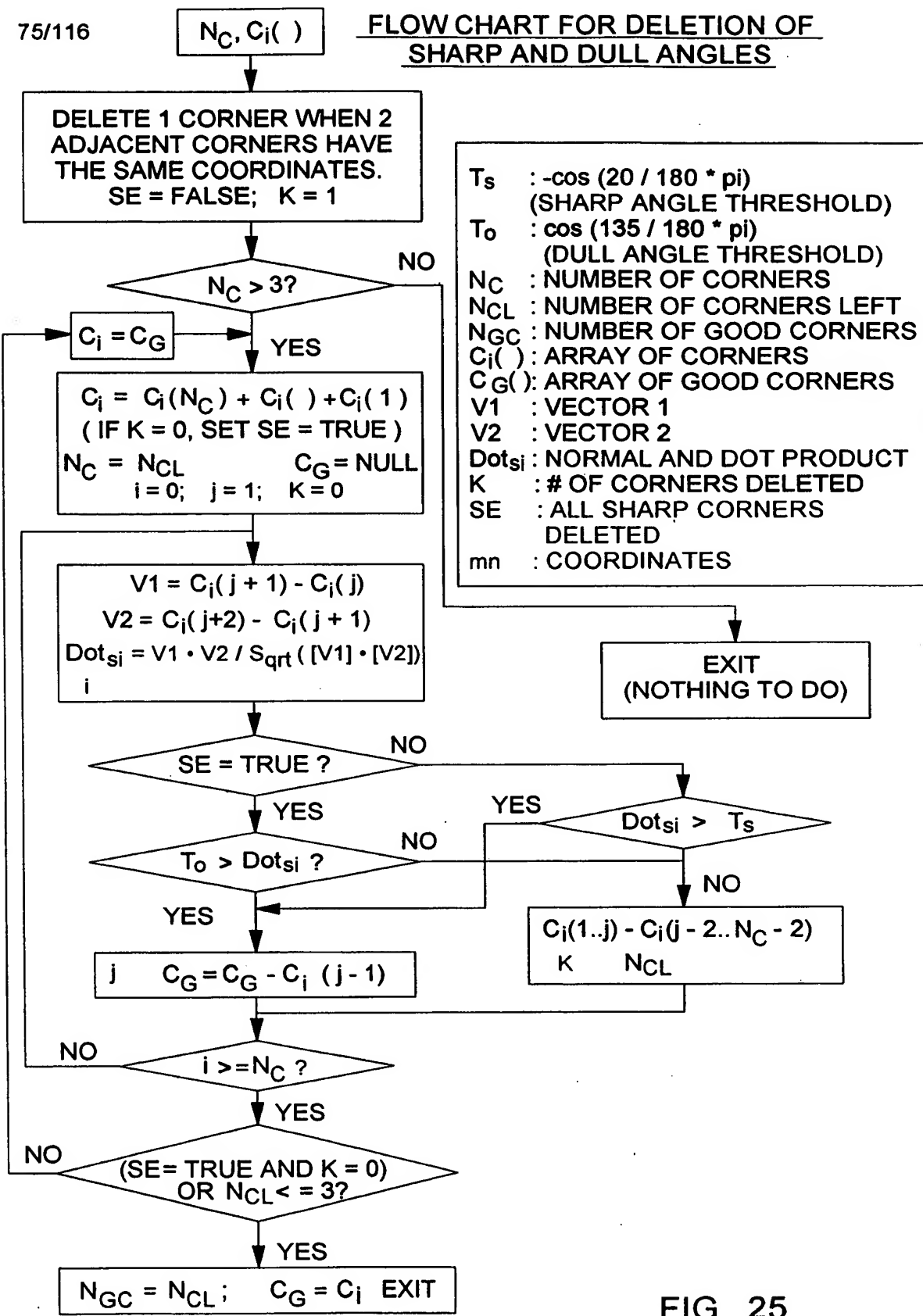


FIG. 25

76/116

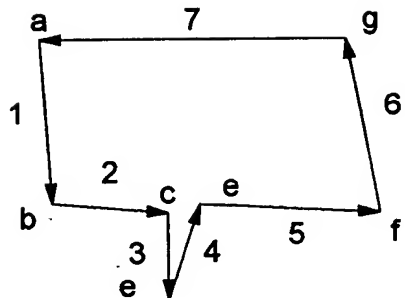


FIG. 26A

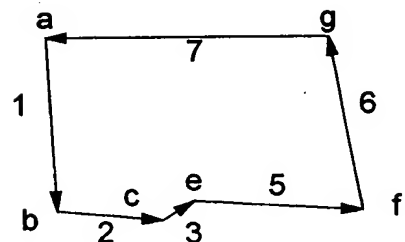


FIG. 26B

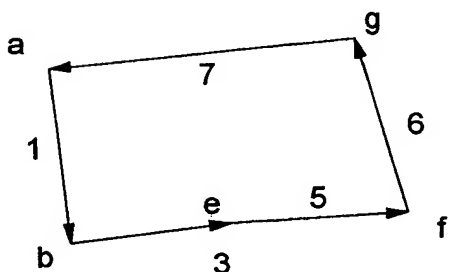


FIG. 26C

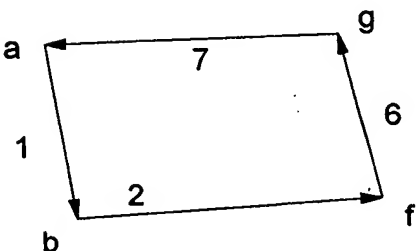


FIG. 26D

77/116

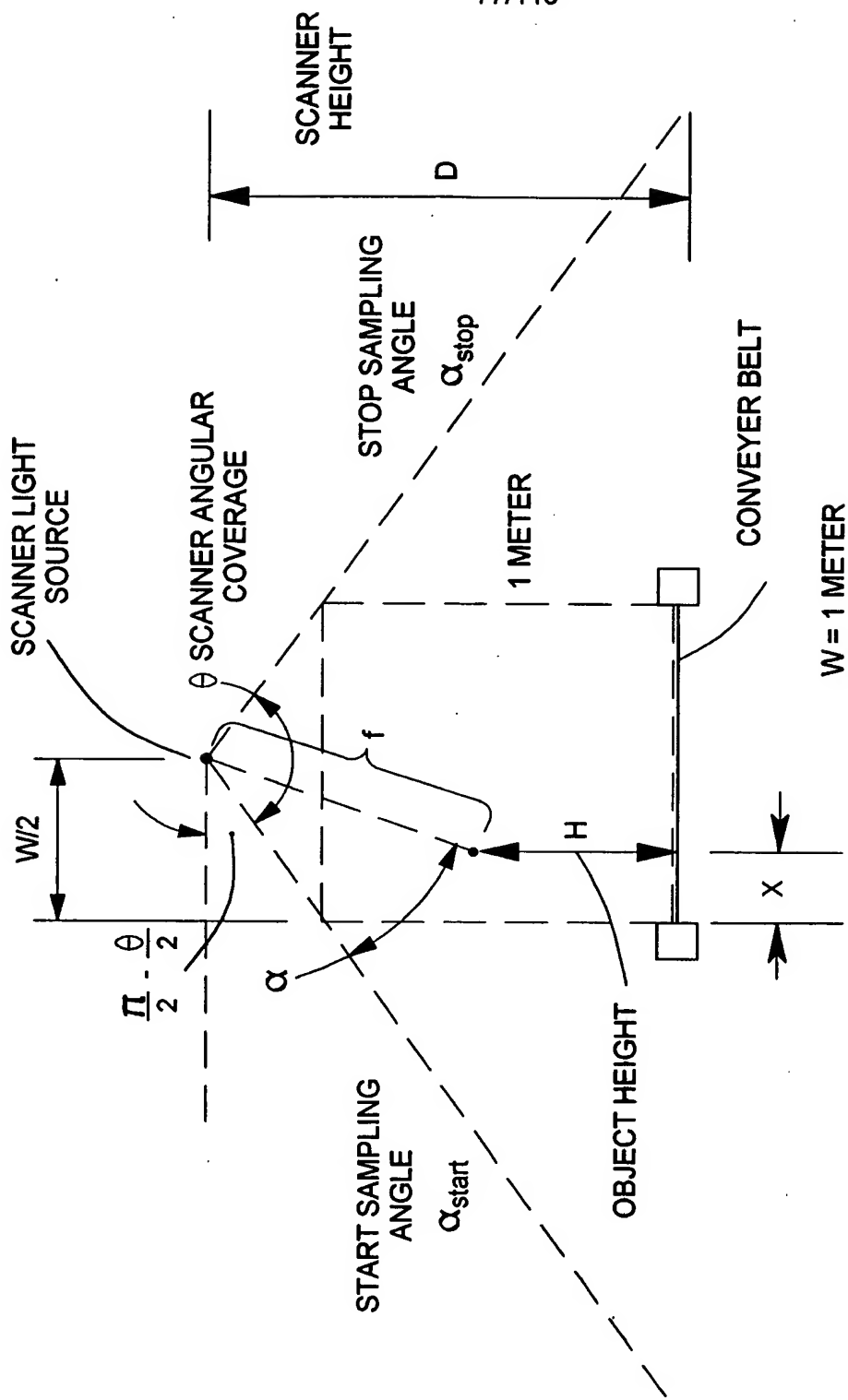


FIG. 27

78/116

FLOW CHART FOR PACKAGE AREA COMPUTATION

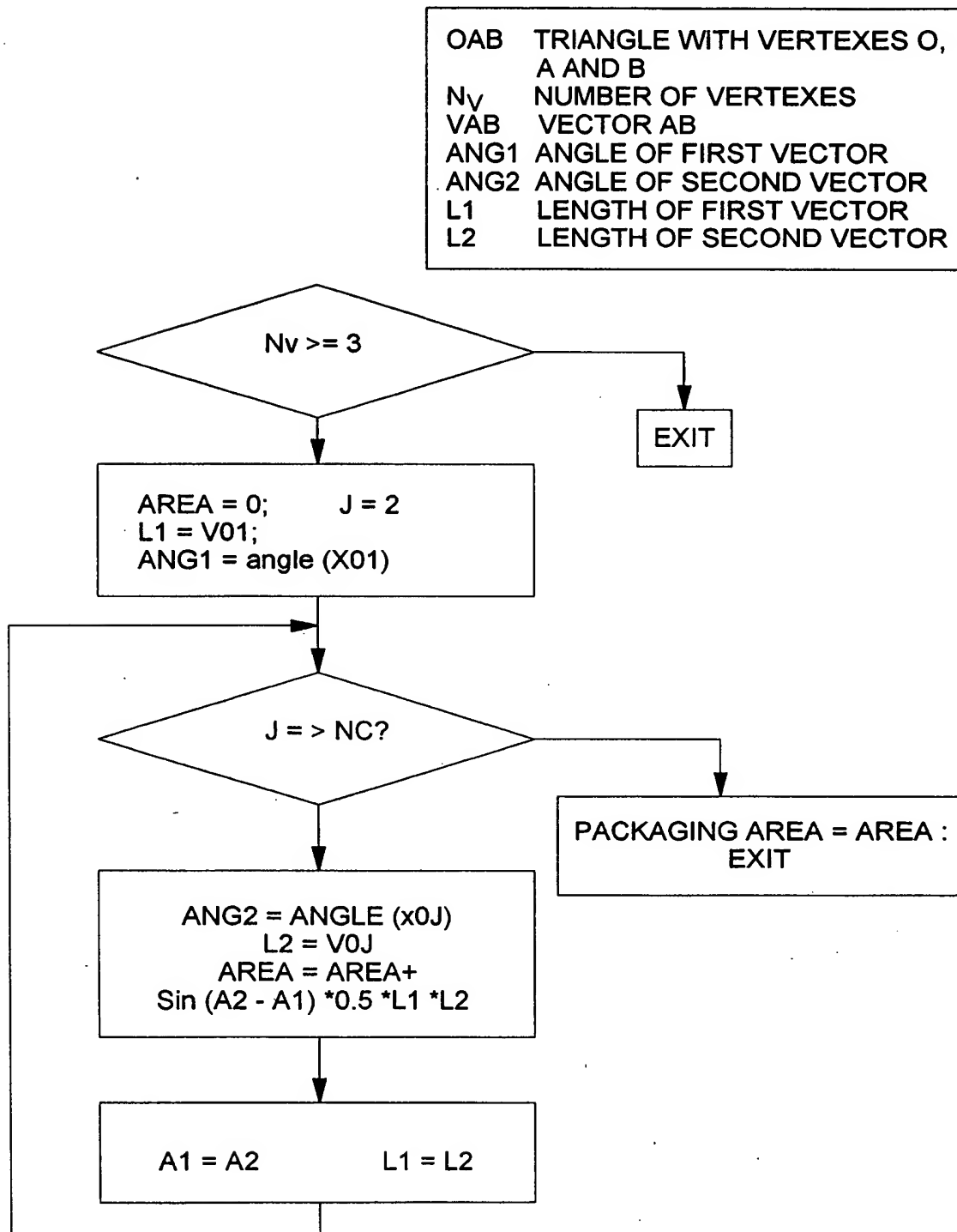


FIG. 28

79/116

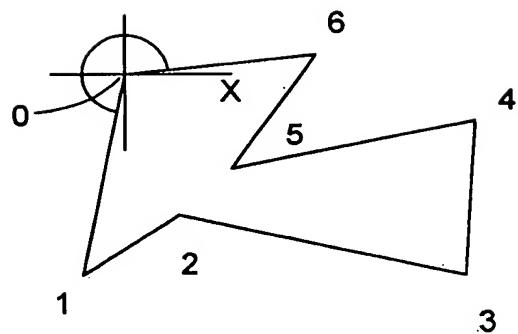


FIG. 29A

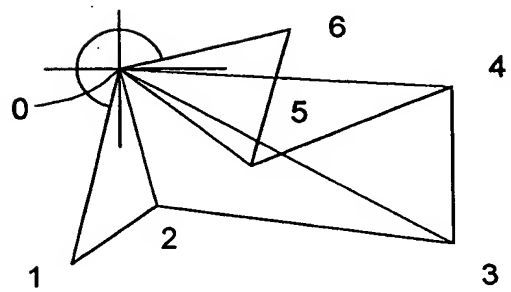


FIG. 29B

80/116

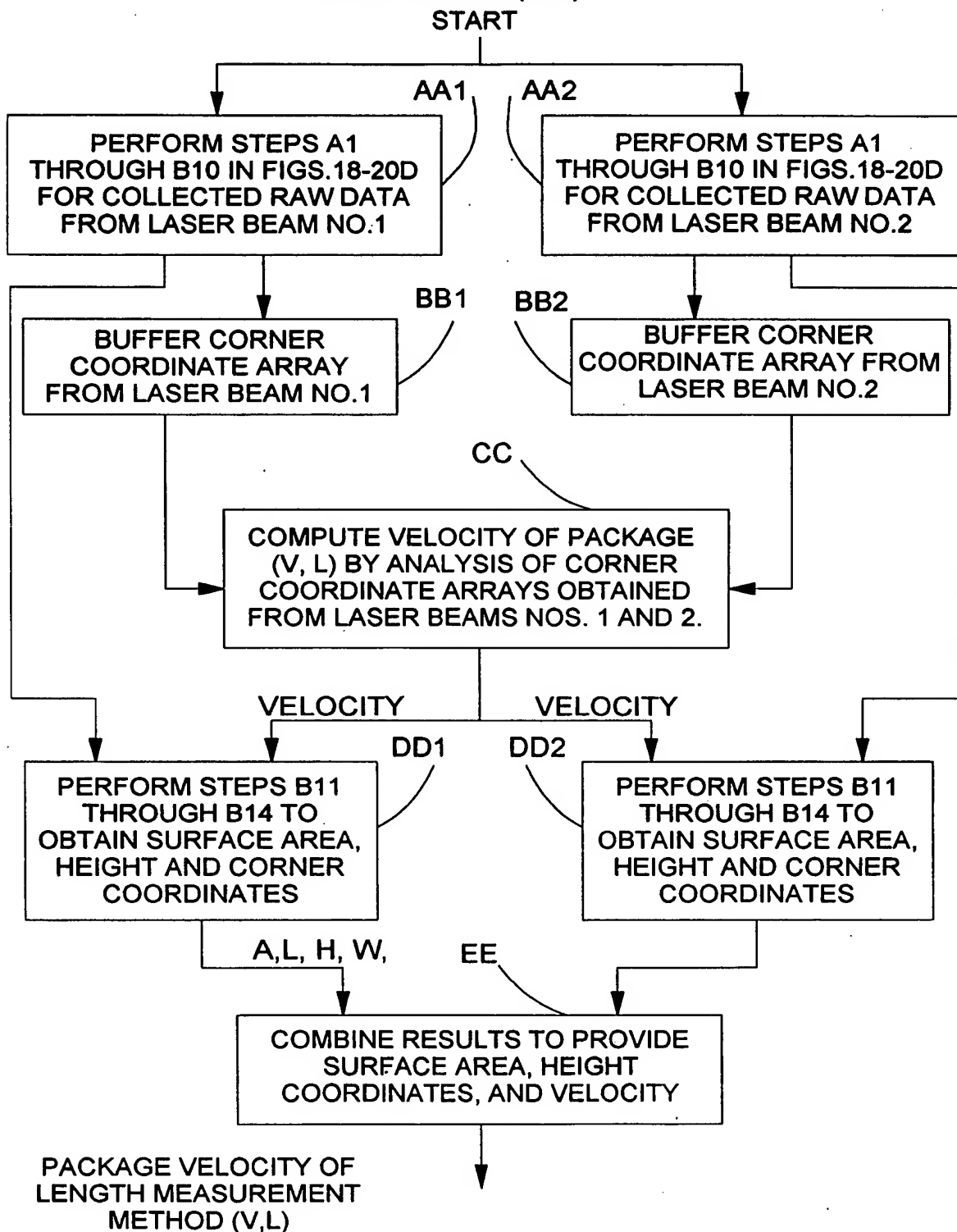
PACKAGE VELOCITY MEASUREMENT
SUBSYSTEM (400)

FIG. 30

81/116

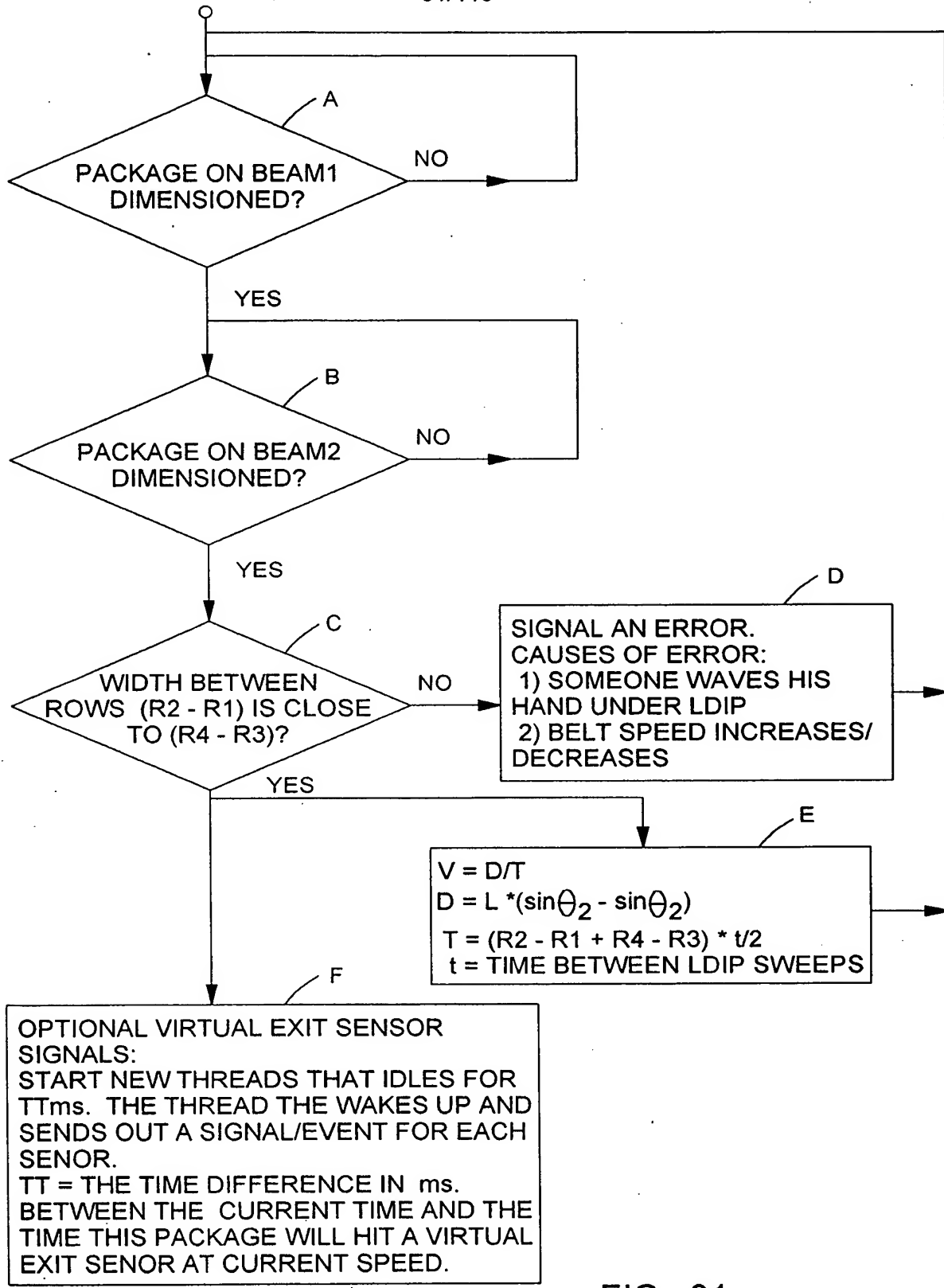


FIG. 31

82/116

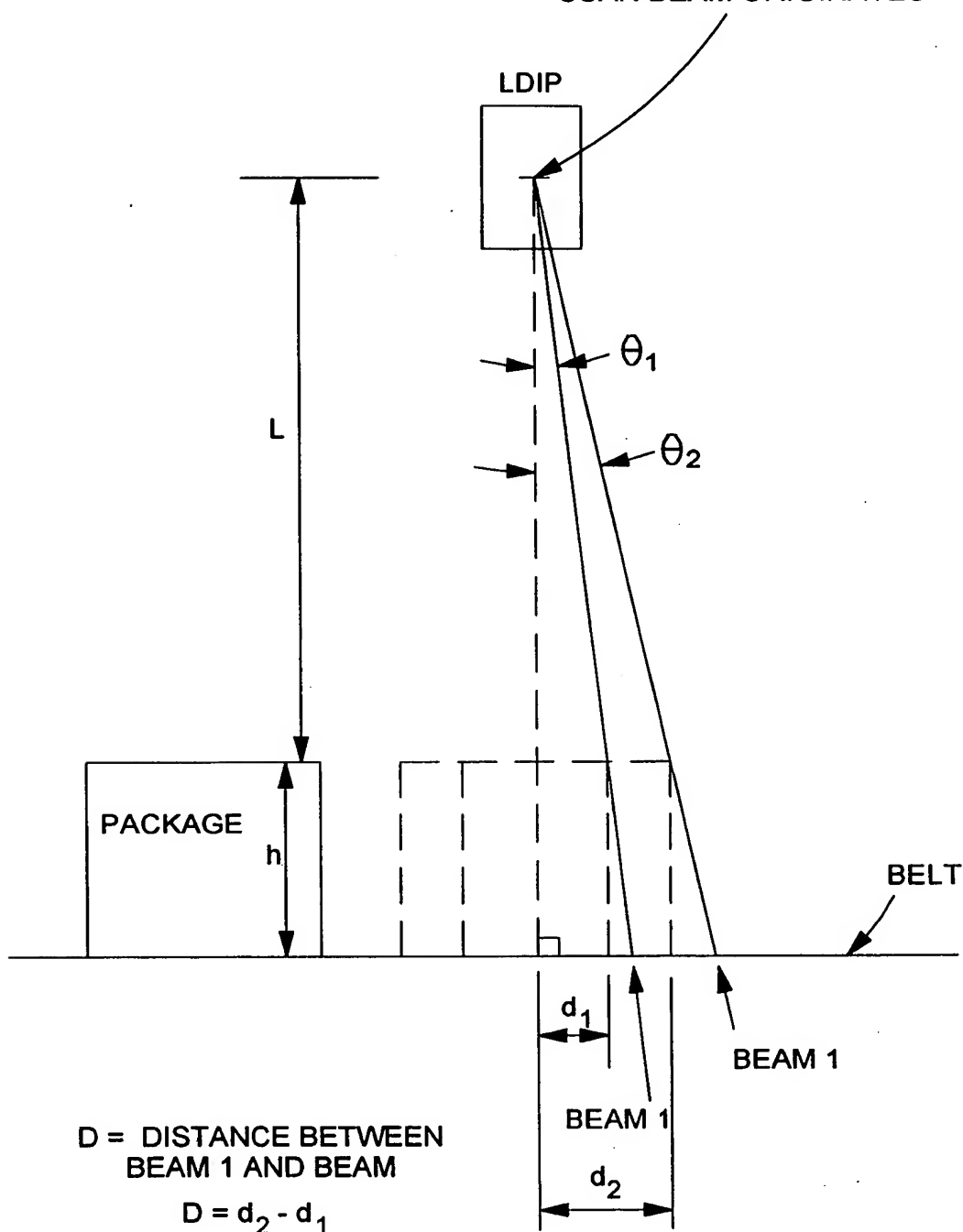
VIRTUAL POINT OF WHERE
SCAN BEAM ORIGINATES

FIG. 32

83/116

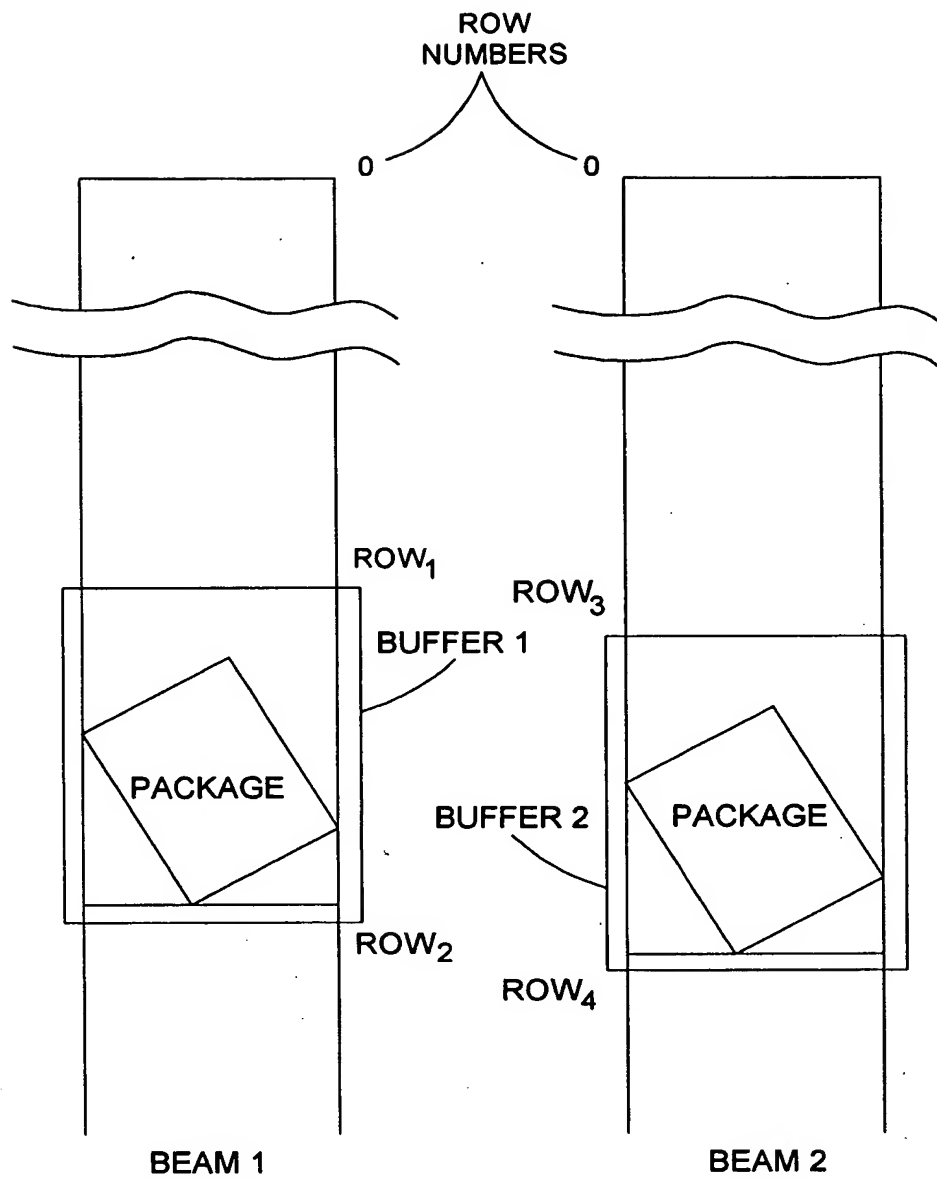


FIG. 33A

FIG. 33B

84/116

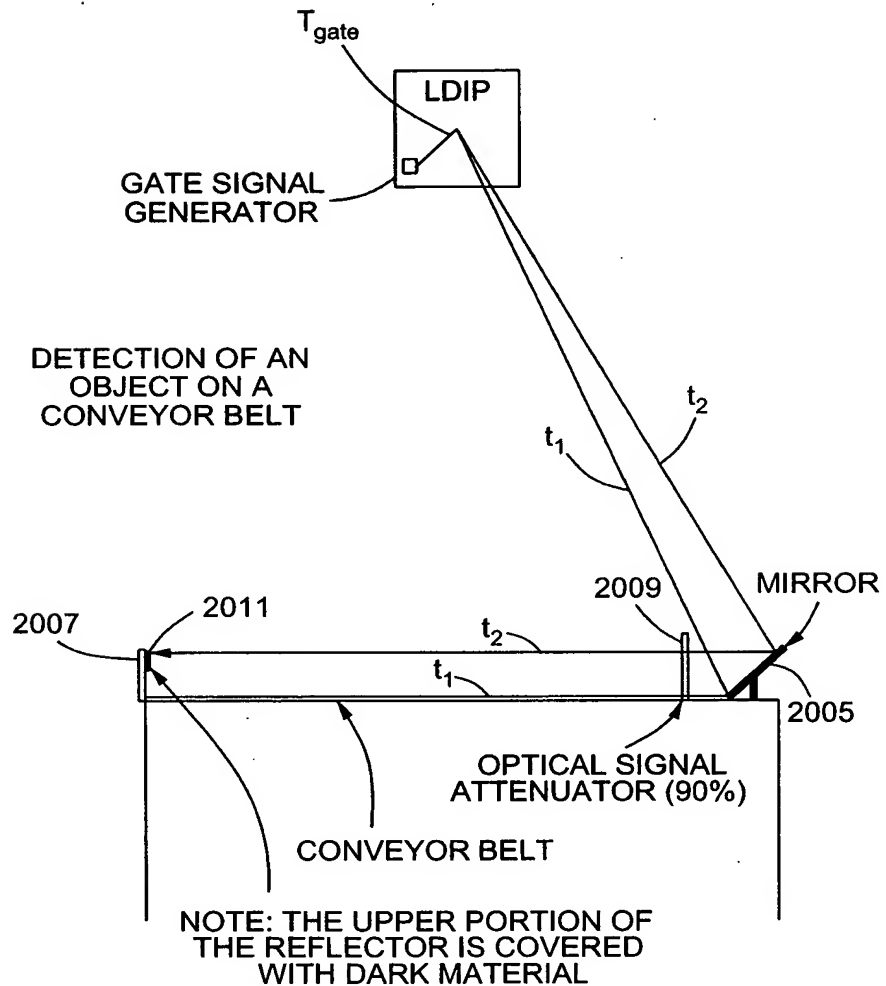
PACKAGE IN TUNNEL (PITT) INDICATION
SUBSYSTEM (500)

FIG. 33C

85/116

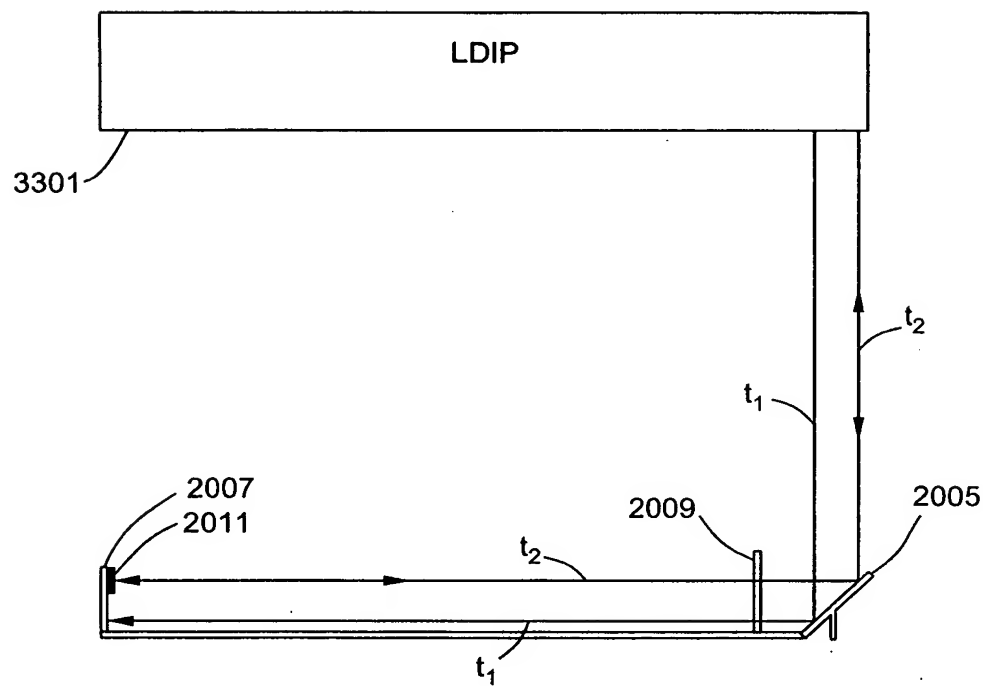


FIG. 33D

86/116

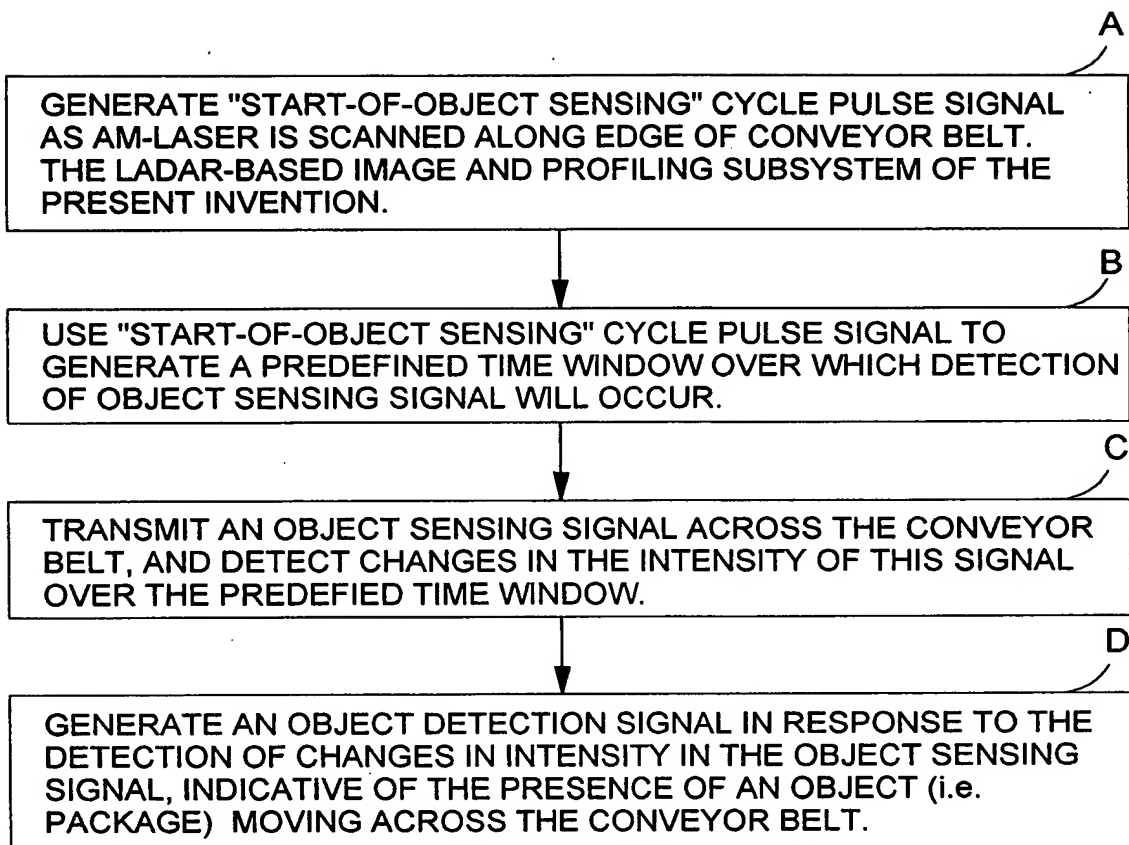


FIG. 34

87/116

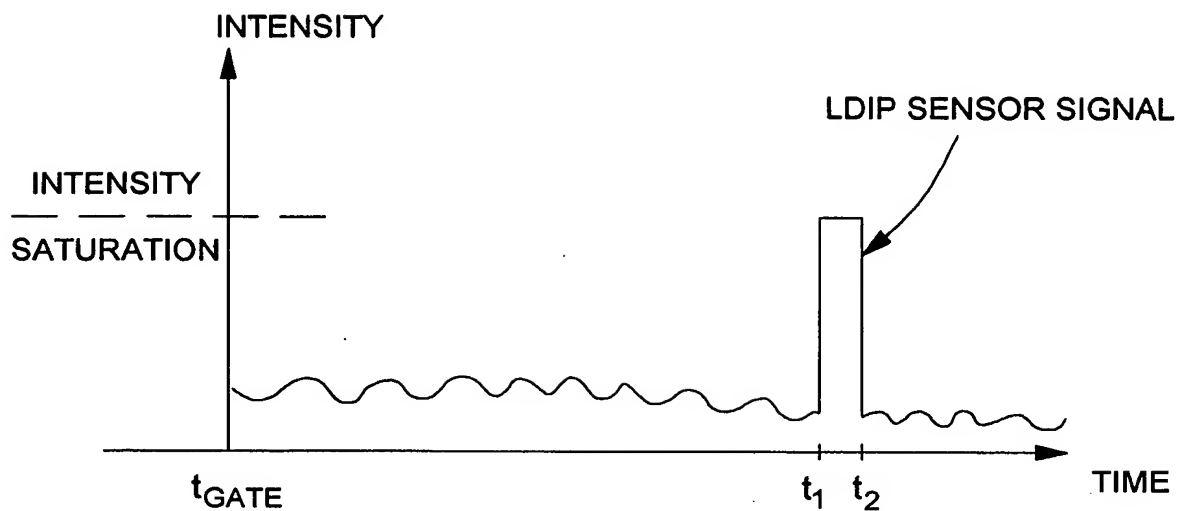


FIG. 35A

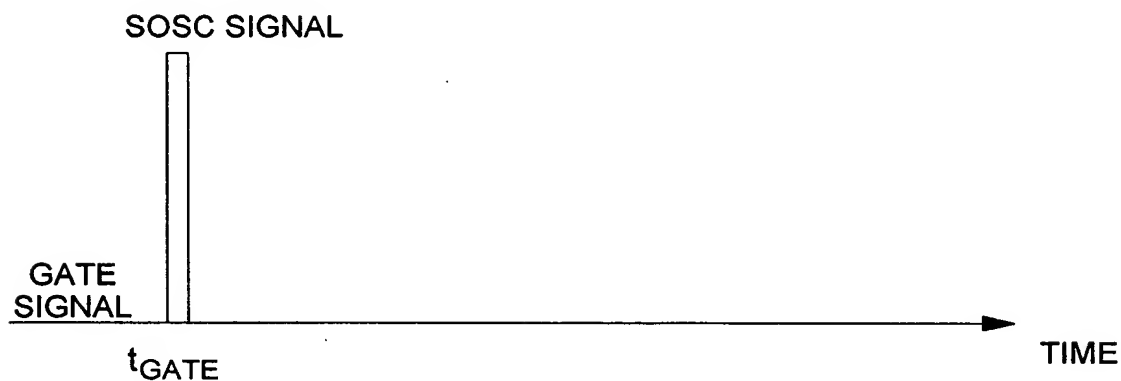


FIG. 35B

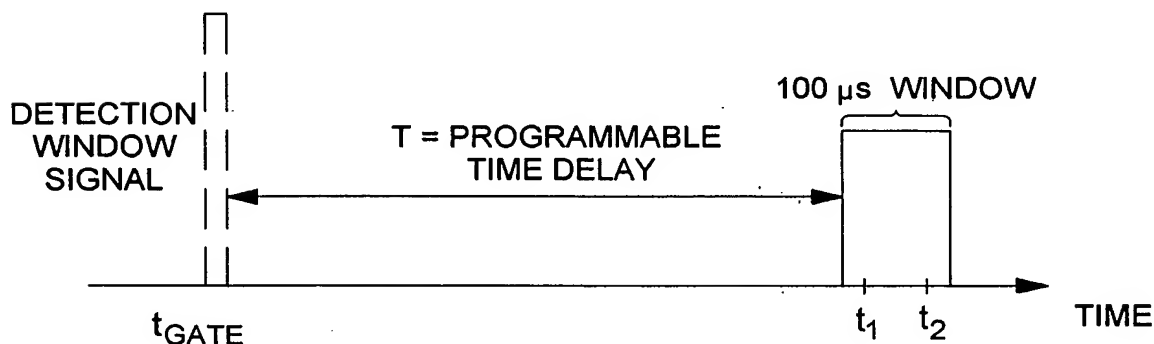


FIG. 35C

TABLE 1

TABLE 2

FIR FILTER TABS						
-0.2	0.25	-0.33	0.5	-1	0	1

FIG. 36A

88/116

TABLE 3

FIG. 36C

89/116

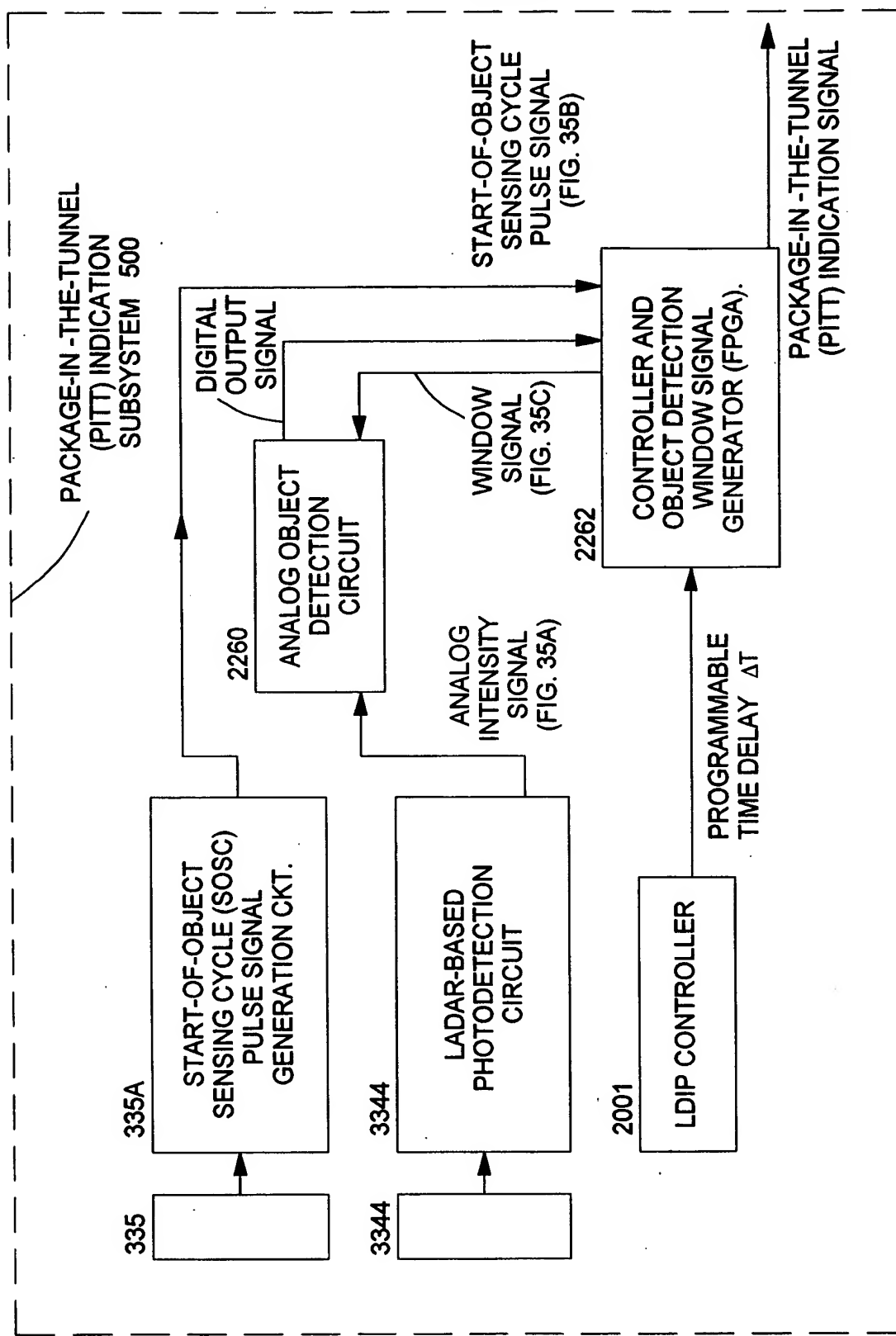


FIG. 37

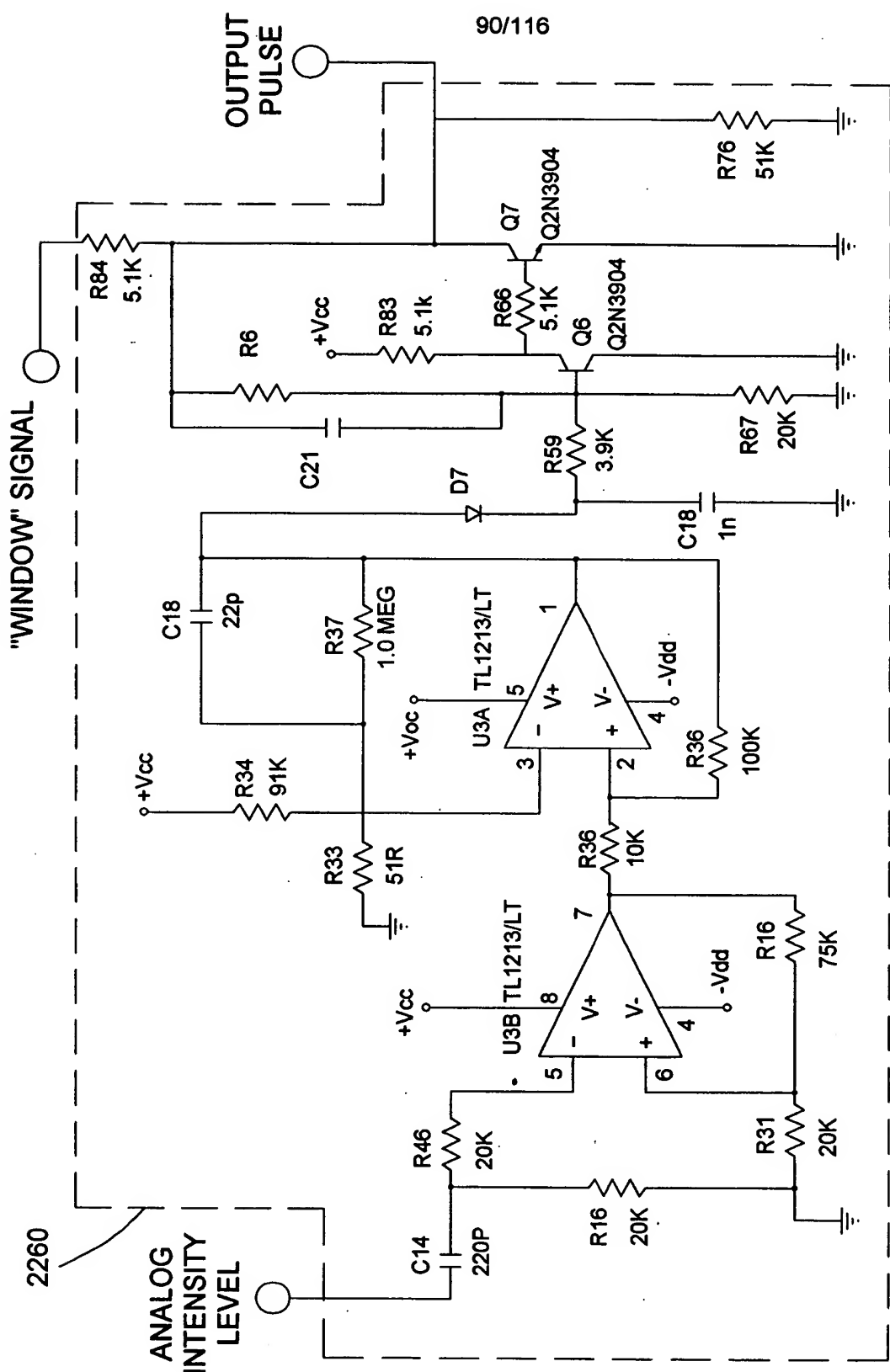
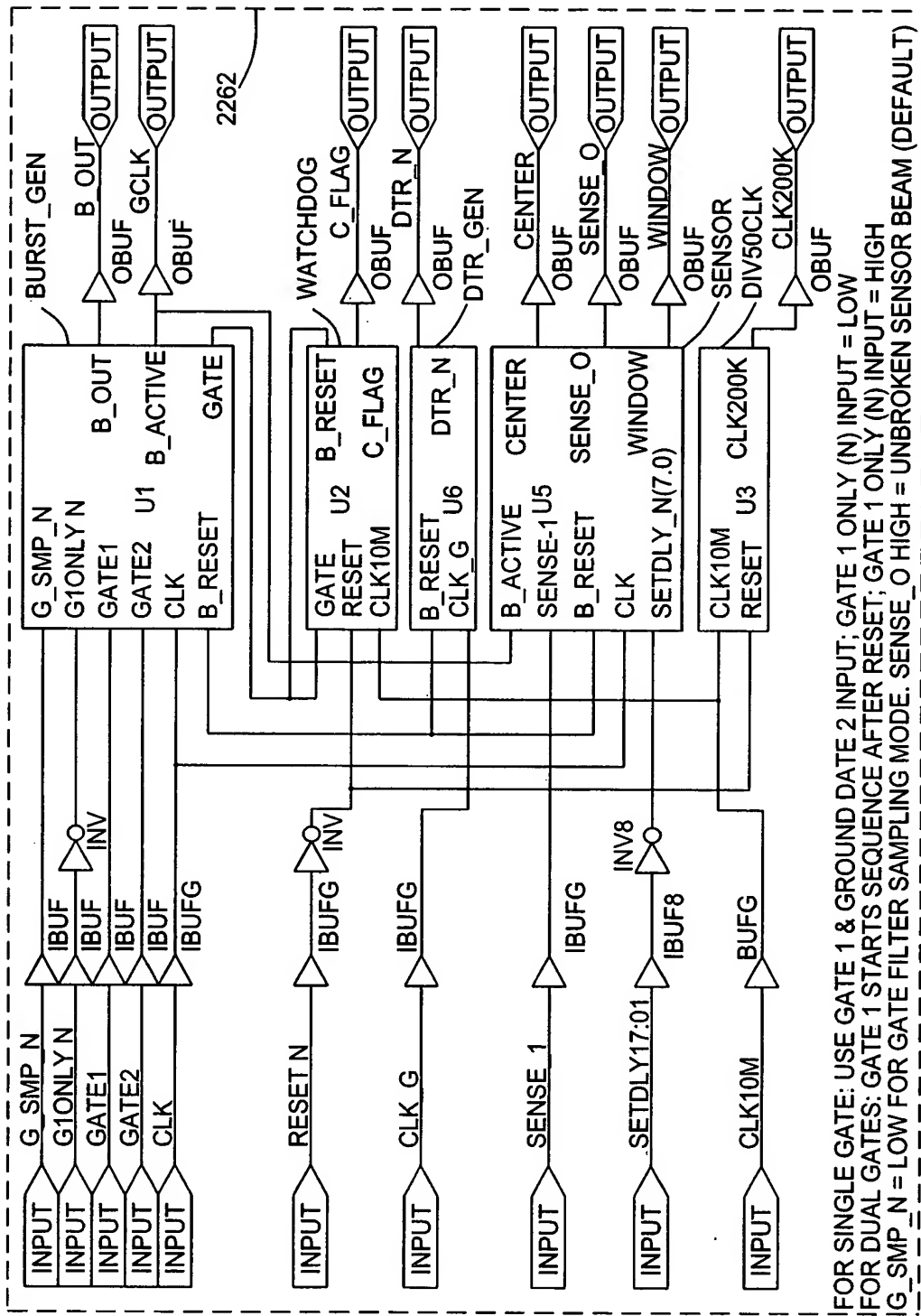


FIG. 38

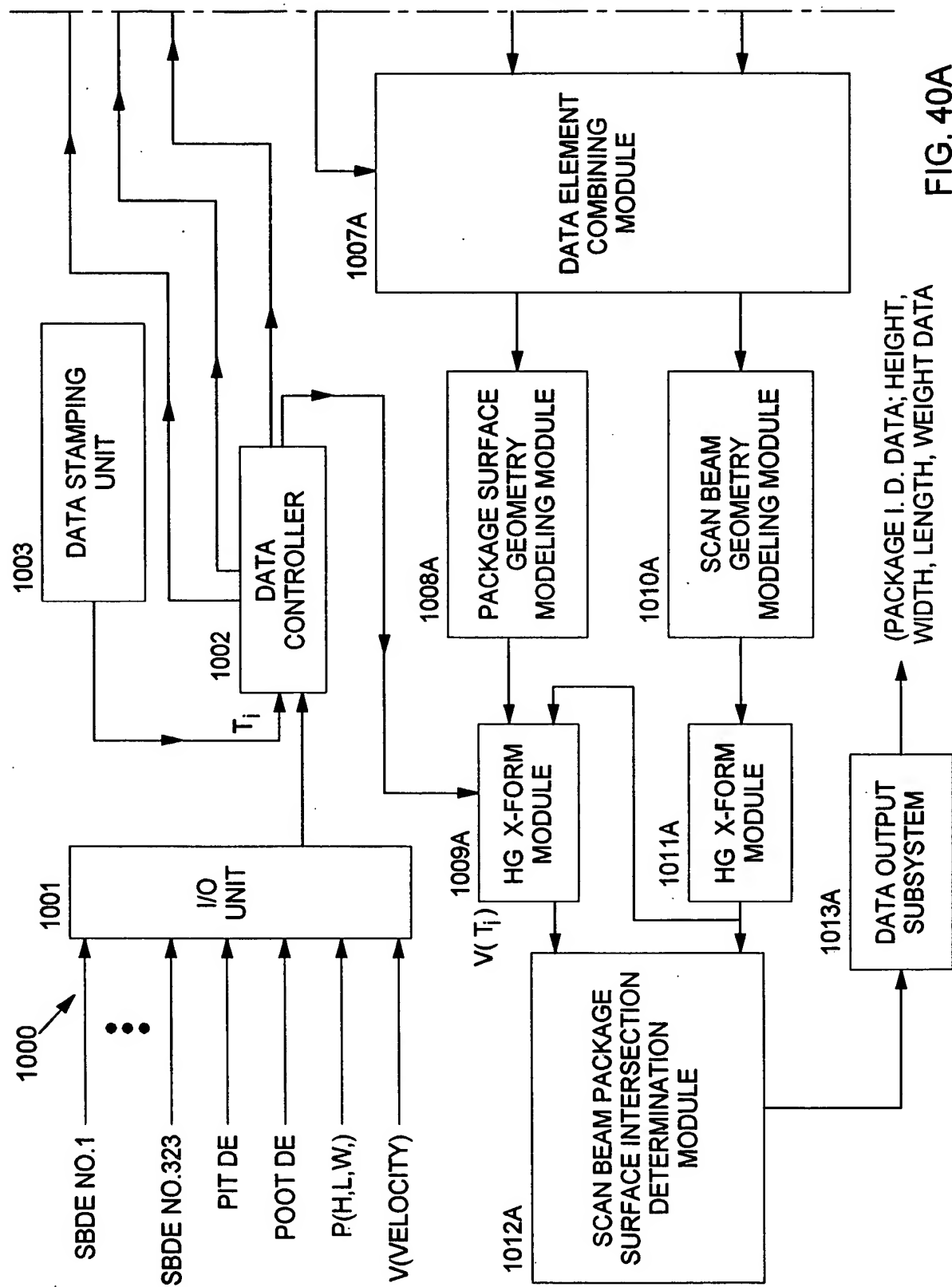
91/116



FOR SINGLE GATE: USE GATE 1 & GROUND GATE 2 INPUT; GATE 1 ONLY (N) INPUT = LOW
 FOR DUAL GATES: GATE 1 STARTS SEQUENCE AFTER RESET; GATE 1 ONLY (N) INPUT = HIGH
 G_SMP_N = LOW FOR GATE FILTER SAMPLING MODE. SENSE_O HIGH = UNBROKEN SENSOR BEAM (DEFAULT)

FIG. 39

92/116



93/116

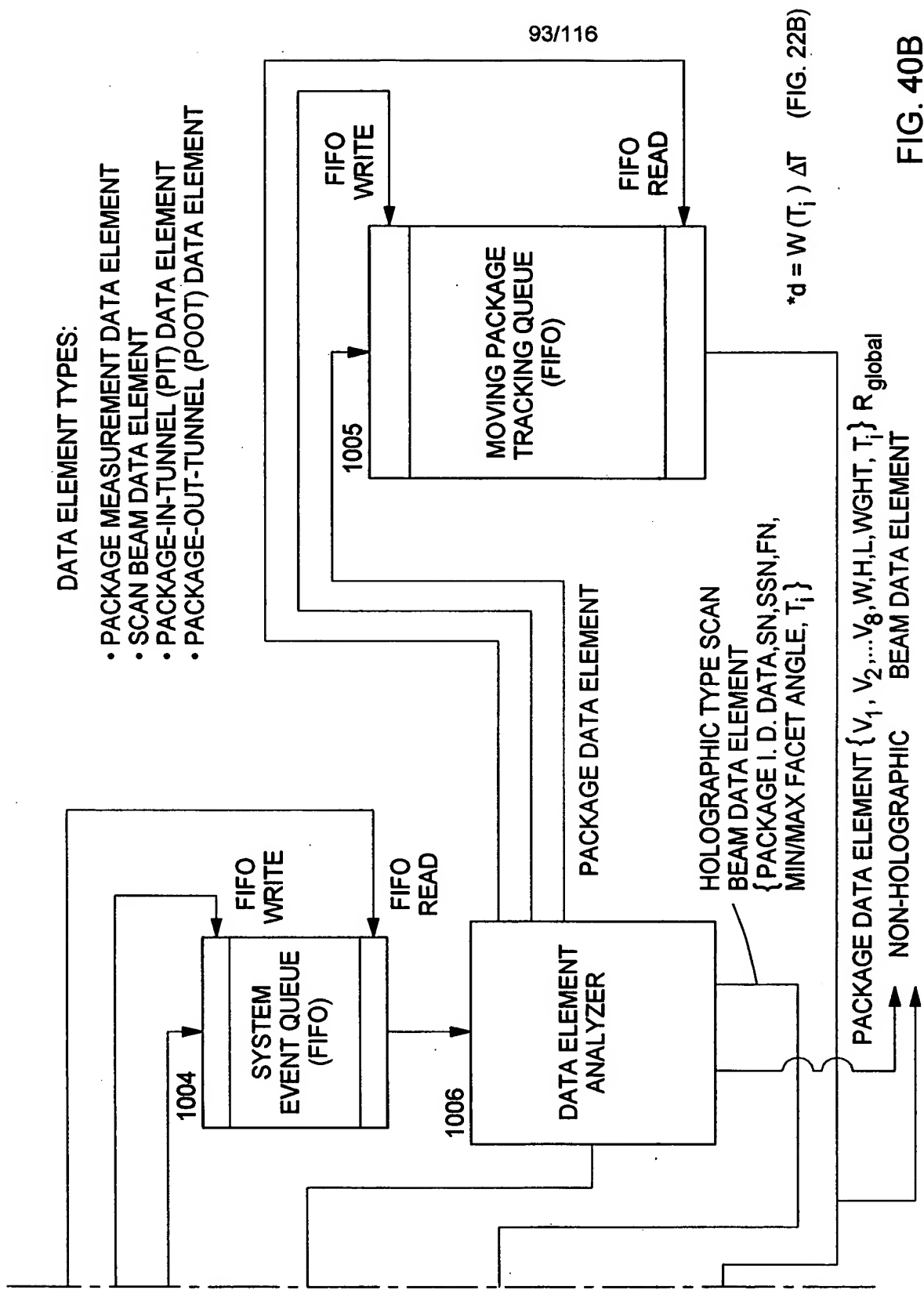


FIG. 40B

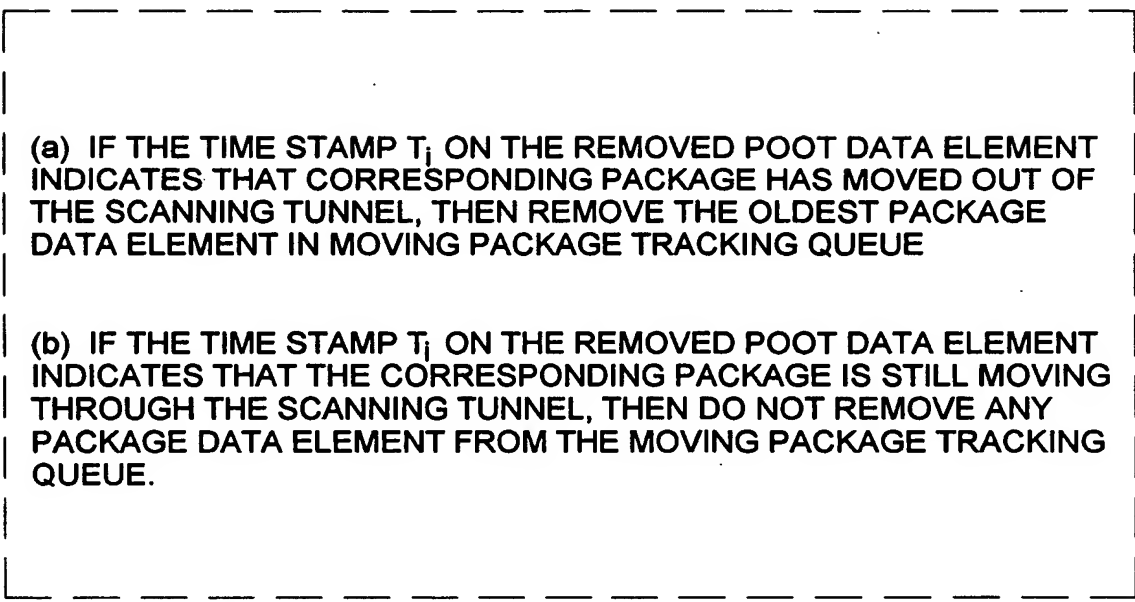
94/116

DATA ELEMENT HANDLING RULES

- 1. WHEN A PACKAGE DATA ELEMENT (PDE) OF ANY TYPE IS REMOVED FROM THE SYSTEM EVENT QUEUE, THEN IT IS PLACED IN THE MOVING PACKAGE TRACKING QUEUE**
- 2. WHEN A SCAN BEAM DATA ELEMENT (SBDE) IS REMOVED FROM THE SYSTEM EVENT QUEUE, THEN IT IS COMBINED WITH EACH PACKAGE DATA ELEMENT IN THE MOVING PACKAGE TRACKING QUEUE AND THEN EACH RESULTING DATA ELEMENT PAIR IS PROCESSED ALONG THE PACKAGE DATA ELEMENT CHANNEL AND SCAN DATA ELEMENT CHANNEL AS SHOWN IN FIGS. 40A & 40B**
- 3. WHEN A PACKAGE-IN-TUNNEL (PIT) DATA ELEMENT IS REMOVED FROM THE SYSTEM EVENT QUEUE, THEN THE OLDEST PACKAGE DATA ELEMENT IN THE MOVING PACKAGE TRACKING QUEUE IS REMOVED THERE FROM**
- 4. WHEN A PACKAGE OUT-OF TUNNEL (POOT) DATA ELEMENT IS REMOVED FROM THE SYSTEM EVENT QUEUE, THEN THE FOLLOWING OPERATIONS ARE CARRIED OUT**

FIG. 41A

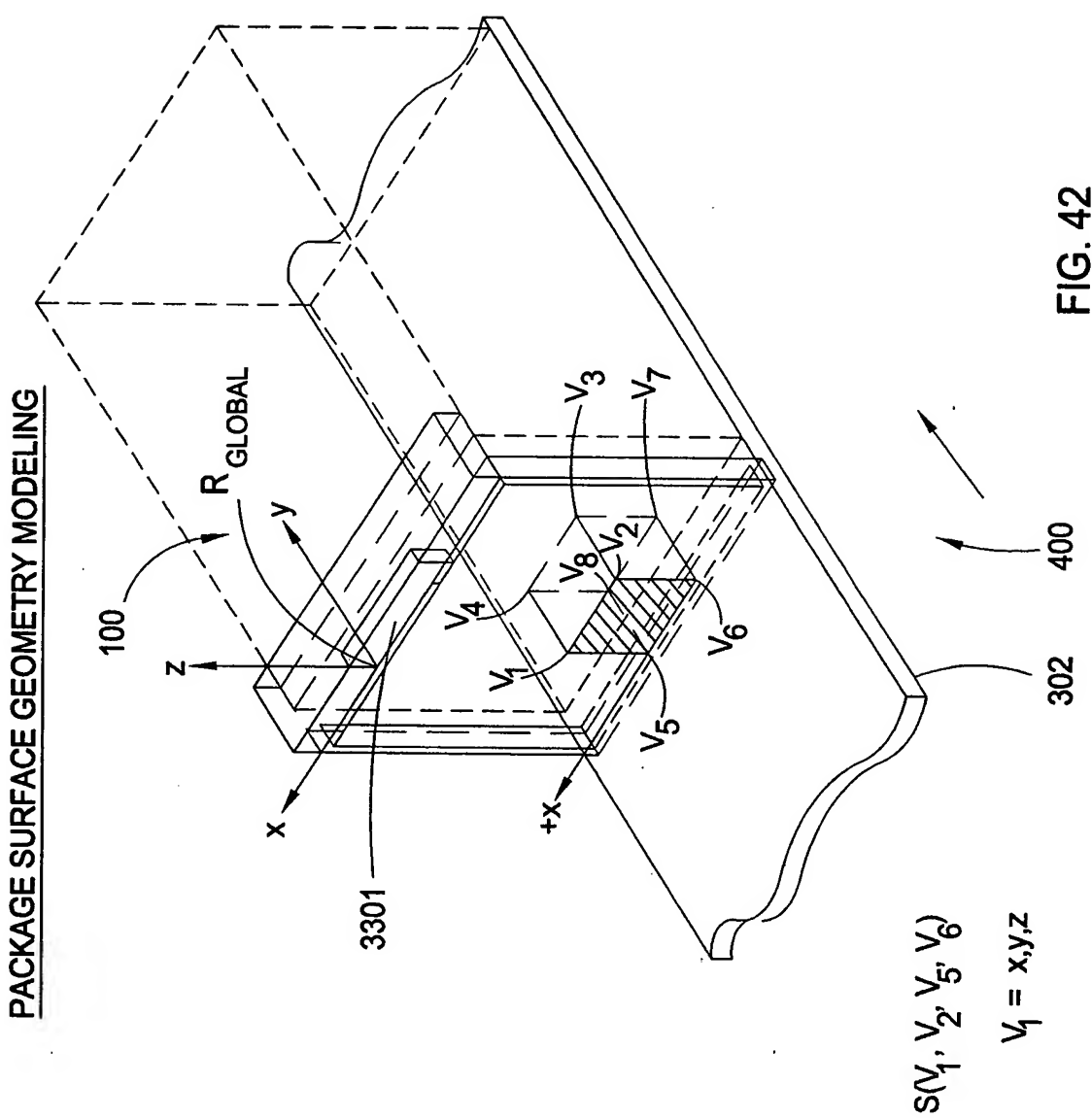
95/116



- (a) IF THE TIME STAMP T_i ON THE REMOVED POOT DATA ELEMENT INDICATES THAT CORRESPONDING PACKAGE HAS MOVED OUT OF THE SCANNING TUNNEL, THEN REMOVE THE OLDEST PACKAGE DATA ELEMENT IN MOVING PACKAGE TRACKING QUEUE
- (b) IF THE TIME STAMP T_i ON THE REMOVED POOT DATA ELEMENT INDICATES THAT THE CORRESPONDING PACKAGE IS STILL MOVING THROUGH THE SCANNING TUNNEL, THEN DO NOT REMOVE ANY PACKAGE DATA ELEMENT FROM THE MOVING PACKAGE TRACKING QUEUE.

FIG. 41B

96/116



97/116

**VECTOR-BASED SURFACE MODELING OF PACKAGES MOVING
IN SCANNING TUNNEL**

**MATHEMATICAL FORM OF EACH SURFACE ON THE PACKAGE:
VECTOR-BASED MODEL CONSISTING OF (1) AT LEAST THREE
VERTEX POINTS WITHIN THE PLANE OF THE PACKAGE SURFACE,
AND (2) NORMAL VECTOR FOR THE PLANE.**

PROCEDURE:

- (1) USE POSITION VECTOR (REFERENCED TO $X=0, Y=0, Z=0$ IN R_{global}), FOR SPECIFYING THE POSITION OF EACH VERTEX IN THE PACKAGE SURFACE PLANE; AND**
- (2) USE NORMAL VECTOR FOR SPECIFYING THE SURFACE DIRECTION OF THE PACKAGE SURFACE (AT WHICH LIGHT REFLECTS)**
- (3) USE THESE FOUR VECTORS TO SPECIFY THE SURFACE OR THE PACKAGE IN COORDINATE REFERENCE FROM R_{global}**

FIG. 43

98/116

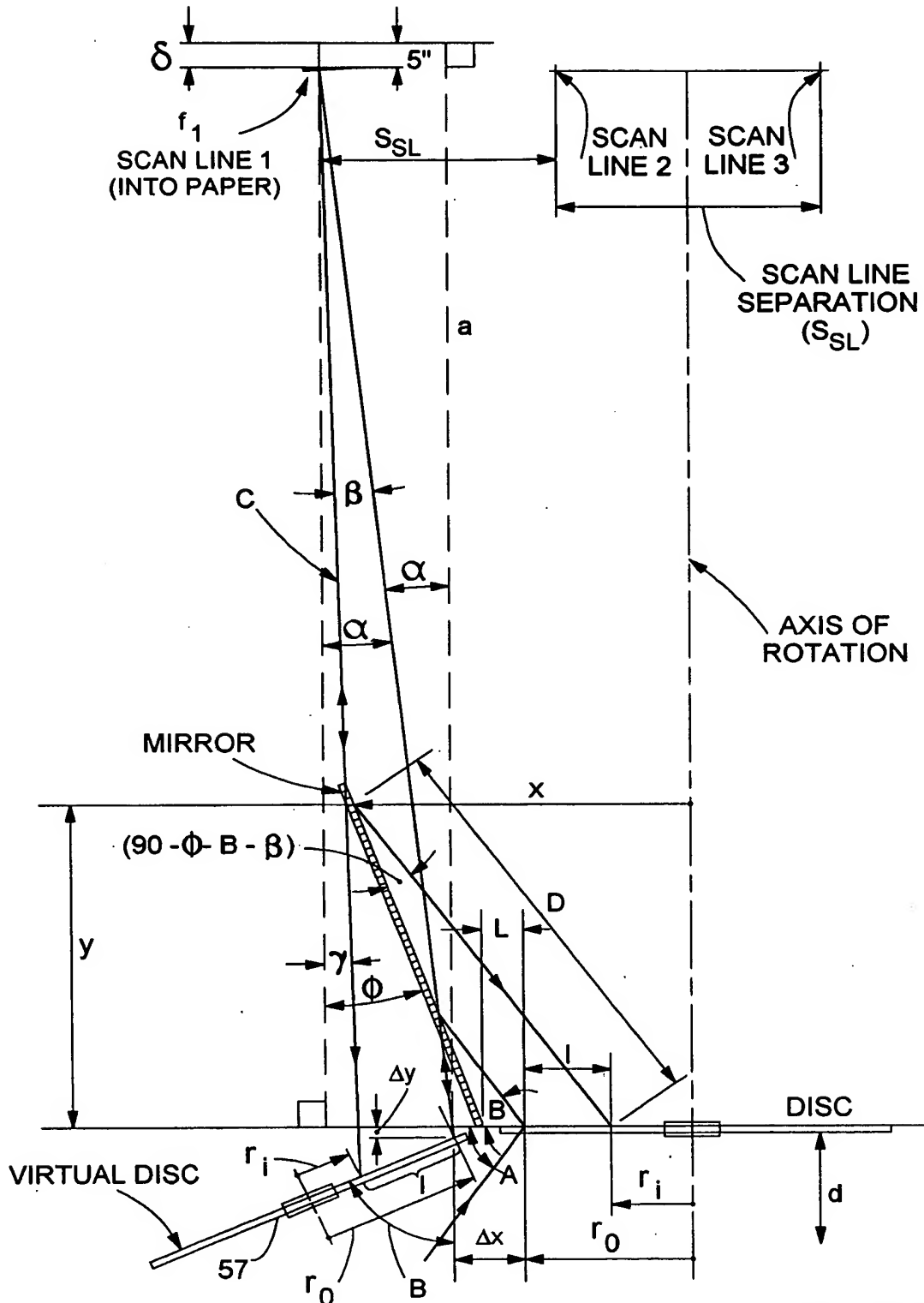
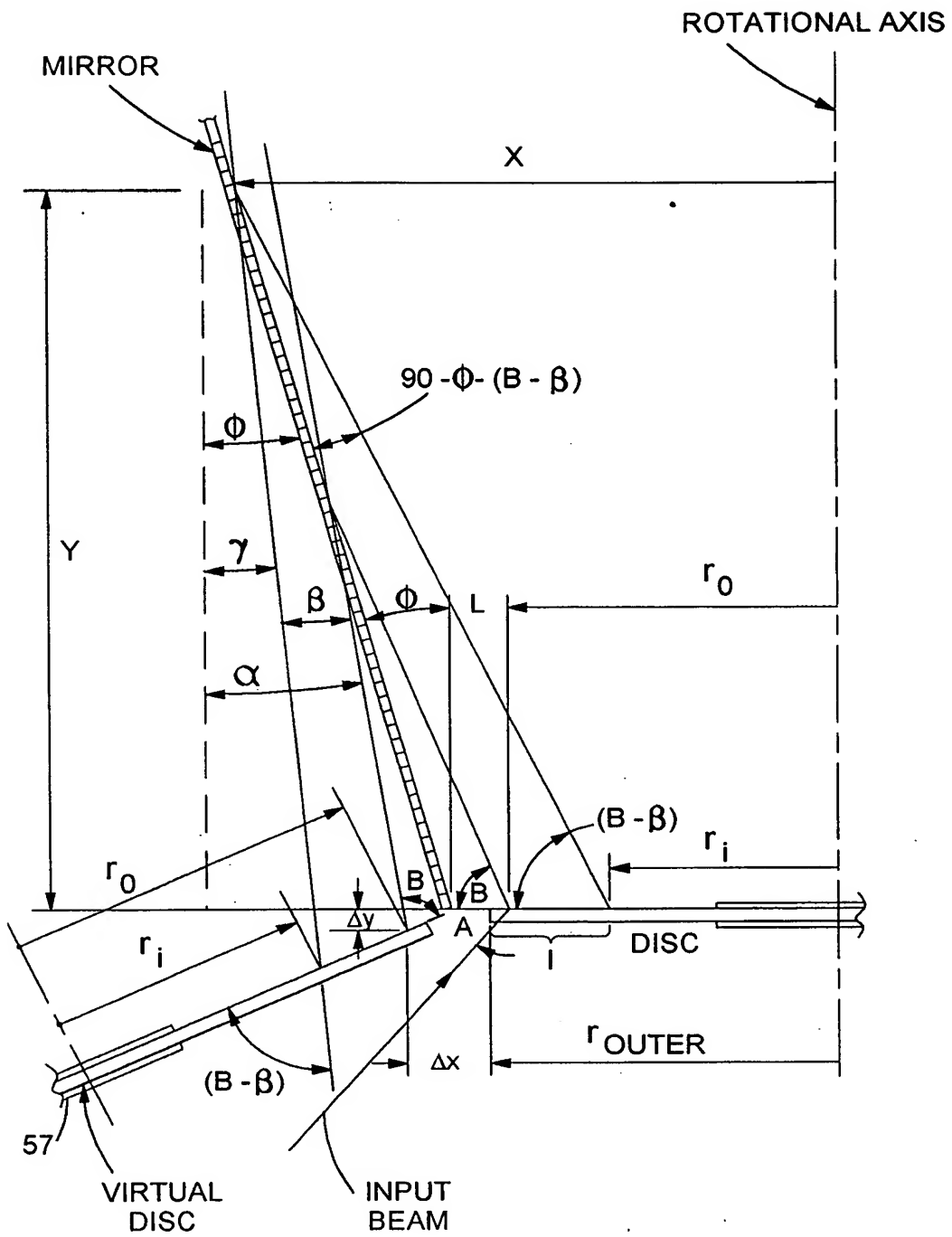


FIG. 44A1

99/116



β = ANGULAR RANGE OF
RETURN BEAM RAY ANGLES

FIG. 44A2

100/116

- (1) THE RADIUS TO BEAM-INCIDENT-POINT ON THE HOLOGRAPHIC SCANNING DISC, ASSIGNED THE SYMBOLIC NOTATION " r_0 "
- (2) SCANLINE SEPARATION BETWEEN ADJACENT SCANLINES AT THE FOCAL PLANE OF THE (i,j)-TH SCANLINE, ASSIGNED THE SYMBOLIC NOTATION " s_{SL} "
- (3) THE SCANLINE LENGTH (MEASURED INTO PAPER) FOR THE (i,j)-TH SCANLINE, ASSIGNED THE SYMBOLIC NOTATION " L_{SL} "
- (4) THE DISTANCE MEASURED FROM THE SCANNING DISC TO THE FOCAL PLANE OF THE (i,j)-TH SCANLINE, ASSIGNED THE SYMBOLIC NOTATION a_i
- (5) THE DISTANCE FROM RADIUS TO BEAM-INCIDENT-POINT r_0 TO BEAM FOLDING MIRROR, ASSIGNED THE SYMBOLIC NOTATION "L"
- (6) THE TILT ANGLE OF THE J-TH BEAM FOLDING MIRROR ASSOCIATED WITH GENERATION OF THE (i,j)-TH SCANLINE, ASSIGNED THE SYMBOLIC NOTATION " ϕ_j "
- (7) THE TILT ANGLE OF THE VIRTUAL SCANNING DISC, ASSIGNED THE SYMBOLIC NOTATION " 2ϕ "
- (8) THE LATERAL SHIFT OF THE BEAM INCIDENT POINT ON THE VIRTUAL SCANNING DISC, ASSIGNED THE SYMBOLIC NOTATION " Δx "
- (9) THE VERTICAL SHIFT OF THE BEAM INCIDENT POINT ON THE VIRTUAL SCANNING DISC, ASSIGNED THE SYMBOLIC NOTATION " Δy "
- (10) THE DISTANCE FROM THE ROTATION AXIS TO THE BEAM INCIDENT POINT ON THE VIRTUAL SCANNING DISC, ASSIGNED THE SYMBOLIC NOTATION " $r_0 + \Delta x$ "
- (11) THE DISTANCE FROM THE BEAM INCIDENT POINT ON THE VIRTUAL SCANNING DISC TO THE FOCAL PLANE WITHIN WHICH THE (i,j)-TH SCANLINE RESIDES, ASSIGNED THE SYMBOLIC NOTATION " f_i "
- (12) THE DIAMETER OF THE CROSS-SECTION OF THE LASER BEAM SCANNING STATION, ASSIGNED THE SYMBOLIC NOTATION " d_{BEAM} "
- (13) THE ANGULAR GAP BETWEEN ADJACENT HOLOGRAPHIC SCANNING FACETS, ASSIGNED THE SYMBOLIC NOTATION " d_{GAP} "
- (14) THE OUTER RADIUS OF THE AVAILABLE LIGHT COLLECTION REGION ON THE HOLOGRAPHIC SCANNING DISC, ASSIGNED THE SYMBOLIC NOTATION " r_{OUTER} "

FIG. 44B1

(15) THE INNER RADIUS OF THE AVAILABLE LIGHT COLLECTION REGION ON THE HOLOGRAPHIC SCANNING FACET, ASSIGNED THE SYMBOLIC NOTATION " r_{INNER} "

(16) ONE-HALF OF THE DEPTH OF FIELD OF THE (i, j)-TH SCANLINE, ASSIGNED THE SYMBOLIC NOTATION " δ "

(17) THE DISTANCE FROM THE MAXIMUM READ DISTANCE ($f_i + 5"$) TO THE INNER RADIUS r_i OF THE SCANNING FACET, ASSIGNED THE SYMBOLIC NOTATION "C"

(18) THE OUTER RAY ANGLE MEASURED RELATIVE TO THE NORMAL TO THE i-TH HOLOGRAPHIC FACET, ASSIGNED THE SYMBOLIC NOTATION " α "

(19) THE INNER RAY ANGLE MEASURED RELATIVE TO THE NORMAL TO THE i-TH HOLOGRAPHIC FACET, ASSIGNED THE SYMBOLIC NOTATION " γ "

(20) THE LIGHT COLLECTION ANGLE MEASURED FROM THE FOCAL POINT OR THE i-TH FACET TO THE LIGHT COLLECTION AREA OF THE SCANNING FACET, ASSIGNED THE SYMBOLIC NOTATION " β "

(21) THE INTERSECTION OF THE BEAM FOLDING MIRROR AND LINE C, ASSIGNED THE SYMBOLIC NOTATION "X"

(21A) THE INTERSECTION OF THE BEAM FOLDING MIRROR AND LINE C, ASSIGNED THE SYMBOLIC NOTATION "Y"

(22) THE DISTANCE MEASURED FROM THE INNER RADIUS TO THE POINT OF MIRROR INTERSECTION, ASSIGNED THE SYMBOLIC NOTATION "D"

(23) THE DISTANCE MEASURED FROM THE BASE OF THE SCANNER HOUSING TO THE TOP OF THE j-TH BEAM FOLDING MIRROR, ASSIGNED THE SYMBOLIC NOTATION "h"

(24) THE DISTANCE MEASURED FROM THE SCANNING DISC TO THE "d" BASE OF THE HOLOGRAPHIC, ASSIGNED THE SYMBOLIC NOTATION

(25) THE FOCAL LENGTH OF THE i-TH HOLOGRAPHIC SCANNING FACET FROM THE CORRESPONDING FOCAL PLANE WITHIN THE SCANNING VOLUME, ASSIGNED THE SYMBOLIC NOTATION " f_i "

(26) INCIDENT BEAM ANGLE, ASSIGNED THE SYMBOLIC NOTATION " A_i "

(27) DIFFRACTED BEAM ANGLE, ASSIGNED THE SYMBOLIC NOTATION " B_i "

FIG. 44B2

102/116

(28) THE ANGLE OF THE J-TH LASER BEAM MEASURED FROM THE VERTICAL, ASSIGNED THE SYMBOLIC NOTATION " $-\alpha$ "

(29) THE SCAN ANGLE OF THE LASER BEAM, ASSIGNED THE SYMBOLIC NOTATION " θ_{si} "

(30) THE SCAN MULTIPLICATION FACTOR FOR THE I-TH HOLOGRAPHIC FACET, ASSIGNED THE SYMBOLIC NOTATION " M_i "

(31) THE FACET ROTATION ANGLE FOR THE I-TH HOLOGRAPHIC FACET, ASSIGNED THE SYMBOLIC NOTATION " θ_{ROTi} "

(32) ADJUSTED FACET ROTATION ANGLE ACCOUNTING FOR DEADTIME, ASSIGNED THE SYMBOLIC NOTATION " θ'_{ROTi} "

(33) THE LIGHT COLLECTION EFFICIENCY FACTOR FOR THE I-TH HOLOGRAPHIC FACET, NORMALIZED RELATIVE TO THE 16TH FACET, ASSIGNED THE SYMBOLIC NOTATION " ξ_i "

(34) THE MAXIMUM LIGHT COLLECTION FOR THE I-TH HOLOGRAPHIC FACET, ASSIGNED THE SYMBOLIC NOTATION " $Area_i$ "

(35) THE BEAM SPEED AT THE CENTER OF THE (i, j)-TH SCANLINE, ASSIGNED THE SYMBOLIC NOTATION " V_{CENTER} "

(36) THE ANGLE OF SKEW OF THE DIFFRACTED LASER BEAM AT THE CENTER OF THE I-TH HOLOGRAPHIC FACET, ASSIGNED THE SYMBOLIC NOTATION " ϕ_{SKEW} "

(37) THE MAXIMUM BEAM SPEED OF ALL LASER BEAMS PRODUCED BY THE HOLOGRAPHIC SCANNING DISC, ASSIGNED THE SYMBOLIC NOTATION " V_{MAX} "

(38) THE MINIMUM BEAM SPEED OF ALL LASER BEAMS PRODUCED BY THE HOLOGRAPHIC SCANNING DISC, ASSIGNED THE SYMBOLIC NOTATION " V_{MIN} "

(39) THE RATIO OF THE MAXIMUM BEAM SPEED TO THE MINIMUM BEAM SPEED, ASSIGNED THE SYMBOLIC NOTATION " V_{MAX} / V_{MIN} "

(40) THE DEVIATION OF THE LIGHT RAYS REFLECTED OFF THE PARABOLIC LIGHT REFLECTING MIRROR BENEATH THE SCANNING DISC, FROM THE BRAGG ANGLE FOR THE FACET, ASSIGNED THE SYMBOLIC NOTATION " δ_e "

FIG. 44B3

103/116

**PARAMETER EQUATION USED IN THE SPREADSHEET
DESIGN OF THE SCANNER**

$$(1) \Delta x := L (1 + \cos(2\phi))$$

$$(2) \Delta y := L \sin(2\phi)$$

$$(3) \Delta y := r_0 + \Delta x$$

$$(4) C := \sqrt{(f + \delta)^2 + l^2 + 2(f + \delta)l \cos(B)}$$

LAW OF COSINES, WHERE: $l = r_{\text{outer}} - r_{\text{inner}}$

$$\beta = \alpha - \gamma = B + 2\phi - 90 - \gamma$$

$$(5) \alpha := B - 90 + 2\phi$$

$$(6) r := \alpha - \cos \left[\frac{(f + \delta)^2 + C^2 - l^2}{2(f + \delta)C} \right]$$

$$(7) \beta := \alpha - \gamma$$

$$(8) X := D \cos(B - \beta) + r_i$$

$$(9) Y := D \sin(B - \beta)$$

$$(10) D := \frac{[r_0 + L - r_i] \sin(90 + \gamma)}{\sin(90 - B + \beta - \phi)} \quad \text{LAW OF SINES}$$

$$(11) h := Y + d$$

FIG. 44C1

104/116

$$(12) \quad f_i := \sqrt{a_i^2 + [m S_{SL} - [r_0 + \Delta x]]^2}$$

m IS A FACTOR THAT VARIES FROM SCAN LINE TO SCAN LINE AND DETERMINED BY SCAN LINE SEPARATION AND DISTANCE FROM THE ROTATIONAL AXIS OF THE DISC.

$$(13) \quad B_i := \tan \left[\left[\frac{m S_{SL} - [r_0 + \Delta x]}{a_i} \right] \right] + 90 - 2\phi$$

$$(14) \quad \Phi_{Si} := 2 \tan \left[\left[\frac{\frac{1}{2} \text{ScanLineLength}}{f_i} \right] \right]$$

$$(15) \quad M_i := \frac{r_0}{f_i} + \cos(\lambda_1) + \cos(B_i)$$

$$(16) \quad \Theta_{roti} := \frac{\Theta_{Si}}{M_i}$$

$$(17) \quad \Theta'_{roti} := \Theta_{roti} + \underbrace{\frac{d_{beam}}{r_0} + \frac{d_{gap}}{r_0}}_{\Theta_{dead}}$$

$$(18) \quad \xi_i := \left[\frac{f_i}{f_{16}} \right]^2 \frac{\sin[B_{16}]}{\sin(B_i)} H_i$$

$$(19) \quad \text{Area}_i := \pi \left[r_{\text{outer}}^2 + r_{\text{inner}}^2 \right] \frac{\xi_i}{\sum_{i=1}^{16} [\xi_i]} \quad i = 1, 2, \dots, 16$$

FIG. 44C2

105/116

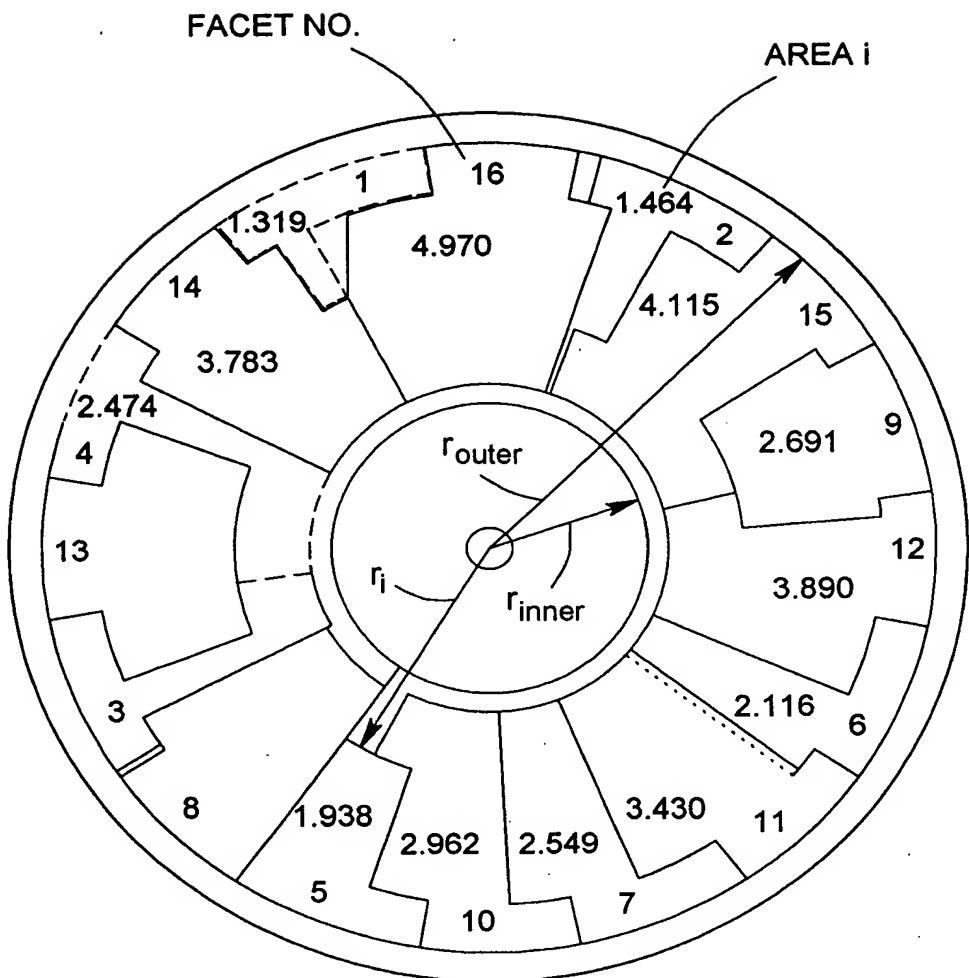


FIG. 44D

106/116

**VECTOR MODELING OF LASER SCAN BEAMS IN
HOLOGRAPHIC SCANNING SUBSYSTEMS**

**MATHEMATICAL FORM FOR EACH LASER SCAN BEAM:
VECTOR-BASED MODEL OF OPTICAL PATH OF BEAM FROM DISC TO
MIRROR TO FOCAL PLANE (∞)**

PROCEDURE:

- (1) USE POSITION VECTOR REFERENCED FROM $X=0, Y=0, Z=0$ IN $R_{\text{local scanner}}$ FOR SPECIFYING THE STARTING POINT OF LASER SCAN BEAM ON DISC, AND DIRECTION VECTOR FOR SPECIFYING THE DIRECTION OF LASER BEAM THE BEAM FOLDING MIRROR; AND
- (2) USE POSITION VECTOR FOR SPECIFYING POINT ON MIRROR WHERE BEAM IS REFLECTED FROM BEAM FOLDING MIRROR TOWARDS FOCAL PLANE OF FACET, EXTENDING TO INFINITY, AND DIRECTION VECTOR FOR SPECIFYING THE DIRECTION OF LASER BEAM TOWARDS DESIGNATED FOCAL PLANE
- (3) THESE FOUR VECTORS SPECIFY THE LASER BEAM RAY IN LOCAL COORDINATE REFERENCE $R_{\text{local scanner}}$

FIG. 45

107/116

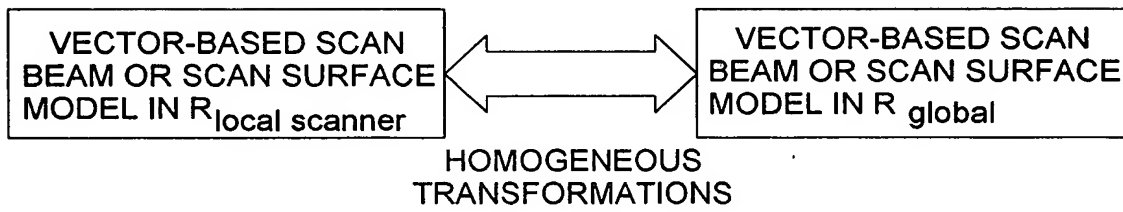
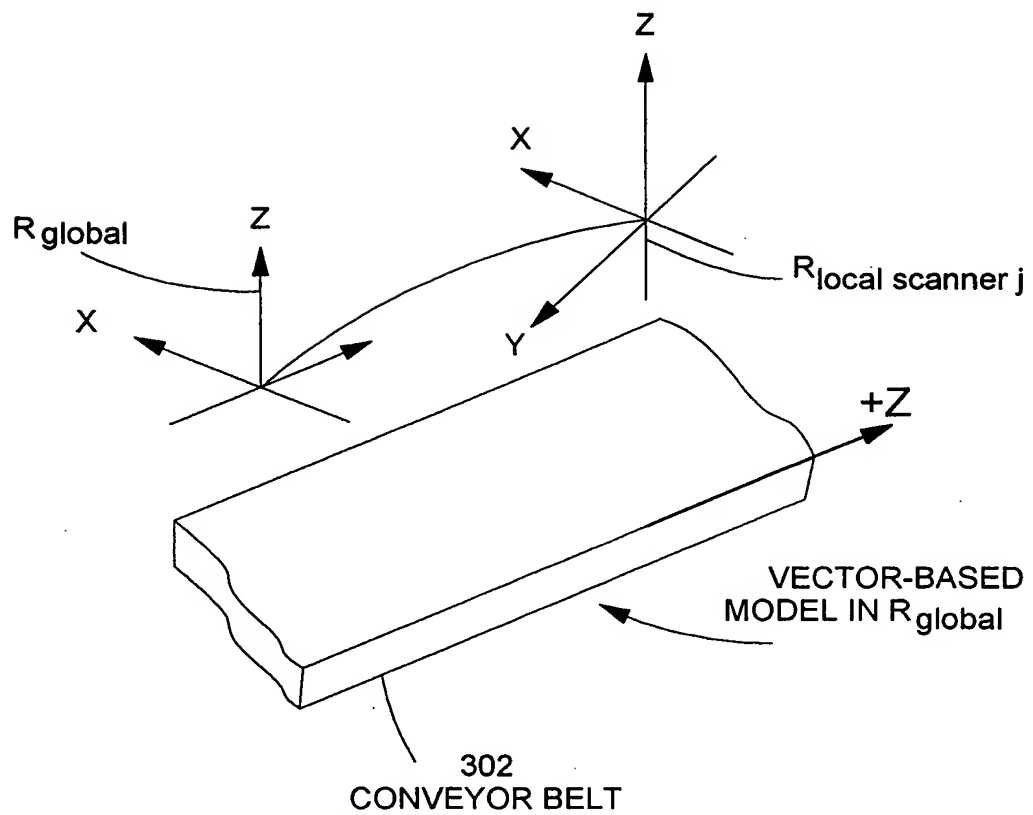
VECTOR-BASED
MODEL IN $R_{\text{local scanner}}$ 

FIG. 46

108/116

COORDINATE CONVERSION OF VECTOR-BASED MODELS OF
PACKAGE SURFACES

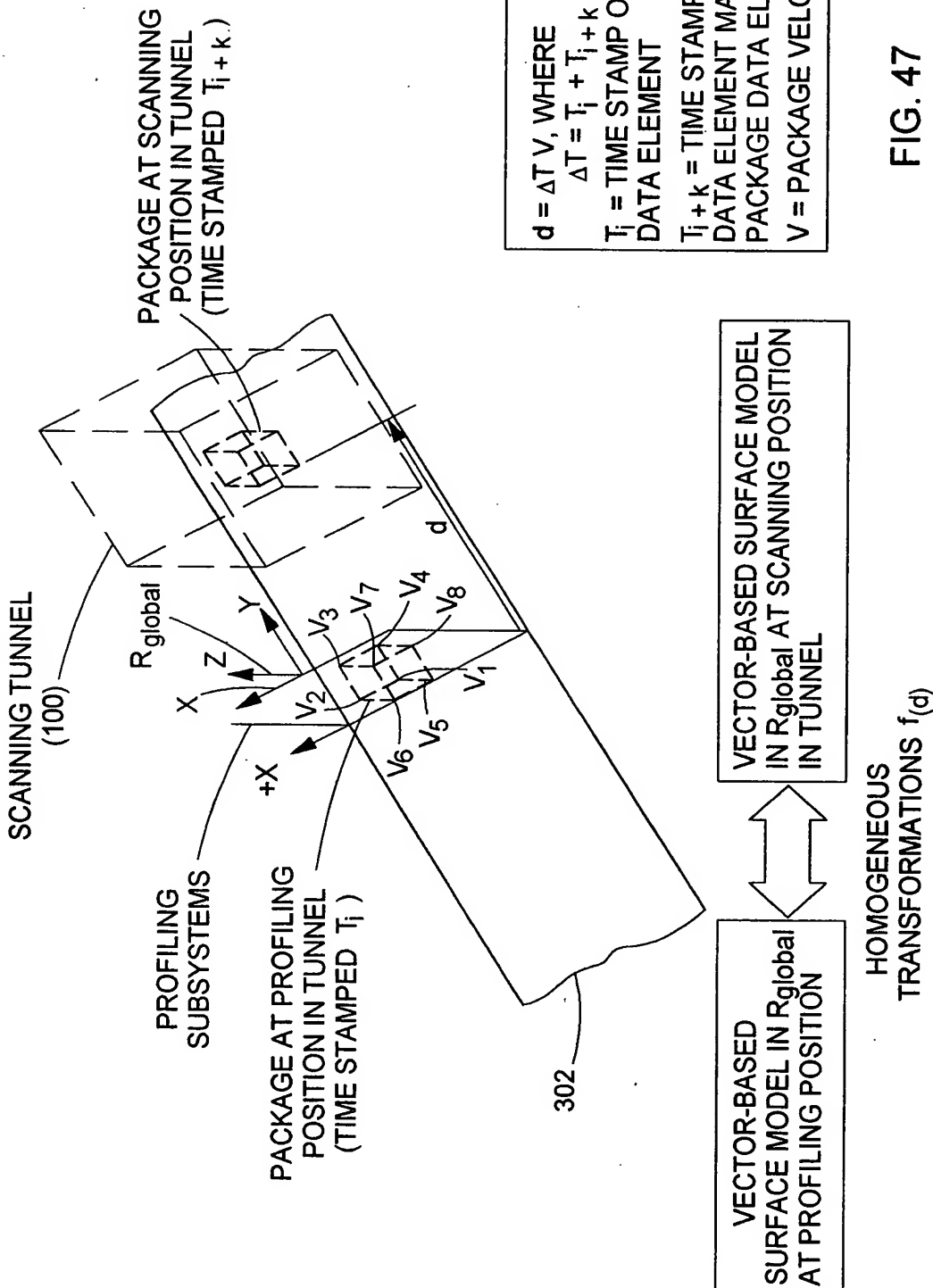
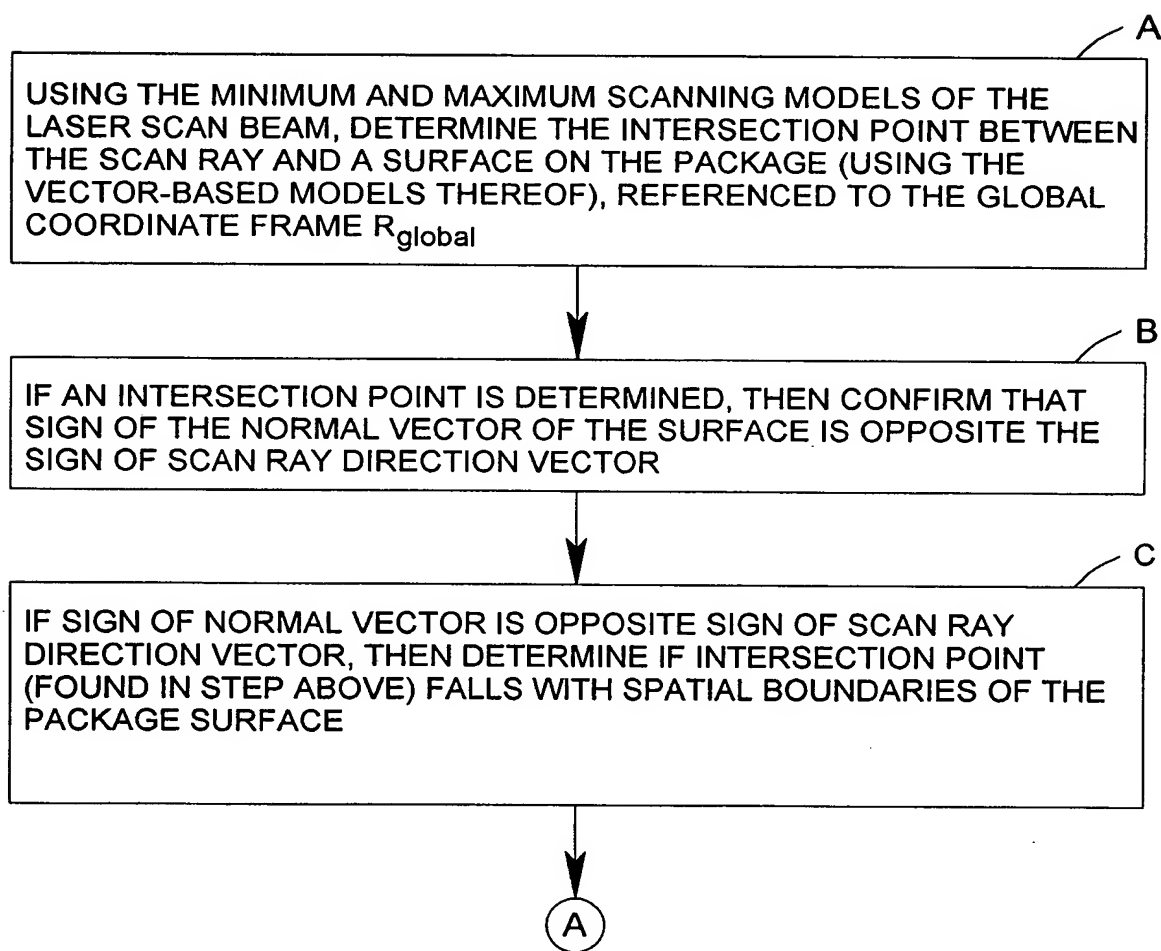


FIG. 47

109/116

**SCAN BEAM/PACKAGE SURFACE INTERSECTION DETERMINATION
METHOD FOR SCAN DATA ELEMENTS PRODUCED FROM
HOLOGRAPHIC SCANNING SUBSYSTEMS**



110/116

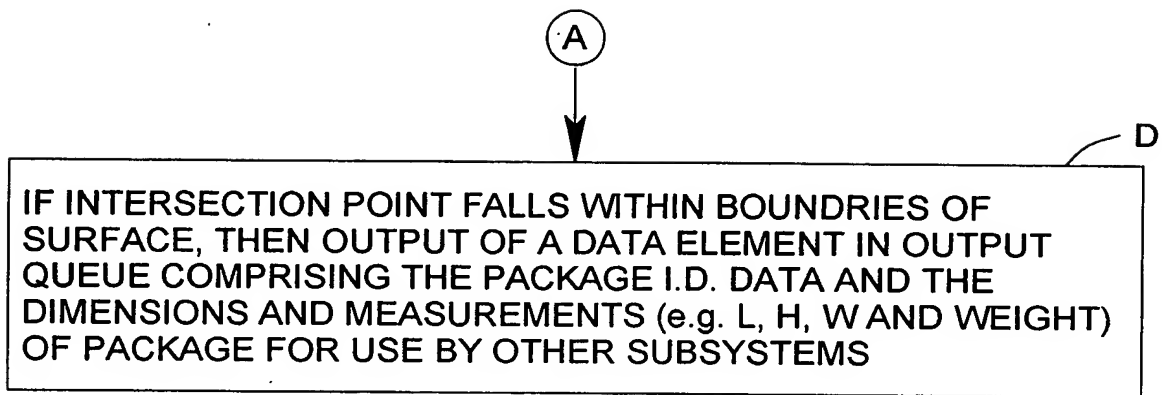
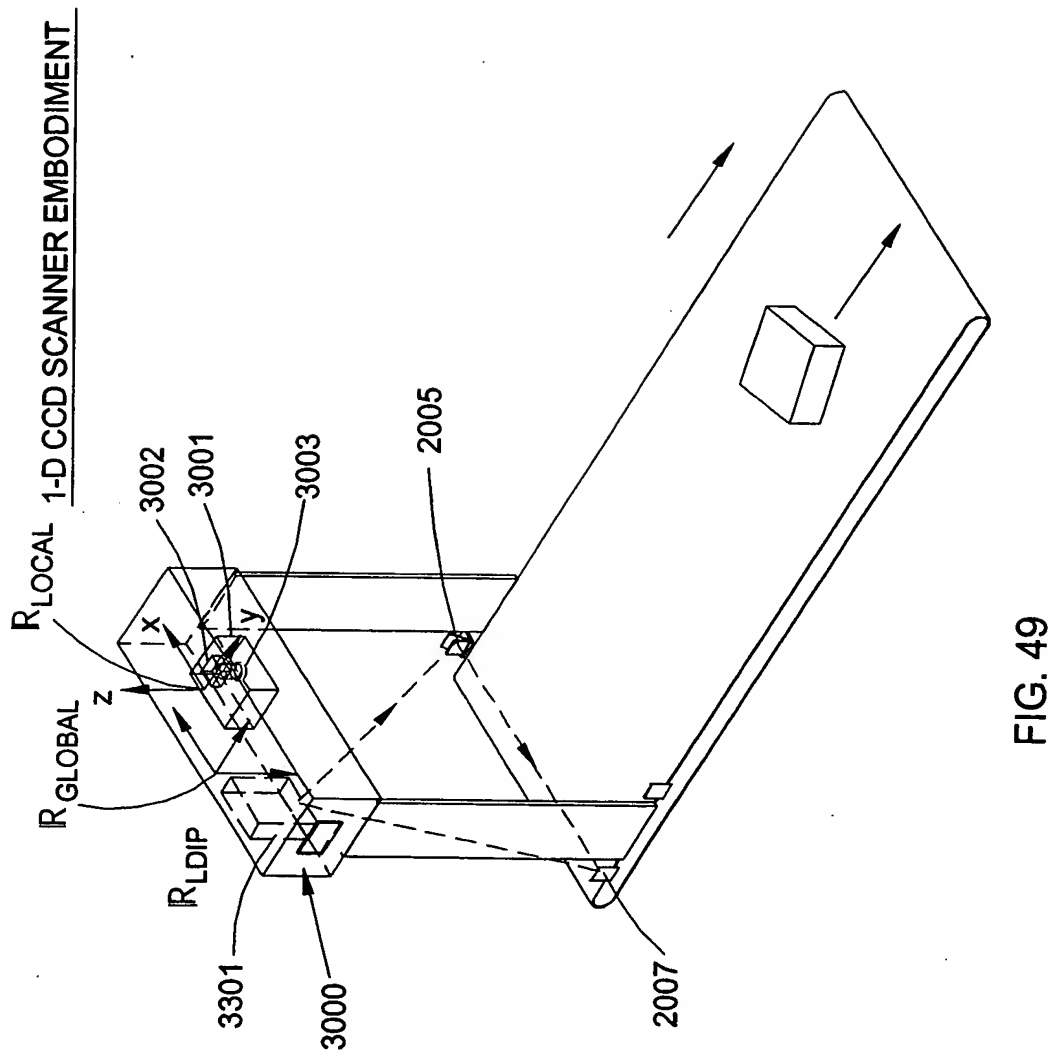


FIG. 48B

111/116



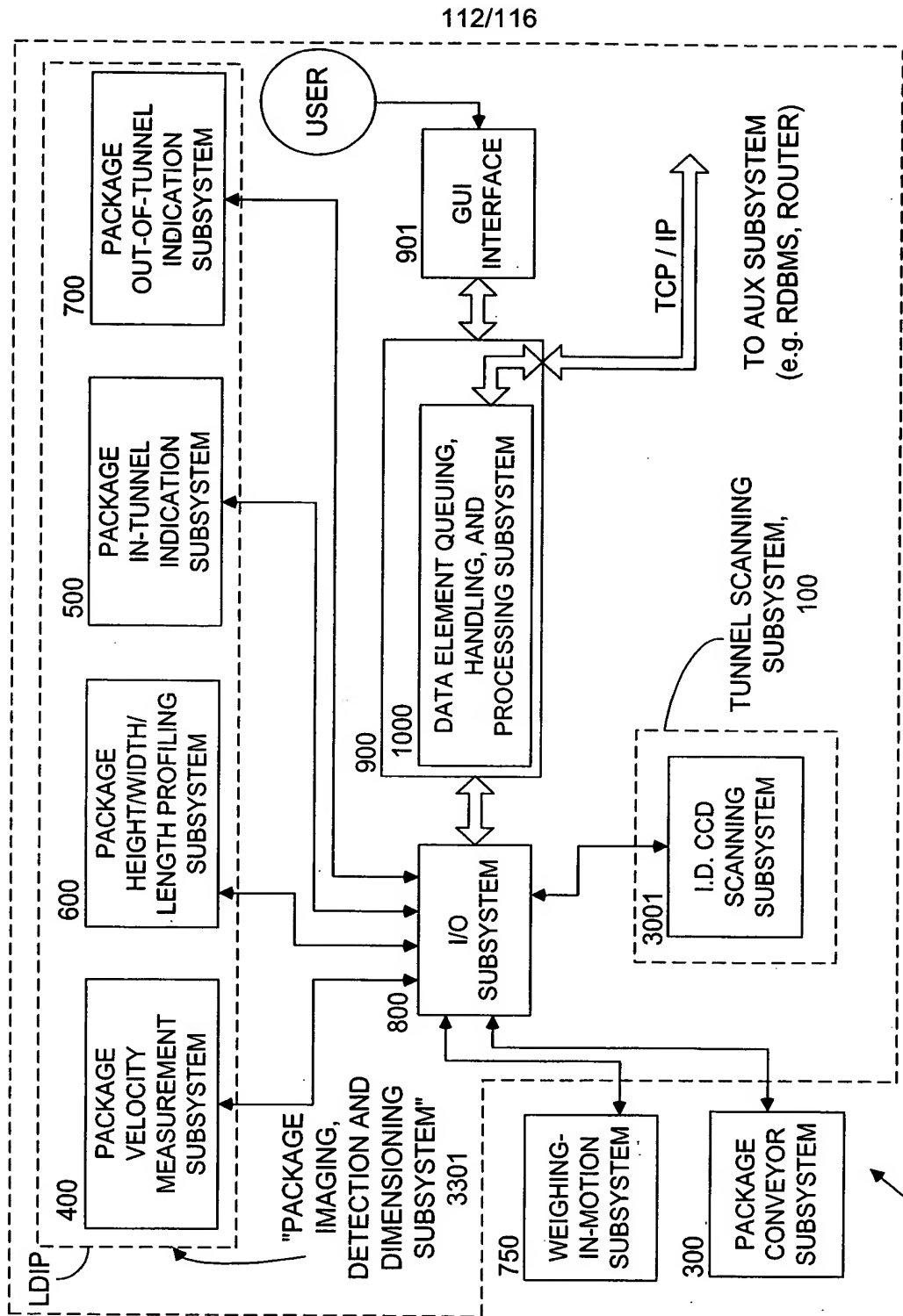


FIG. 50

113/116

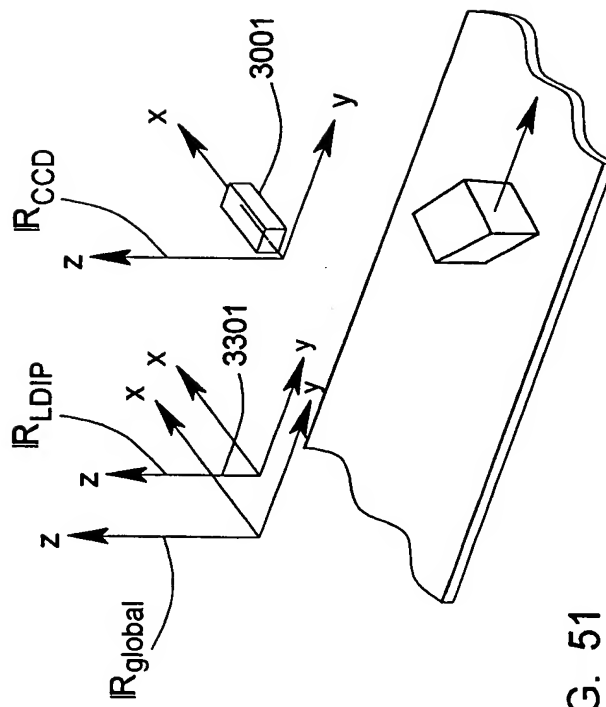


FIG. 51

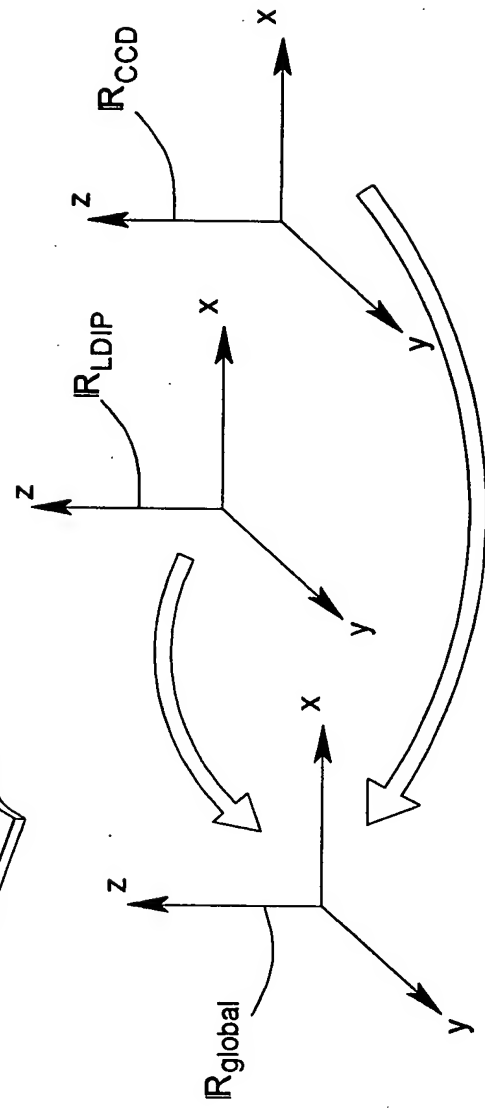


FIG. 52

114/116

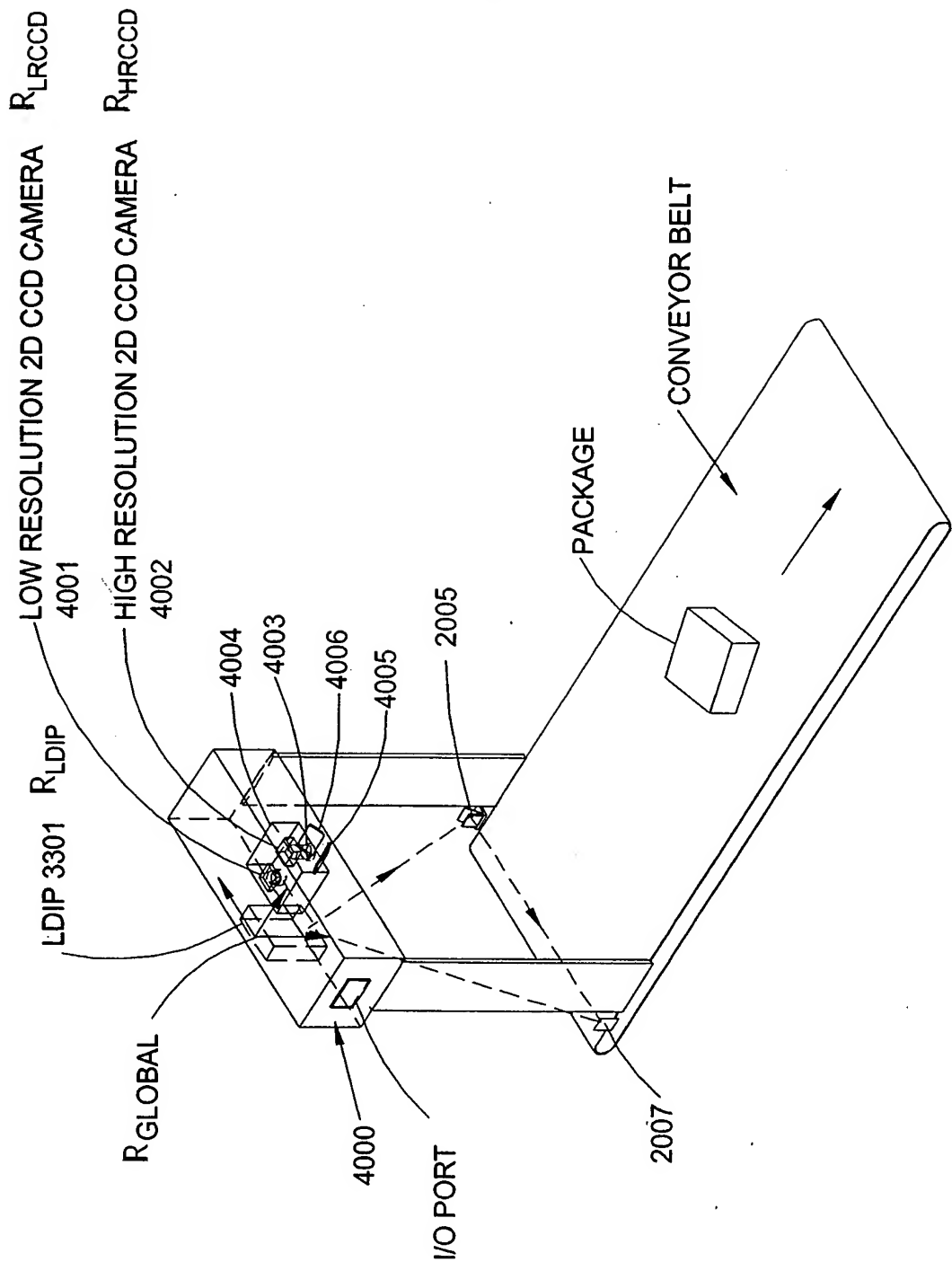


FIG. 53

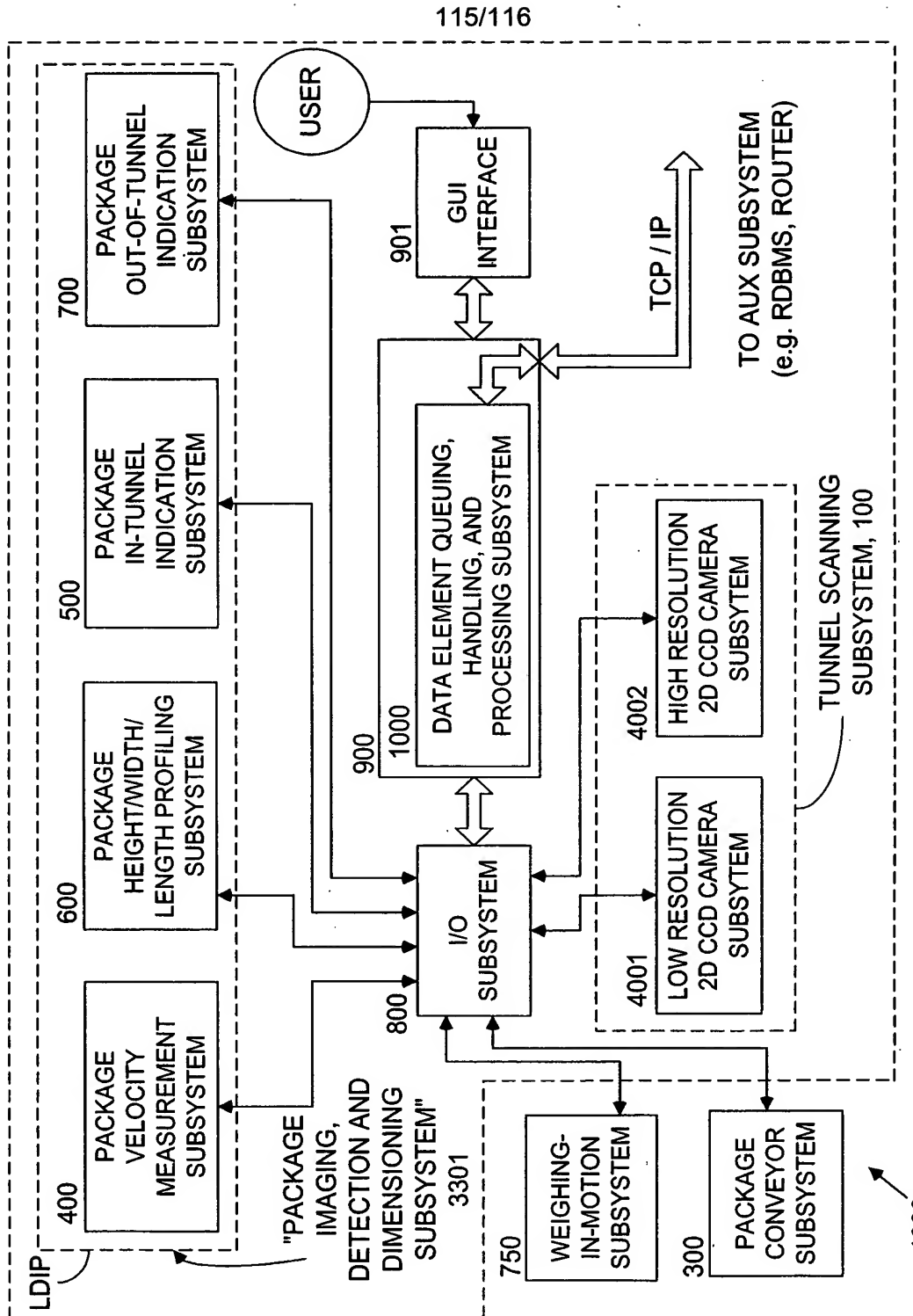


FIG. 54

116/116

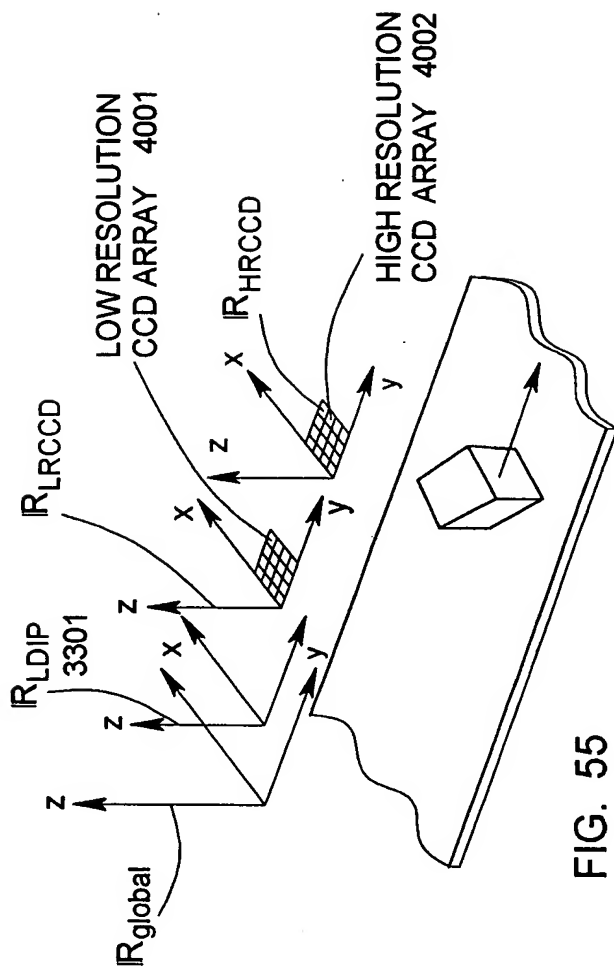


FIG. 55

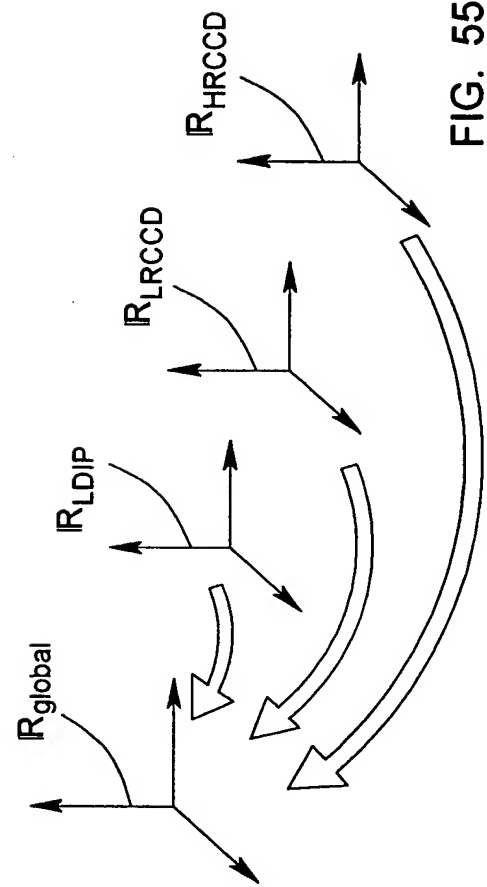


FIG. 55